SAND2019-7575PE

Optical Diagnostics in Combustion

Robert Barlow
Sandia National Laboratories

Objectives of this lecture

- Motivate experimental combustion research
- Highlight the role of optical diagnostics in combustion research
- Introduce basic concepts of light-matter interaction, lasers, detectors, turbulent flow
- Cover principles of some commonly applied combustion diagnostics
- Highlight some things we have learned about fundamental combustion phenomena

- The emphasis will be on turbulent gas-phase combustion

Outline

Motivation

- Projections from IEA
- Scenario 2DS, very limited CO_2 emissions
- Growing demand, electrification
- Fossil + Biofuels still 2/3 of total in 2050

International Energy Agency
Energy Technology Perspectives 2017
https://webstore.iea.org/energy-technology-perspectives-2017 (free)

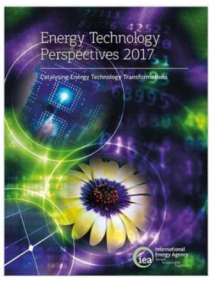

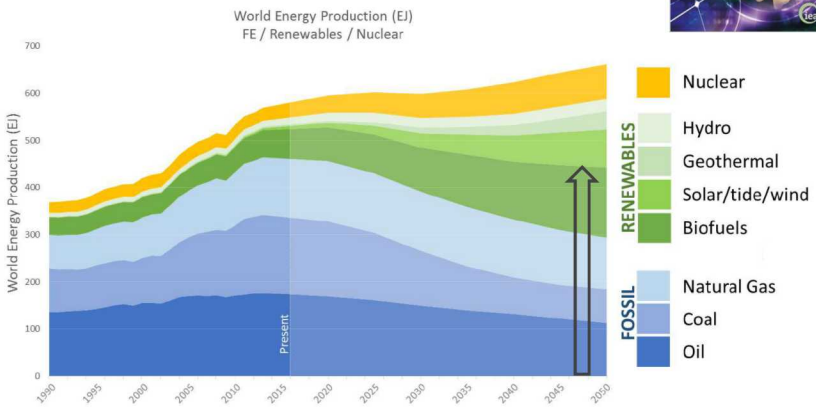

Motivation

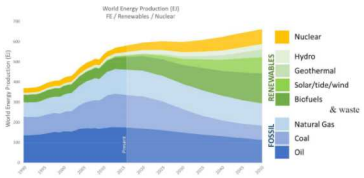

- Combustion will remain a big part of the world energy economy for decades, and climate change demands that combustion systems be as clean and efficient as possible
- Turbulent combustion is a complex, multi-scale, multi-physics problem that we don't fully understand and are not very good at predicting, yet

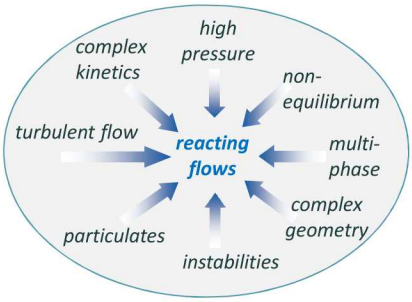

Sandia National Laboratories

5

Motivation

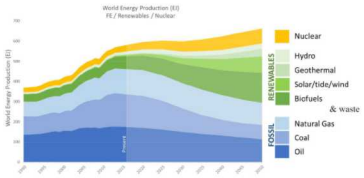

- We want our experiments to be useful
  - New or improved techniques (*diagnostic demonstration experiments*)
  - Fundamental insights on physical phenomena (*exploratory science experiments*)
  - Benchmark data sets for testing of models (*validation experiments*)
  - Technology development; sensing and control (*solve practical problems*)
- Suggestions on doing useful experiments:
  - Collaborate with experimental and computational people
  - Apply multiple diagnostics (simultaneously, if possible)
  - Design experiments to address BOTH science and validation objectives
  - Pay attention to things that can render your data useless
    - flow calibrations!!!
    - repeatability checks using known reference conditions
    - avoid uncontrolled or overly complex boundary conditions
    - ask yourself, "What am I really measuring? What are the potential errors?"
- Contribute to the development of predictive models for the design of future combustion technologies

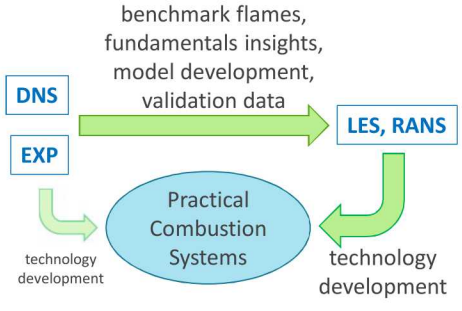

Sandia National Laboratories

6

A good place to find collaborators (www.tnfworkshop.org)

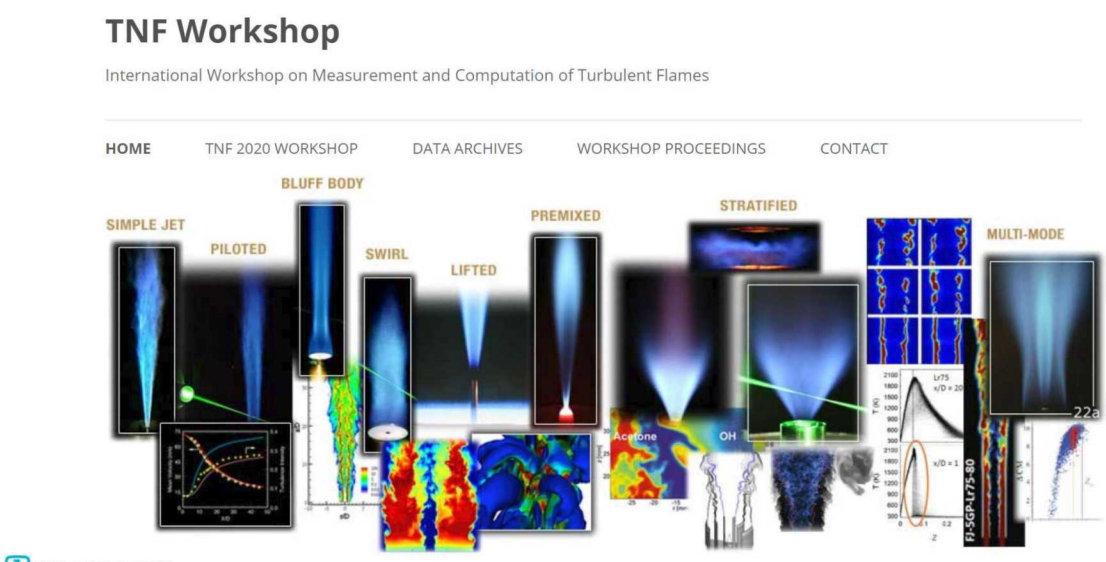

Sandia National Laboratories

7

International Workshop on Measurement and Computation of Turbulent Flames

- Framework for collaboration among experimental and computational researchers
  - Isolate aspects of **turbulence-chemistry interaction** that are poorly understood and challenging to model (parametric variation)
  - Use **simple fuels** to minimize uncertainty
  - Apply **complementary diagnostics** to the same flames
    - velocity, scalars, statistics, dynamics
    - careful attention to boundary condition
  - Joint **comparisons of multiple simulations** against experiments

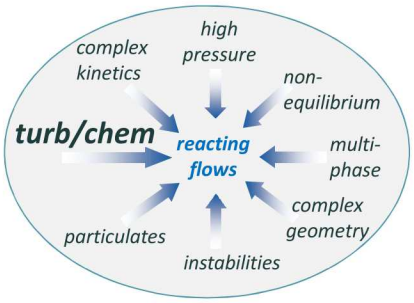

TNF1	TNF8	TNF14
1996	2006	2018
•non-premixed	•premixed •stratified •lifted jet in hot coflow	•multi-regime •multi-dimensional (4D) •flame-wall •enclosed, high-P

- One of several workshops:
  - ISF, PTF, ECN, TCS, RCM, LII, Flame Chemistry, High P…

Sandia National Laboratories

8

Things we would like to measure

- Flow field
  - Mean, fluctuations, correlations (1-2-3 components)
  - Strain, vorticity (gradients in 2D or 3D)
  - Length and time scales of turbulence, coherent structures
- Scalar field
  - Mean, fluctuation of temperature, major and minor species concentrations
  - Equivalence ratio or mixture fraction
  - Scalar gradients and length scales
  - Structural information based on 2D- or quasi 3D-diagnostics
  - Heat release rate (where, when, how much)
- Multiphase flow and particulates (e.g., coal, spray, soot, synthesis)
  - Particle size, number density, volume fraction, velocity, …
- Boundary and inflow conditions
  - Flow and scalar fields
  - Surface temperatures
- Information on unsteadiness and flow dynamics (4D)
  - Temporal sequences of flow and scalar fields, pressure fluctuations

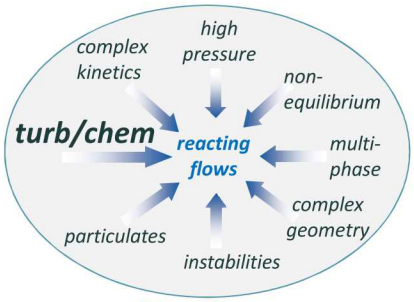

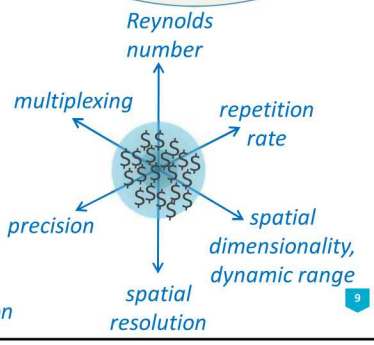

Sandia National Laboratories

Everything simultaneously in 3D with temporal evolution

9

Why laser diagnostics?

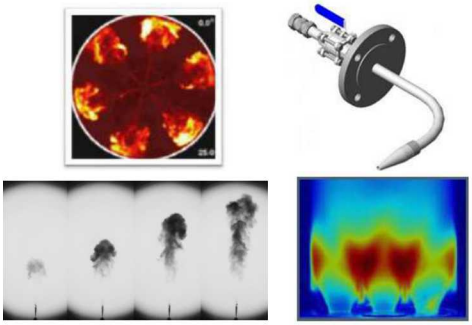

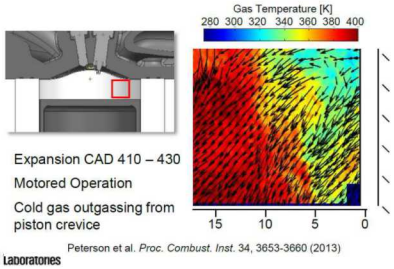

Peterson et al. *Proc. Combust. Inst.* 34, 3653-3660 (2013)

Sandia National Laboratories

- You can learn a lot without lasers
  - Physical probes for T, gas sampling
  - Chemiluminescence and soot luminosity
  - Shadowgraph and Schlieren imaging
  - Combine with high-speed cameras
  - Acoustic sensors
  - Include just looking and listening!
- But lasers offer many advantages
  - Temporal resolution (pulsed lasers)
  - Spatial resolution (focused beams, sheets)
  - Spectral selectivity (tunable lasers)
  - High sensitivity (LIF, laser absorption)
  - High power and repetition rate (pulse burst)
  - Non-intrusive (but not always)
  - Can be applied simultaneously

10

Classification

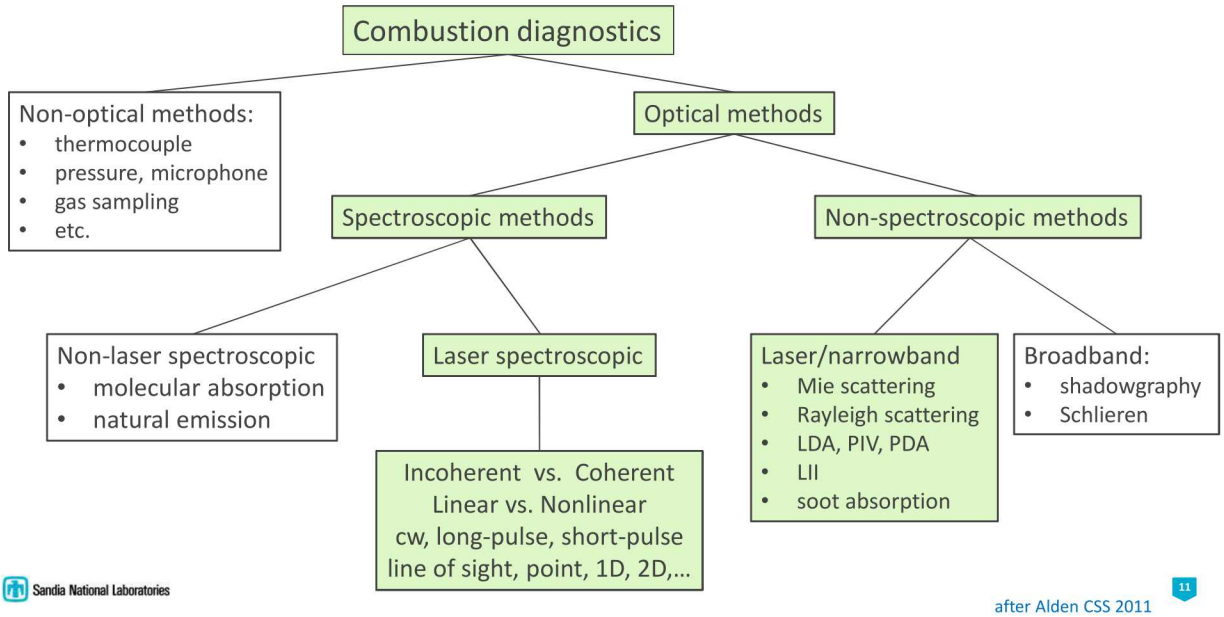

Sandia National Laboratories

after Alden CSS 2011

11

Enabling technologies and related fields

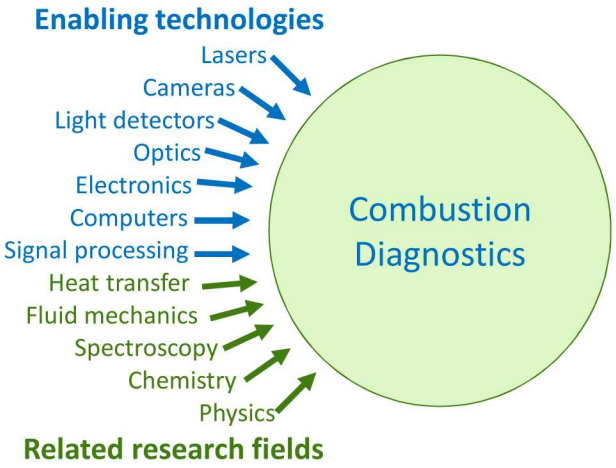

- Many advances in laser diagnostics have been enabled by technological advances from other fields:
  - Low noise CCD detectors for astronomy
  - Scientific CMOS detectors in bio research
  - Infrared (IR) diode lasers, fiber optics, and detectors for telecommunications
  - Lasers developed for medical and industrial applications, and other research fields
  - IR spectroscopy database (HITRAN) for atmospheric science and remote sensing
  - Tomographic analysis from medical imaging
  - Signal and image denoising based on wavelet methods for image compression
- Most velocity diagnostics were originally developed for nonreacting flow research

Sandia National Laboratories

12

Today's menu of major laser diagnostic techniques

- **Gas velocity**
  - **Laser Doppler anemometry (LDA)** — Mie scattering from particles seeded into the flow
  - **Particle imaging velocimetry (PIV)** — Mie scattering from particles seeded into the flow
  - Particle tracking velocimetry (PTV)
- **Gas temperature and species concentrations**
  - **Laser absorption spectroscopy (LAS)** — CISS lecture notes: Alden 2011, Linne 2016, Hanson 2018
  - **Laser induced fluorescence (LIF)** — CISS lecture notes: Alden 2011, Linne 2016, Hanson 2018
  - **Laser Rayleigh scattering (LRS)**
  - **Spontaneous Raman scattering (SRS)**
  - Coherent anti-Stokes Raman spectroscopy (CARS) — CISS lecture notes: Alden 2011, Linne 2016
- **Soot**
  - Laser absorption/scattering
  - Laser induced incandescence (LII) — Michelson et al., Progress in Energy and Combustion Science 51 (2015)
- **Droplets and sprays**
  - Phase Doppler anemometry (PDA)
  - Tracer LIF — Schulz, Sick, Progress in Energy and Combustion Science 31 (2005)
  - Structured illumination (SLIPI) — Linne, Progress in Energy and Combustion Science 39 (2013);
  - Ballistic imaging, X-ray imaging — Linne, CISS 2016 lecture notes

Sandia National Laboratories

https://www.combustioninstitute.org/resources/cisummerschool/

13

Application example: High-speed imaging of velocity and OH

Flame	P_{th} (kW)	ϕ	$\dot{m}_{air}$ (g/s)	$\dot{m}_{CH4}$ (g/s)	p' (Pa)	f_a (Hz)	S (Hz)	f_{pvc} (Hz)
1	7.6	0.55	4.7	0.15	85	302	0.55	507
2	10	0.65	5.4	0.20	130	305	0.55	555
3	10	0.75	4.7	0.20	220	308	0.55	515

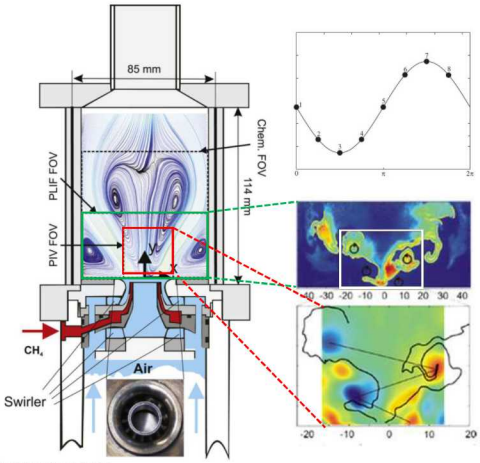

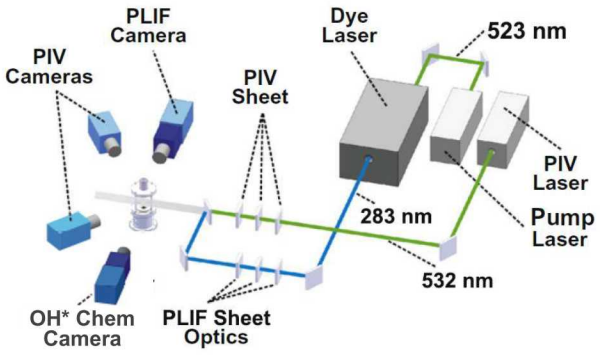

- Simultaneous stereo PIV, OH PLIF, and chemiluminescence imaging
- Three flames with different strength of acoustic instability
- Pressure fluctuations and PVC at different frequencies; data are doubly phase resolved

Sandia National Laboratories

Steinberg et al. CNF 157 (2010); AIAA J 50 (2012)

14

Application example: High-speed imaging of velocity and OH

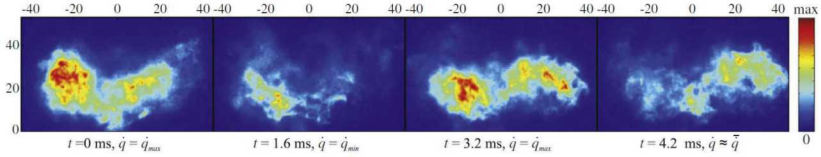

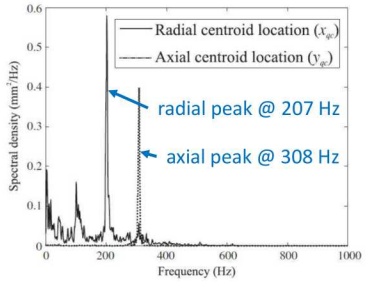

- Time sequence of OH* chemiluminescence
- Spectra of axial and radial OH* centroid locations have different peaks
- Pressure and volume flow fluctuation at 308 Hz (phase shift)
- Precessing vortex core revolves at 515 Hz (207 Hz = 515 Hz – 308 Hz)
- Complex interactions
- Doubly phase resolved flow-field and combustion statistics

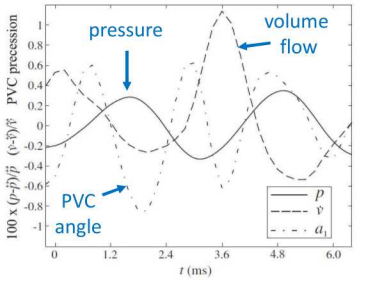

Sandia National Laboratories

Steinberg et al. CNF 157 (2010); AIAA J 50 (2012)

Periodic flow-flame interactions – Stable flame

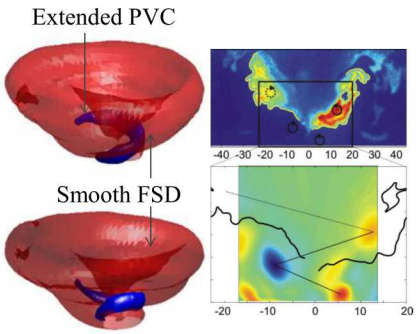

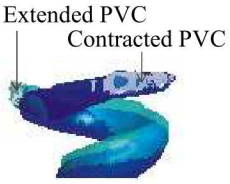

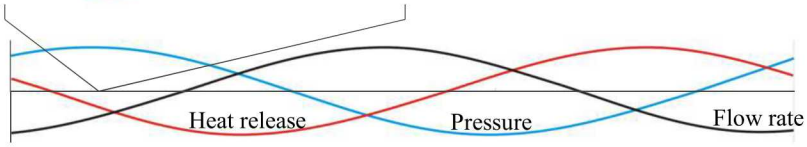

Sandia National Laboratories

16

Steinberg et al. CNF 157 (2010); AIAA J 50 (2012)

Periodic flow-flame interactions – Stable flame

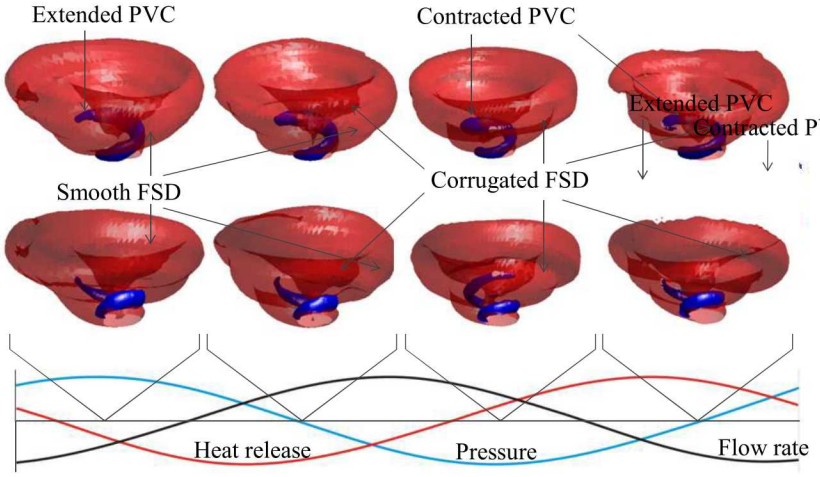

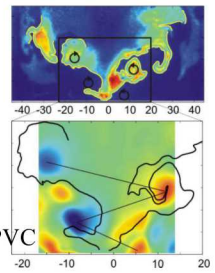

Sandia National Laboratories

Steinberg et al. CNF 157 (2010); AIAA J 50 (2012)

17

Setting up the diagnostic system is only a first step

- Design experiments with clear objectives regarding the combustion physics you what to investigate. (Your advisor should be able to guide you on this, but the best students eventually come up with better ideas than their advisors.)
- Do you have the right tools to get the data you need?
- Try to get an early look at your data to catch problems before too much time has been invested
- Read the literature
- Ask lots of questions
- Analysis to pull new understanding and physical insight is usually a much larger time investment that the actual experiments.
- Be prepared to find something unexpected; your objectives may evolve as you gain understanding of your experimental target

Sandia National Laboratories

18

Coming up: Basics concepts of …

- Electromagnetic spectrum (light)
- Polarization
- How lasers work
- Common lasers used in combustion diagnostics
- Optical tidbits
- Light detectors


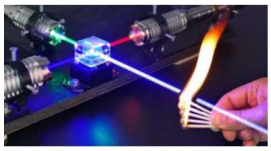

Sandia National Laboratories

19

Light is electromagnetic radiation

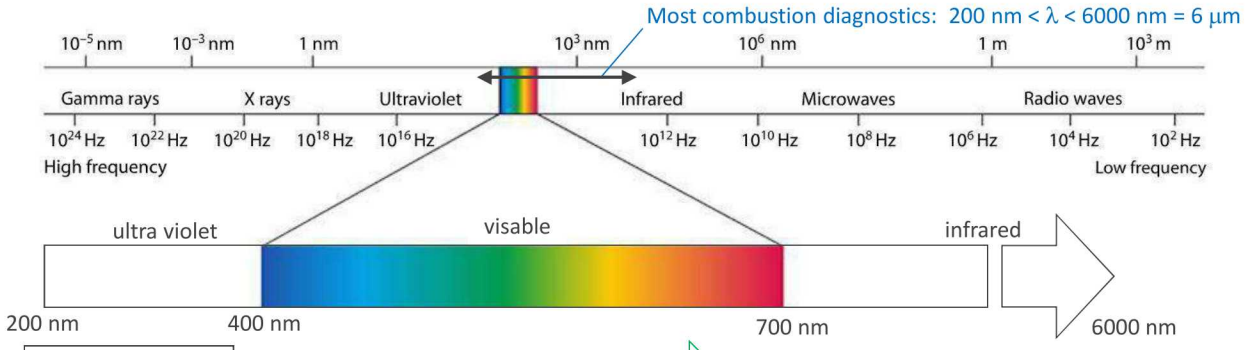

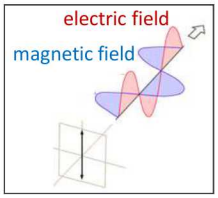

increasing wavelength, λ

increasing frequency, ν

c = speed of light in a vacuum = 3.0×10^8 m/s
u = speed of light in a material
$u = c/n$, where n = material index of refraction
$\nu = c/\lambda_o = u/\lambda$ (Hz), where λ_o = vacuum wavelength
$E = h\nu$ = photon energy (J)
where h = 6.63e-34 J·s (Planck's constant)

Note: Spectroscopists often use wavenumbers (cm^{-1}) = ν/c or = $10{,}000{,}000/\lambda_o$ with λ_o in nm

https://www.miniphysics.com/electromagnetic-spectrum_25.html

Sandia National Laboratories

20

Light is electromagnetic radiation

- In optics, 'polarization' denotes the electric field orientation, since optical interactions are electronic

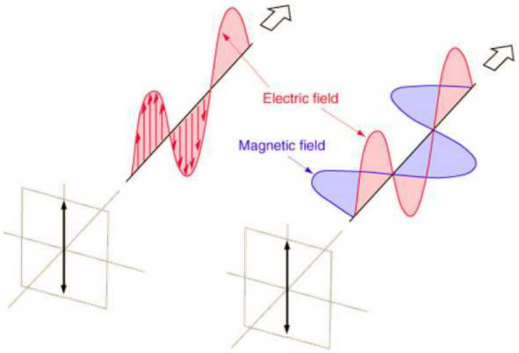

linearly polarized light
vertical polarization

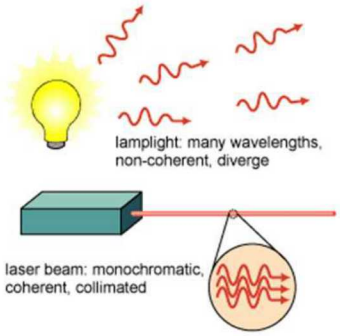

Many lasers are designed to generate linearly polarized light. The laser beam is also collimated, and wave propagation is coherent.

Random polarization

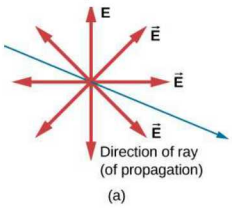

Linear polarization

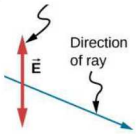

Sandia National Laboratories

See Mark Linne CISS 2016 Lecture 3 for a detailed treatment of electromagnetism

21

Light is electromagnetic radiation

- Three types of polarization: linear, circular, and elliptical

linear polarization

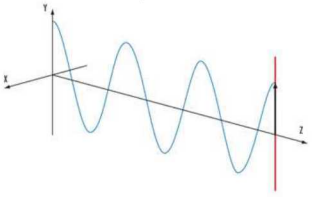

*The electric field is confined to a **single plane** along the direction of propagation.*

circular polarization

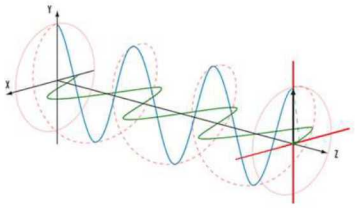

*The electric field consists of two perpendicular, equal in amplitude, linear components that have a **phase difference of π/2**. The resulting electric field describes a circle.*

elliptical polarization

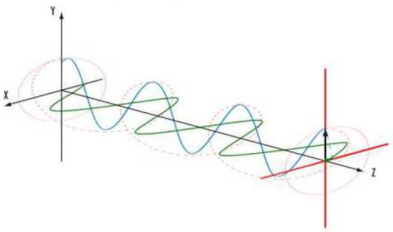

*The electric field consists of two perpendicular linear components with **any amplitude and any phase difference**. The resulting electric field describes an ellipse.*

Sandia National Laboratories

https://www.edmundoptics.com/resources/application-notes/optics/introduction-to-polarization/

22

Light is electromagnetic radiation

- Optical materials can be used to manipulate polarization.

https://www.edmundoptics.com/resources/application-notes/optics/understanding-waveplates/

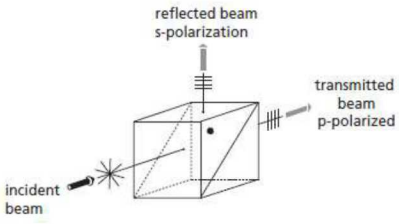

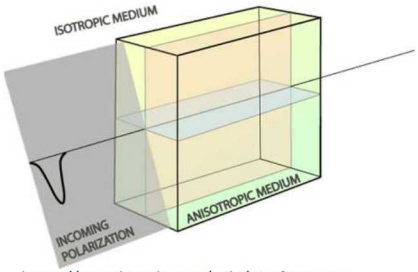

https://en.wikipedia.org/wiki/Birefringence

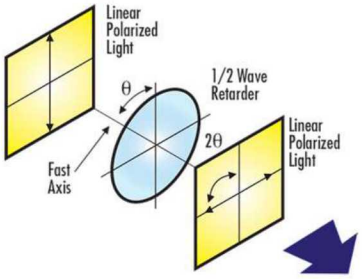

A **polarizer** separates an incident beam into two linear components

A **birefringent material** (e.g., crystal) has a different index of refraction parallel vs. perpendicular to the optical axis of the material. Components travel at different speed

Example: a **half wave plate** rotates the polarization of a linearly polarized beam by twice the angle between its optical axis and the polarization axis of the incoming beam

Sandia National Laboratories

Combine a half wave plate with a polarizer to make a **variable beam splitter** or **variable attenuator** for a linearly polarized laser beam.

23

Basics of lasers, optics, and detectors

- Consider a typical setup for OH LIF (point, line, or planar)

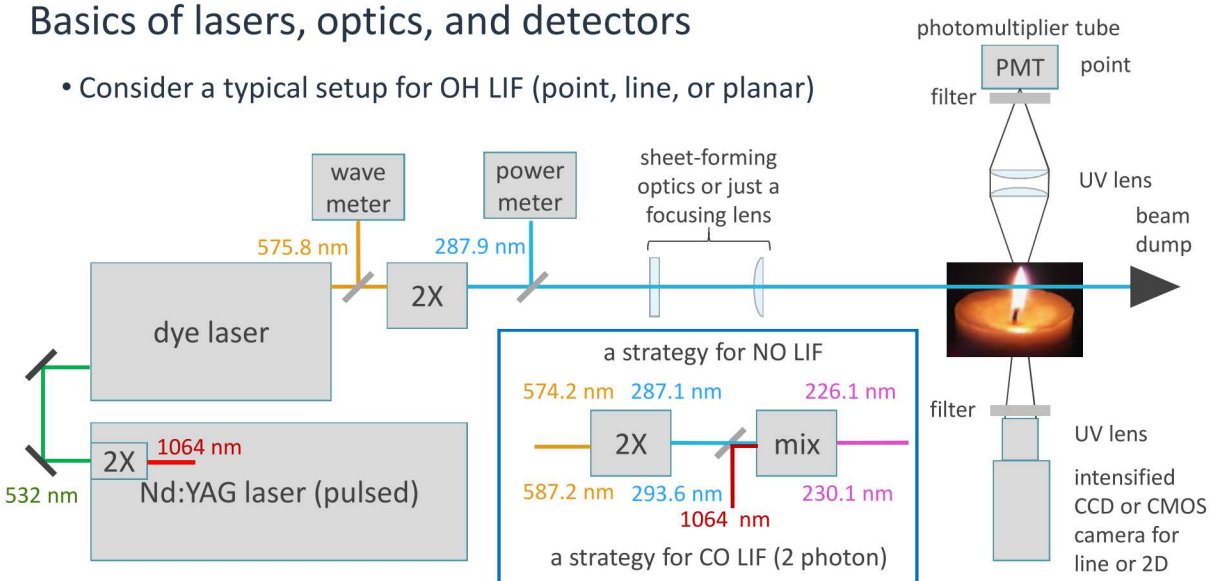

Sandia National Laboratories

24

Common lasers in combustion diagnostics

- Flashlamp-pumped, Q-switched Nd:YAG lasers
- Dye lasers

long history of combustion diagnostics with 10 ns,10 Hz Nd:YAG and dye lasers: LIF, CARS, Rayleigh, Raman, LII, …

- Diode-pumped, Q-switched Nd:YAG lasers
- High rep rate dye lasers

high-speed PIV and PLIF

- Visible and IR diode lasers (many)

https://en.wikipedia.org/wiki/Laser_diode

- Mode-locked ultrashort pulse lasers
  (e.g., ~100 fs pulses, 800 nm @ ~80 MHz rep rate)

https://www.rp-photonics.com/ultrafast_lasers.html
https://www.rp-photonics.com/picosecond_lasers.html

Sandia National Laboratories

Length of laser pulse at c = 3.0e8 m/s = 30 cm/ns:
10 ns pulse is 3 m long; 100 fs pulse is 30 μm long

25

Basic components of a laser

Light **A**mplification by **S**timulated **E**mission of **R**adiation

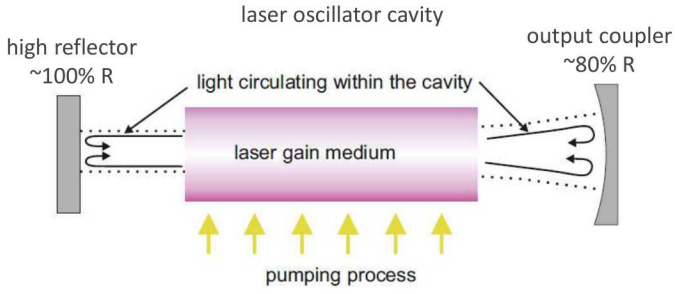

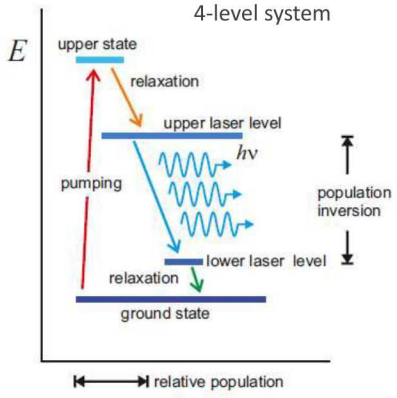

- The stimulated emission process is coherent; the photons inside the cavity and exiting in the laser beam are coherent with each other

Sandia National Laboratories

Linne CISS 2016

26

Flashlamp-pumped, Q-switched Nd:YAG lasers

- Work horse laser in combustion diagnostics
- Gain medium is Nd in a glass host, yttrium aluminum garnet (YAG)
- Pumped by broadband flashlamps in a water-cooled reflective chamber
- Q-switch (Pockels cell and polarizer) blocks oscillation while stored energy builds up
- Pulsed laser beam at 1064 nm (IR, not visible, therefore dangerous!)
- Usually oscillator and one or two amplifiers
- Typical specs:
  - 10 Hz (most common, up to 100 Hz)
  - Up to 2.5 J/pulse @ 1064 nm (even 7 J/pulse*)
  - 6-10 ns pulse width (also variable pulse width versions, 50 ns to ~3 μs)
- Can be injection seeded by small narrowband cw laser
- Nonlinear crystals for harmonic generation: 532 nm, 355 nm, 266 nm

Sandia National Laboratories

* www.rrcat.gov.in/newsletter/NL/nl2018/issue2/pdf/L6.pdf

27

Flashlamp-pumped, Q-switched Nd:YAG lasers

- Lasing starts randomly in an unseeded laser
- Temporal pulse shape of an unseeded laser shows beating of many longitudinal modes; changes from pulse to pulse
- Spatial beam profile fluctuates

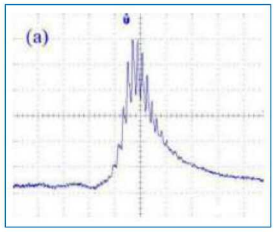

unseeded temporal pulse

- Injection seeding:
- Light from a small single-frequency diode-pumped cw Nd:YAG laser is injected along the axis of the pulsed laser cavity (slave oscillator)
- Better, more repeatable temporal and spatial beam characteristics
- Narrower bandwidth
  - necessary for some applications, e.g., filtered Rayleigh scattering
  - useful in many other applications.

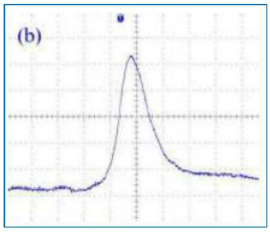

seeded temporal pulse

Sandia National Laboratories

Linne CISS 2016

28

Dye lasers

- Lasing medium is a fluorescent dye in liquid solvent (e.g., methanol) circulating through a dye cell
- Pump source is usually another laser (e.g., pulsed Nd:YAG @ 532 or 355 nm)
- A grazing incidence grating in the oscillator selects the wavelength that can be amplified, so the output is tunable and can be narrowband (< 0.1 cm^{-1})
- Combine different pump wavelengths and dyes with doubling and mixing crystals (~190-900nm)

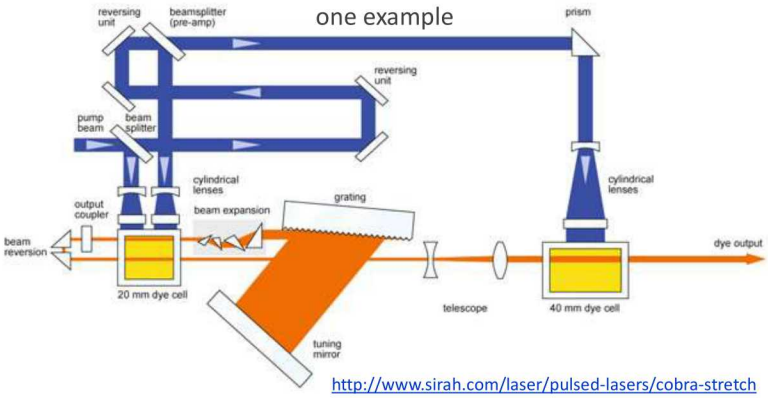

http://www.sirah.com/laser/pulsed-lasers/cobra-stretch

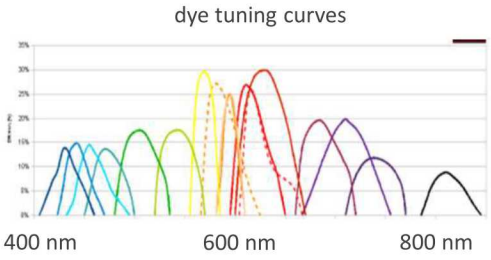

https://www.radiant-dyes.com/index.php/products/laser-dyes

29

Nonlinear crystals for frequency conversion

- Crystals with non-cubic crystal structures are often birefringent
- Phase matching by angle tuning (efficiency <50%)

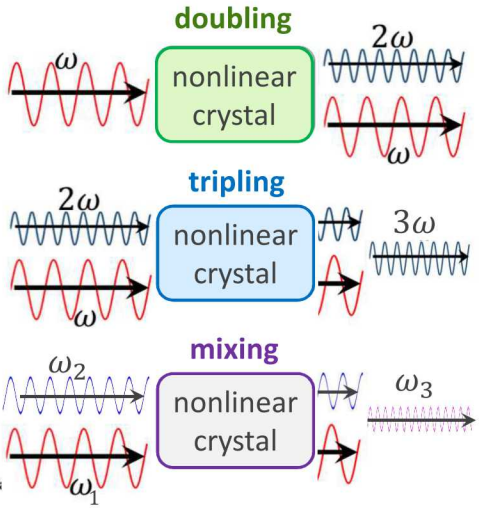

$$\omega_3 = \omega_1 + \omega_2$$

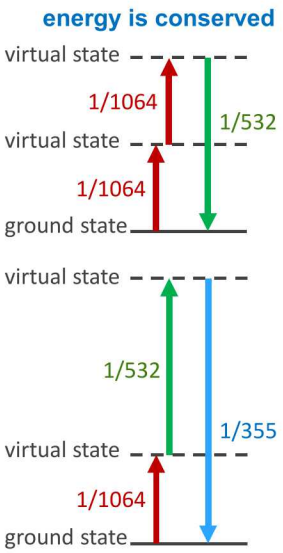

https://en.wikipedia.org/wiki/Nonlinear_optics

30

Diode-pumped, Q-switched Nd:YAG lasers and matched dye lasers

- 808 nm wavelength infrared GaAlAs laser diodes pump the Nd:YAG rod
  - pulse energy up to 120mJ
  - pulse length down to 1ns
  - peak power up to 10MW
  - pulse rep. rate **up to 150 kHz**
  - average power up to 800W
  - wavelengths 1064, 532, 355, 266nm
- Dye lasers designed for high repetition rate, similar layout to the 10 Hz dye lasers
- **High speed PIV and PLIF imaging applications**

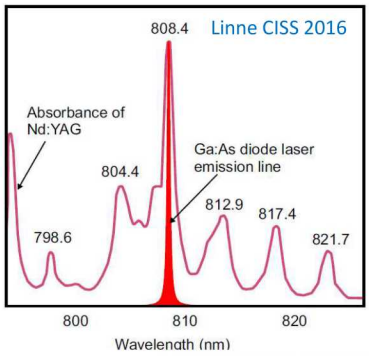

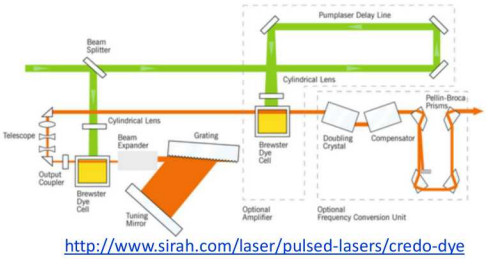

http://www.sirah.com/laser/pulsed-lasers/credo-dye

Sandia National Laboratories

Laser safety

- Lasers used in combustion research are hazardous
  - permanent eye damage
  - skin burns
  - UV skin damage (especially high power 355 nm)
- Personal protective equipment
  - laser glasses/goggles for all wavelengths
  - long sleeves and gloves for 355 nm

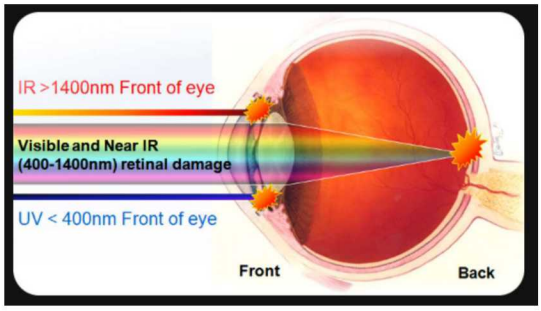

Princeton.edu - Eye Absorption Site vs. Wavelength

- Engineered controls
  - enclose beams wherever practical
  - door interlocks, warning signs & flashing lights outside
  - flashing light at the test section (converted bicycle tail light)
- Proceedures
  - align at lowest possible pulse energy
  - use fluorescent cards to check for stray UV or IR reflections (white business cards for UV, orange card stock for IR)

Sandia National Laboratories

32

Optics (only tidbits)

- Useful info on optics, optical materials, filters, coatings, etc. at the back of the (old) Melles Griot paper catalog, "Fundamental Optics." PDF file available online:
  https://www.cvilaseroptics.com/file/general/Fundamental_Optics_OverviewWEB.pdf

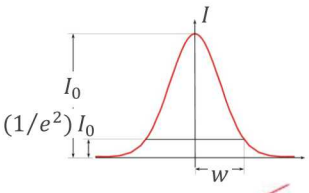

- What's at the focus?
  - Profile at the focus is the spatial Fourier transform of the incoming beam profile
  - Gaussian beam (best possible profile, TEM_{00})
  - Gaussian beam waste, $D = 2w_0 \cong 4\lambda/\pi\Theta$
  - Rayleigh range, $z_R = \pi w_0^2/\lambda$
  - Estimate laser sheet width at center and edge on image
  - Typical laser beam does not focus as well
  - Incoming top hat beam is a sinc function (rings) at the focus

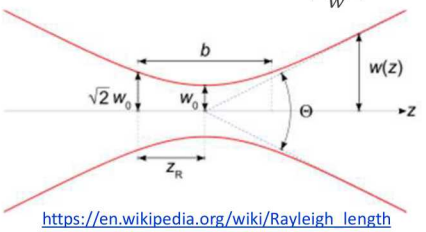

https://en.wikipedia.org/wiki/Rayleigh_length

- Right way and wrong way (let both surfaces do the work)

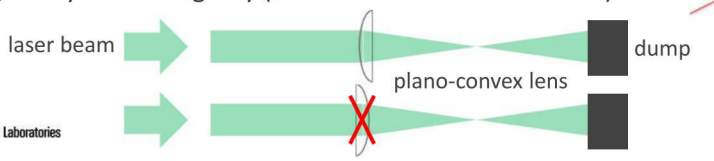

Sandia National Laboratories

33

Photomultiplier tubes

- Good for low level signals (even photon counting)
- Photon hits photocathode material and generates an electron
- Electron cloud is amplified through a dynode chain (~10 stages)
- Custom socket design to optimize performance for pulsed measurements: sensitivity, dynamic range, linearity
- Different photocathode materials for different wavelength ranges
- Combustion diagnostic applications:
  - Pointwise LIF and Raman/Rayleigh
  - LDA

https://en.wikipedia.org/wiki/Photomultiplier_tube

side-on

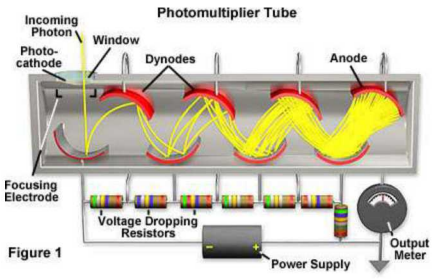

end-on

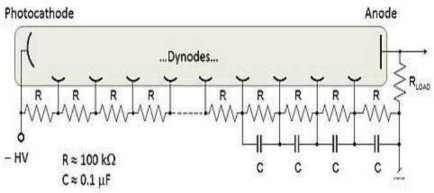

Sandia National Laboratories

34

Photodiodes

- Semiconductor devices that convert light to current
- Diagnostic applications:
  - Laser absorption measurements
  - Laser power/energy monitoring
  - CW and pulsed
  - Chemiluminescence
  - …

Material	Wavelength Range (nm)
Silicon	190-1100
Germanium	400-1700
Indium gallium arsenide	800-2600
Lead sulfide	1000-3500
Mercury cadmium telluride	400-14000

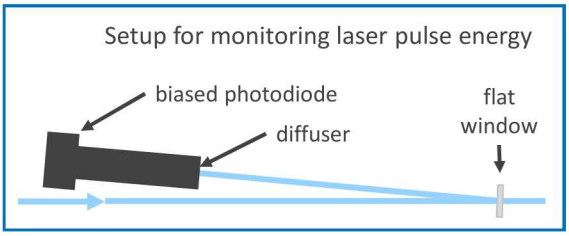

Array detectors (cameras): Fast moving technical area

- Main types in combustion diagnostics: CCD, EMCCD, CMOS, sCMOS
- CCD = charge coupled device
  - Detector of choice for most low rep-rate (CW or 10 Hz) imaging and spectroscopy applications
  - Pixels are read out sequentially through the same circuitry (slower, more accurate)
  - Back-illuminated architecture for high (~90-95%) quantum efficiency
  - Thermoelectric cooling to -100C (cryogenic to -110C) minimizes dark current (determines noise floor)
  - Programmable on-chip binning to reduce readout noise with low-level signals (example: spatial and spectral integration in Raman)
- EMCCD = electron multiplying CCD
  - Allows charge on each pixel to be multiplied before readout; helps with low signal levels, "single photon sensitivity"
- CMOS = complementary metal oxide semiconductor
  - Each pixel has its own amplifier, readout circuitry (faster)
  - High-speed imaging applications (PIV or PLIF at 10+ kHz)
- sCMOS = scientific CMOS
  - Significant improvements in QE, linearity, faster framing than CCDs

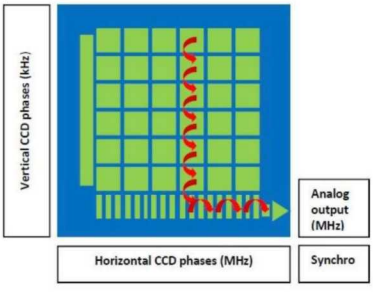

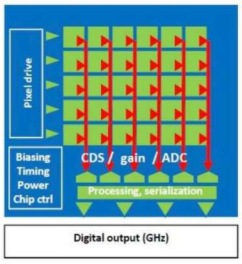

Image intensifiers

- Placed in from of CCD or CMOS detectors to amplify low light signals and/or allow very short gate times (shorter costs more)
- Main elements
  - Photocathode – converts photons to photoelectrons
  - Micro channel plate (MCP) – amplifies electron charge through each micro channel
  - Phospor – converts electrons back to light at a good wavelength for the detector array
- Lens coupled or fiber-optic tapered bundle
  - Lens coupling gives better image quality, allows easy replacement of intensifier, bigger footprint
  - Fiber bundle gives good optical efficiency and compact design, but image quality is not as good (fixed honeycomb pattern, lower resolution)

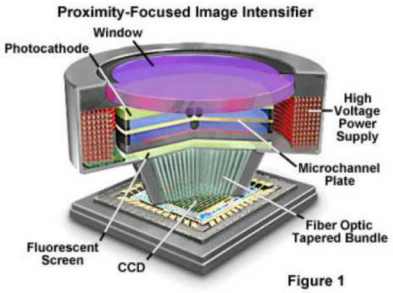

http://hamamatsu.magnet.fsu.edu/articles/proximity.html

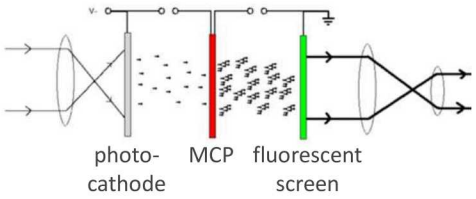

https://en.wikipedia.org/wiki/Image_intensifier

Particle-based velocity measurements

- Mie scattering
- Laser Doppler anemometry (LDA or LDV)
- Particle image velocimetry (PIV)
- Stereo PIV
- Wavelet optical flow velocimetry (wOFV)
- Tomographic PIV

Particle-based velocity measurements: Mie scattering

- Light scattering from particles with size, $d \geq \lambda/\pi$, λ = wavelength
- Theoretical solution for spherical particles (Lorenz Mie Debye)
  - http://www.philiplaven.com/mieplot.htm (free)

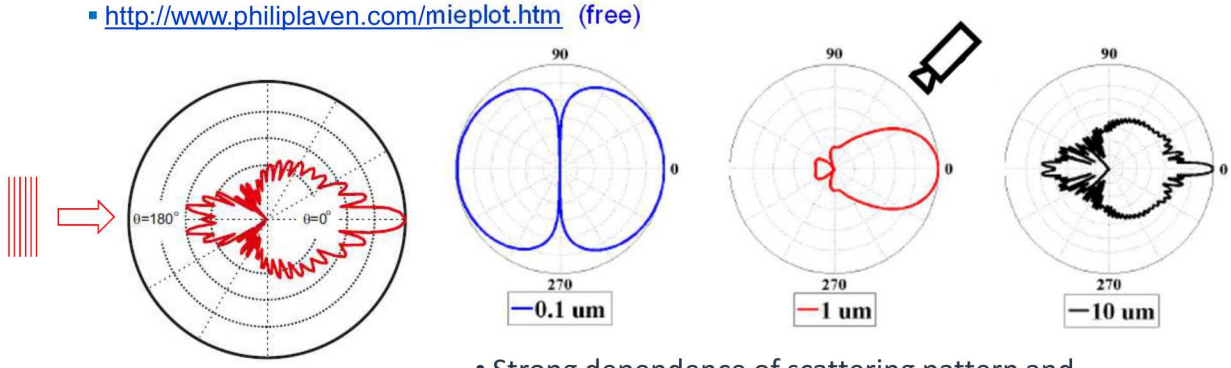

- Strong dependence of scattering pattern and amplitude on particle size

Sandia National Laboratories

Rayleigh scattering if $d < \lambda/\pi$ (coming later)

Laser Doppler anemometry (LDA)

- Pictorial explanation (interference effect is actually realized at the detector)

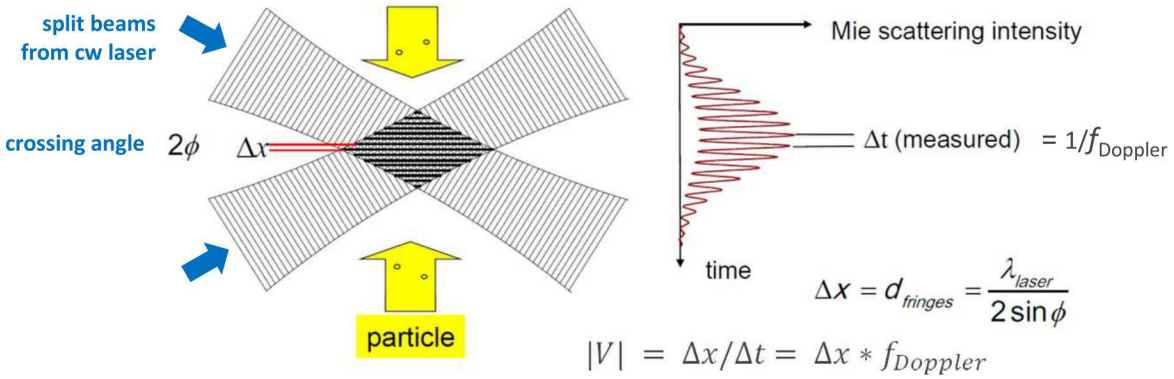

- Component of particle velocity magnitude normal to the stationary "fringes"
- How to resolve direction of flow?

Sandia National Laboratories

Laser Doppler anemometry (LDA)

- Frequency shift one of the beams using acousto-optic (Bragg) cell, 40 MHz

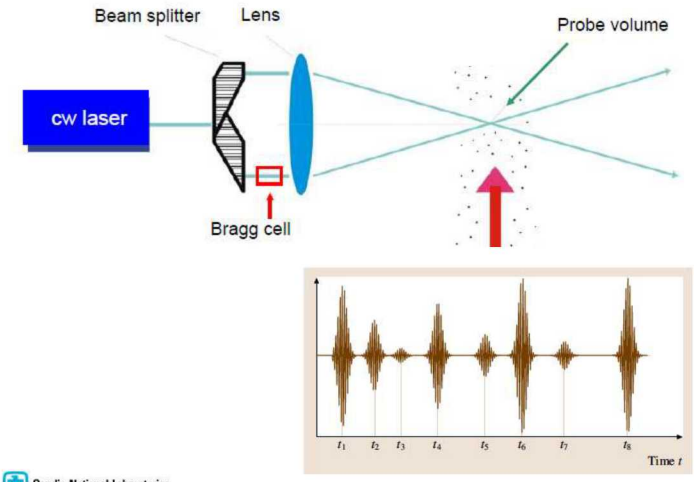

Burst series after high-pass filter

Make "fringes" sweep against the main flow (-40 MHz*Δx); spectrum analyzer subtracts this off.

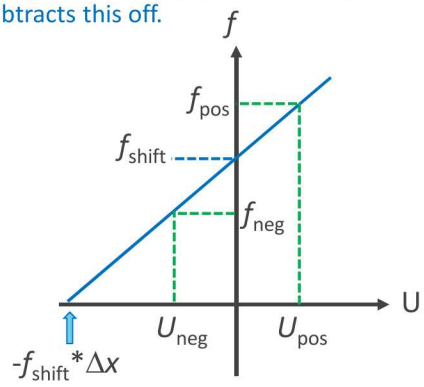

Laser Doppler anemometry (LDA)

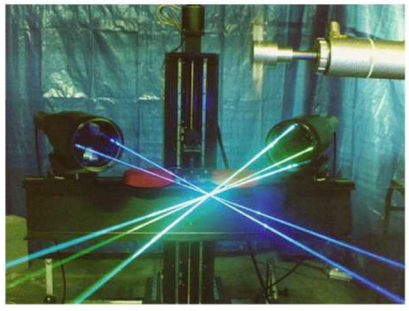

- Three component system uses three colors from cw Ar ion laser (**476.5**, **488.0**, **514.5** nm) or separate diode-pumped solid state lasers (DPSS):

- Commercial systems
  - Fiber optics; easy alignment
  - Analysis software available
- Considerations
  - Backscatter is convenient
  - Off-axis or side scatter is better
    - much smaller probe volume
    - important for high-gradients
    - important for u'v'; time-space coincidence
  - All flow streams should be seeded
  - Proper weighting to avoid velocity bias (not covered here)
  - Particles don't always track the flow (covered after PIV, wOFV, Tomo-PIV)

Particle Image Velocimetry (PIV)

One camera, two components

- "PIV laser" = two Nd:YAG lasers in one box, ΔT between pulses
- CCD up to 29M pixels
- CMOS for high-speed
- Cross correlation of small overlapping windows (16x16 or 32x32 pixels) gives "best" velocity for that window; sub-pixel accuracy
- Optimization of particle density and Δt can be tricky
- Methods for correcting "bad" vectors often need to be applied
- For 2D, 2-component one can calculate vorticity, strain rate, …

Particle Image Velocimetry (PIV)

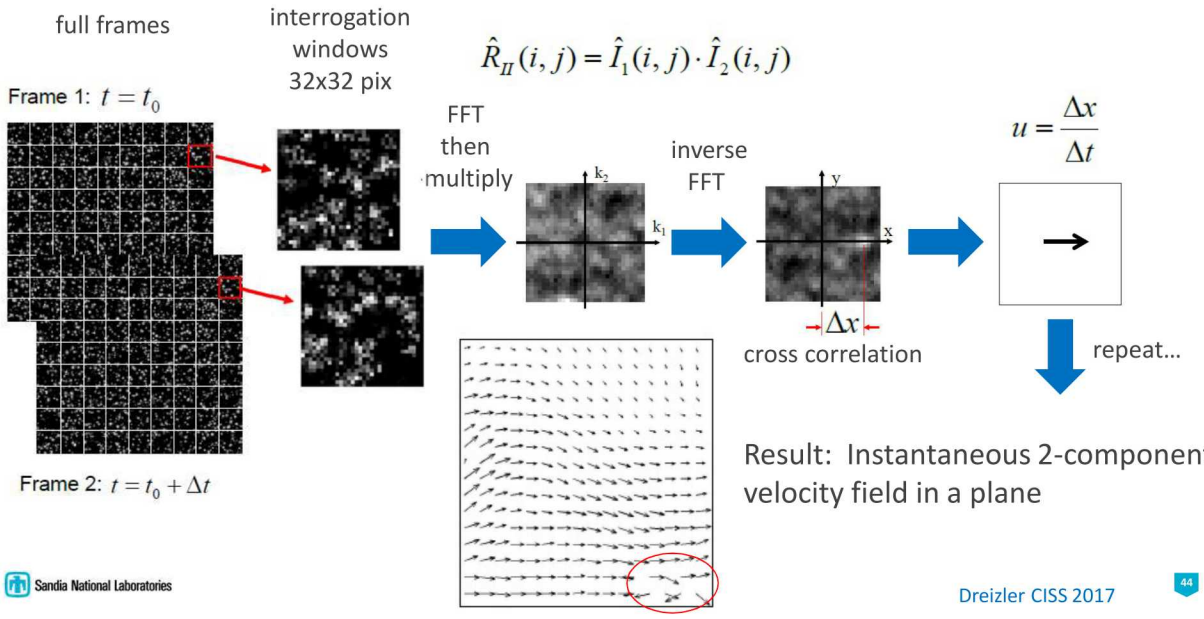

Result: Instantaneous 2-component velocity field in a plane

Stereo PIV

2 cameras, 3 velocity components (u,v,w)

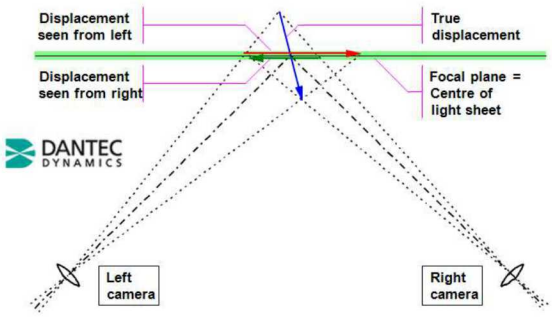

True 3D displacement (Δ X, Δ Y, Δ Z) is estimated from a pair of 2D displacements (Δ x, Δ y) as seen from left and right camera respectively

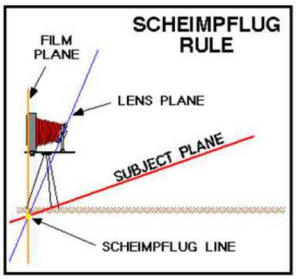

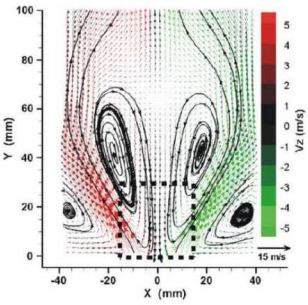

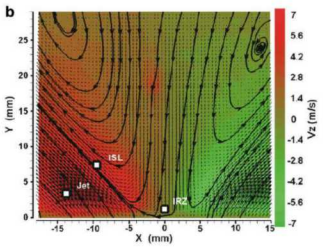

Sandia National Laboratories

Boxx et al., *Combust. Flame* (2010)

45

Wavelet-Based Optical Flow Velocimetry (wOFV)

wOFV slides from Jeff Sutton, OSU

PIV is the most utilized (and *de facto*) measurement technique. It is well established and straight forward to implement. However, PIV uses statistical correlation techniques to estimate the local velocity which yields a "non-dense" solution (i.e., one velocity vector per interrogation window). This greatly limits the spatial resolution, which can result in significant error in high-gradient regions and estimation of derivative quantities.

- Wavelet-based optical flow velocimetry (wOFV)[1,2] is an approach that shows significant promise for accurately estimating velocity in turbulent flows with increased resolution and accuracy
- Assuming stable lighting conditions and conservation of image intensity or "brightness":

$$\frac{\partial I\left(\underline{x},t\right)}{\partial t}+\underline{v}\left(\underline{x},t\right)\cdot\underline{\nabla}I\left(\underline{x},t\right)=0$$

- If the velocity is constant between I_o and I_1, the equation is integrated to yield the displace frame difference (DFD) equation:

$$I_0\left(\underline{x}\right)-I_1\left(\underline{x}+\underline{v}\left(\underline{x}\right)\right)=0$$

Sandia National Laboratories

[1] Dérian, P., et al., *Numerical Mathematics: Theory, Methods and Applications* 6.1 (2013): 116-137.
[2] Schmidt, B. E., Sutton, J.A., *Experiments in Fluids* 60.3 (2019): 37.

46

Wavelet-Based Optical Flow Velocimetry (wOFV)

wOFV slides from Jeff Sutton, OSU

- The velocity field is estimated from the DFD equation by forming a minimization problem

$$\underline{\hat{v}} = \underset{\underline{v}}{\operatorname{argmin}} \; J_D\left(I_0, I_1, \underline{v}\right) + \lambda J_R\left(\underline{v}\right)$$

- Problem is under-constrained; reduce the number of unknowns using wavelets. The formulation described in [2] is a multi-resolution strategy that is not sensitive to individual pixel intensity
- Goal: Find the velocity field that transforms particle image $I(t)$ to $I(t+\Delta t)$

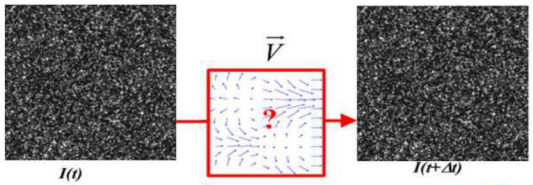

Barlow: "Be wary of this! It can be useful only if effects of out-of-plane motion can be eliminated."

Example concept for estimating velocity from particle images; wOFV also can be applied to scalar fields[3]

[2] Schmidt, B. E., Sutton, J.A., *Experiments in Fluids* 60.3 (2019): 37.
[3] Schmidt, Bryan E., et al. "Evaluation of wavelet-based optical flow velocimetry from OH scalar fields in reacting turbulent flows." *AIAA Scitech 2019 Forum*. 2019.

Sandia National Laboratories

47

Wavelet-Based Optical Flow Velocimetry (wOFV)

wOFV slides from Jeff Sutton, OSU

- Test case: 2D DNS (Sc = 0.7, Re = 3000 isotropic turbulence)[2,4]

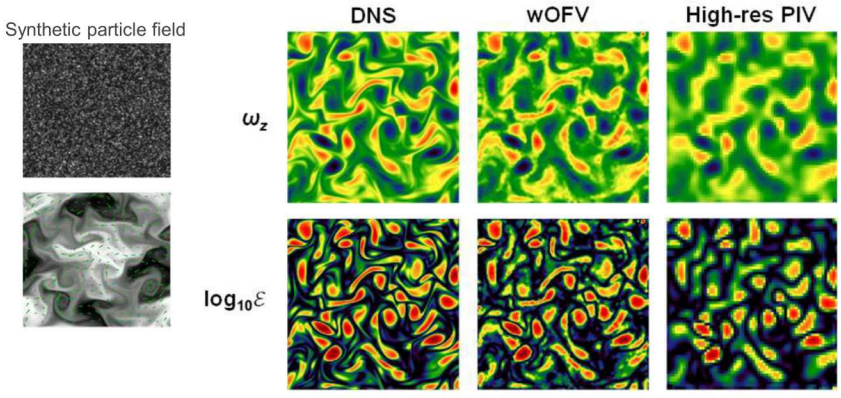

- Velocity accuracy is greatly improved; error is 1/4th that of correlation-based PIV
- Significant improvements in vorticity and enstrophy (ω_z^2) estimations!

[2] Schmidt, B. E., Sutton, J.A., *Experiments in Fluids* 60.3 (2019): 37.
[4] Schmidt, B.E., Sutton, J.A., "Improvements in the accuracy of wavelet-based optical flow velocimetry using an efficient and physically based implementation of velocity regularization", to be submitted, *Experiments in Fluids, 2019.*

Sandia National Laboratories

48

Wavelet-Based Optical Flow Velocimetry (wOFV)

wOFV slides from Jeff Sutton, OSU

- Test case: Michigan Hi-Pilot burner[5,6] (Re_T = 8000)

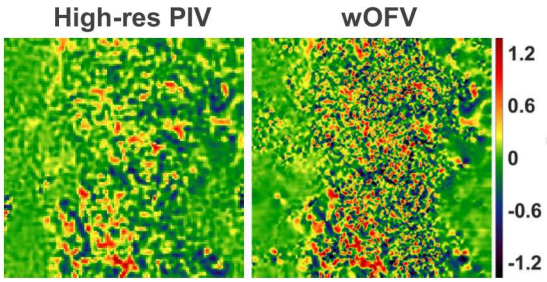

turbulent 1D energy spectrum

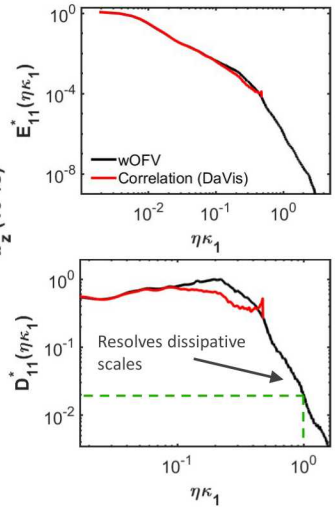

- Velocity measurements resolve dissipation length scales based on measured dissipation spectrum.

Sandia National Laboratories

[5]Wabel, T. M., et al., *Proceedings of the Combustion Institute* 36.2 (2017): 1809-1816.
[6]Schmidt, B.E., et al., "High resolution velocimetry in turbulent premixed flames using a wavelet-based optical flow technique", 11th U.S. National Combustion Meeting, Pasadena, CA, March, 2019

49

Tomographic PIV

- Slab of a few mm thickness
- 4 high-speed cameras
- Tomographic reconstruction
- 3 components in 3D
- Temporal evolution (4D)

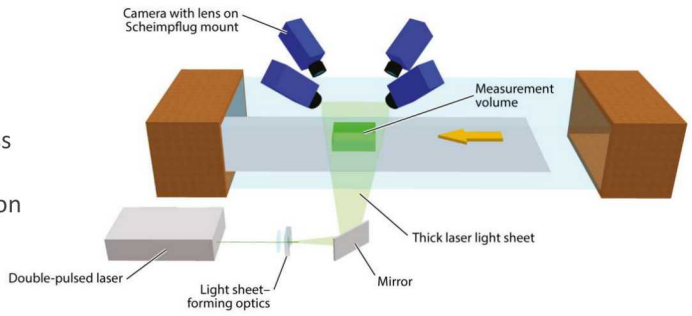

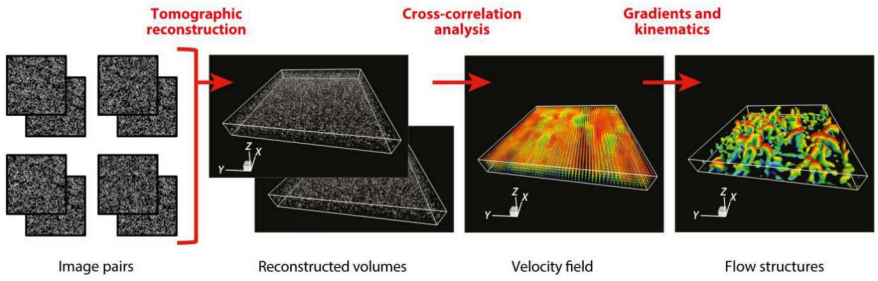

Sandia National Laboratories

Westerweel J, et al. 2013. Annu. Rev. Fluid Mech. 45:409–36

Application example: Tomo-PIV of in-cylinder engine flow

TECHNISCHE UNIVERSITÄT DARMSTADT

- Illumination
  - Dual-cavity laser (PIV400, Spectra Physics)
  - Avg. 375 mJ per single pulse
  - Phase-locked acquisition during intake and compression (<5 Hz)
  - Volume of: 48 x 35 x (4 or 8) mm

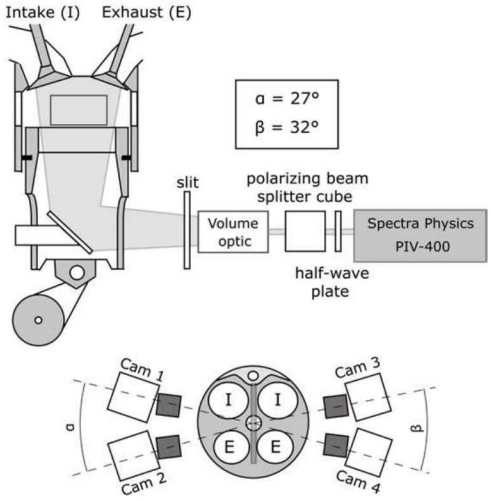

- Detection
  - Interline transfer CCD (ImagerIntense, LaVision, 1376x1040 pixels)
  - Nikon 50 mm, 1.4 (f# 16)
  - Limitation of Camera angles due to cylinder head bolts

Sandia National Laboratories

51

Application example: Tomo-PIV of in-cylinder engine flow

TECHNISCHE UNIVERSITÄT DARMSTADT

- Tomo-PIV processing using DaVis 8.1
- Image pre-processing
  - Subtract sliding average (3px)
  - Local intensity normalization
  - Gaussian smoothing
  - Sharpening filter
- MART Reconstruction (multiplicative algebraic reconstruction technique)

Raw image (270° bTDC)

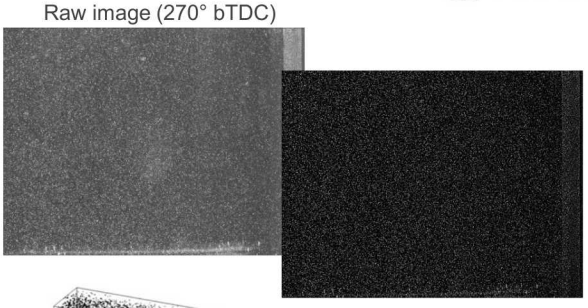

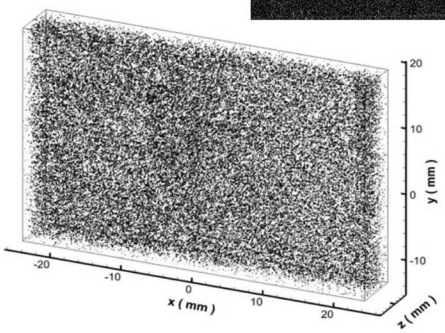

0.04 - 0.05 ppp

Sandia National Laboratories

52

Application example: Tomo-PIV of in-cylinder engine flow

TECHNISCHE UNIVERSITÄT DARMSTADT

- Volume correlation (Finale size)
  - 4mm: 48x48x48 pixel (0.4mm/vector)
  - 8mm: 64x64x64 pixel (0.6mm/vector)
- Post-processing
  - Outlier detection (Neighborhood operation)
  - Gauss smoothing

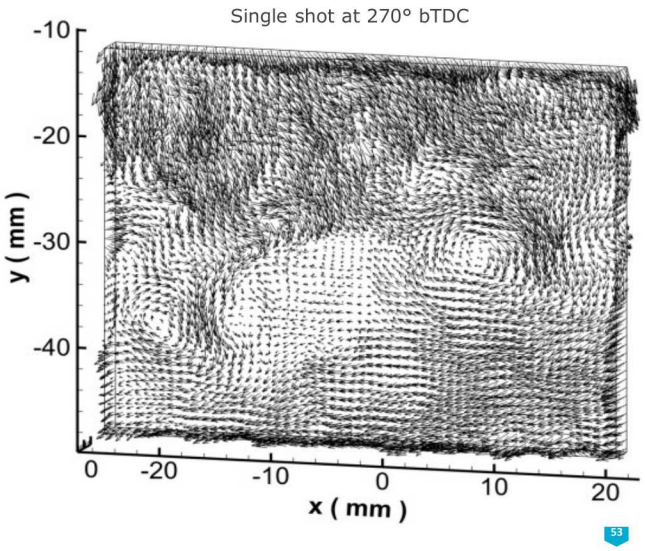

Sandia National Laboratories

53

Application example: Tomo-PIV of in-cylinder engine flow

TECHNISCHE UNIVERSITÄT DARMSTADT

- Iso-surface of average velocity magnitude during intake stroke (270° bTDC)

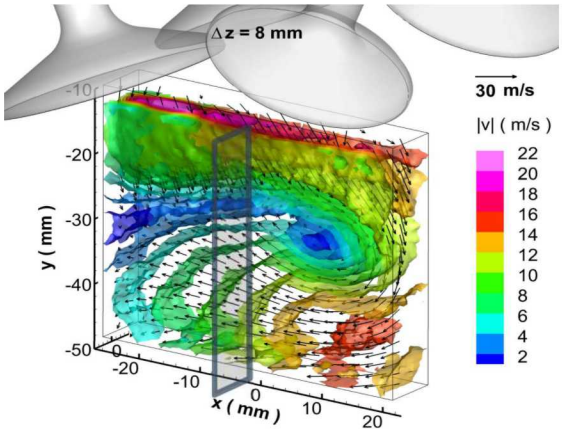

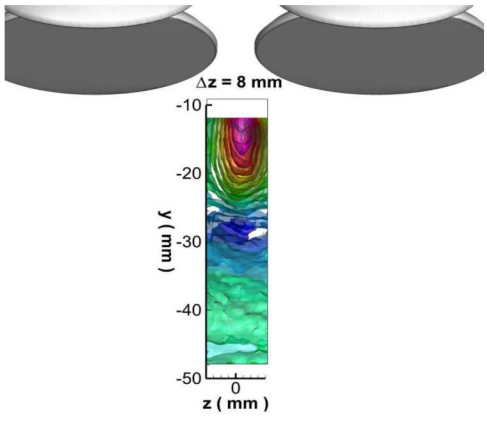

Piston at -51mm

Average over 300 cycles

Sandia National Laboratories

54

High-Speed 3D LIF and Velocity Measurement Capability

Raster scanning of laser sheet
10 kHz duty cycle (1 sweep = 100 us)

acousto-optic deflector cylindrical lens

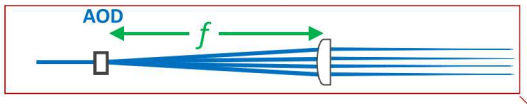

parallel sheets

Pulse Burst + TPIV laser systems

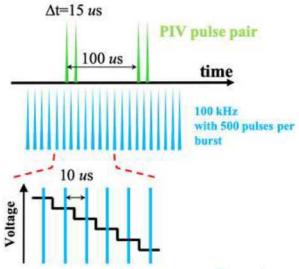

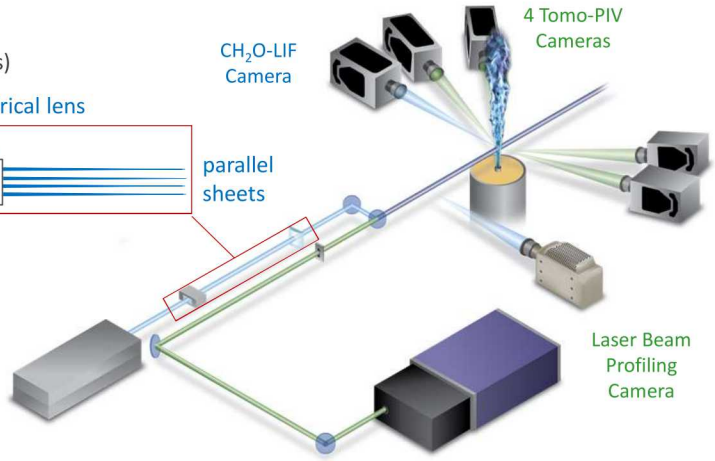

Sandia National Laboratories

Courtesy of Jonathan Frank (not yet published)

CRF

TECHNISCHE UNIVERSITÄT DARMSTADT

55

High-Speed 3D LIF and Velocity at Base of Lifted Jet Flame

Lifted Dimethyl Ether(DME)/Air Jet Flame

102 mm

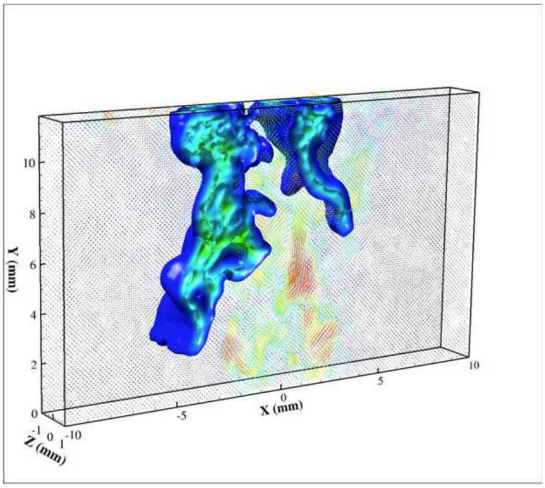

Sandia National Laboratories

Courtesy of Jonathan Frank (not yet published)

CRF

TECHNISCHE UNIVERSITÄT DARMSTADT

56

Particle-based velocity measurements

- Seeding material for turbulent flames
  - Chemically inert
  - Melting point above flame temperatures
  - Small enough to follow the flow (~1 μm typ)

Material	ρ_p (kg/m³)	Melt (K)
MgO	3500	2800
$ZrSiO_4$	3900-4700	2420
TiO_2	4000	1780

$$s = \left|\frac{u_f - u_p}{u_f}\right| < 1\% \qquad \tau_0 = \frac{\rho_p d_p^2}{18\mu} \qquad \mu = \text{dynamic viscosity}$$

  - Cut-off frequency exceeding 1% slip

$$f_c = \frac{\sqrt{(2s - s^2)}}{2\pi\tau_0\sqrt{(1-s^2)\left(1+\frac{\rho_f}{2\rho_p}\right)^2 - \left(\frac{3\rho_f}{2\rho_p}\right)^2}}$$

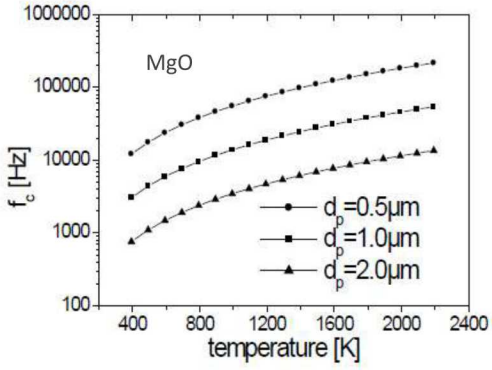

Sandia National Laboratories

Dreizler CISS 2017

Particle-based velocity measurements

- All gas feeds should be seeded, **otherwise results can be biased**
- Volume fraction of seed material must be **adjustable for each flow**
  - Bypass, controlled and variable mass flow
  - Appropriate assembly for addition of seed ("particle seeder")

rotating brush

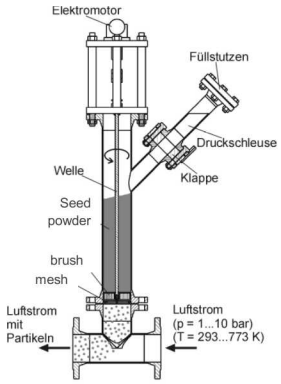

fluidised bed

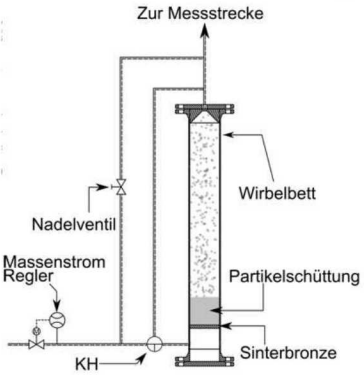

Sandia National Laboratories

Dreizler CISS 2017

58

Summary on velocity measurements

- LDA and PIV are complementary diagnostics for turbulent flames
- LDA is preferred (by some) for single-point statistics of turbulence (validation data)
- PIV has obvious advantages w.r.t. spatially and temporally correlated information (structure and dynamics) and combinations with scalar diagnostics, especially PLIF
- wOFV data processing approach to achieve better spatial resolution
- Other particle or drop methods
  - Phase Doppler anemometry (PDA) is like LDA for velocity of droplets but also gets (spherical) drop size
  - Shake the Box is a 3D (4D) particle tracking approach with 4 cameras (as for TomoPIV)
- Molecular methods (for places where particles can't go, e.g., high speed test facilities)
  - Narrowband Rayleigh; Doppler shift in scattered light changes throughput of molecular filter
  - TDLAS from two directions; doppler shift of absorption wavelength (Hanson et al., CISS 2018 lecture 9 notes)
  - Flow tagging; photodissociation in a grid of pulsed laser lines, followed by PLIF after ΔT (Miles et al., Pitz et al.)
  - Thermal grating velocimetry; crossed lasers beams excite seed molecule, creates thermal grating (Ewart et al.)

Outline

Turbulent length scales and resolution requirements

- Some theory on nonreacting turbulent flow
  - Recall that resolving the dissipation scales was a highlight of the wOFV slides
- What are the turbulent energy and dissipation scales in a flame?
  - Velocity (turbulent kinetic energy)
  - Scalars (fluctuations in temperature, mixture fraction)
- What laser probe resolution is needed to measure scalar variance and dissipation accurately (*and what is scalar dissipation, anyway*?)
- Rayleigh scattering measurements of scalar energy and dissipation spectra and length scales in turbulent jet flames

What is scalar dissipation?

- Important in combustion theory:
  - Peters, Turbulent Combustion (2000)
  - Steady laminar flamelet equation, Z = mixture fraction
  - Scalar dissipation rate, χ (factor 2 not always included)

$$\frac{\varrho}{Le_i}\frac{\chi}{2}\frac{\partial^2\psi_i}{\partial Z^2}+\omega_i=0$$

$$\chi = 2D|\nabla Z|^2$$

- Turbulent non-premixed flames (analog of kinetic energy dissipation):
  - Instantaneous scalar dissipation (Favre fluctuation in Z)

$$\chi = 2D|\nabla Z''|^2$$

- Partially premixed flames:
  - Three dissipation terms arise if normalized progress variable is a function of mixture fraction

$$\chi_{ZZ} = 2D|\nabla Z''|^2 \qquad \chi_{Zc} = 2D(\nabla Z'' \cdot \nabla c'') \qquad \chi_{cc} = 2D|\nabla c''|^2$$

Bray, Domingo, Vervisch, Combust. Flame 141 (2005) 431–437

Length scales and velocity spectra (nonreacting turbulent jet)

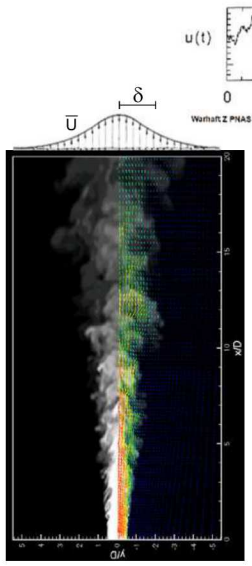

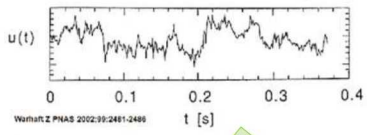

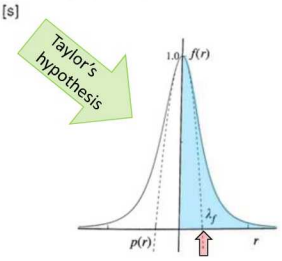

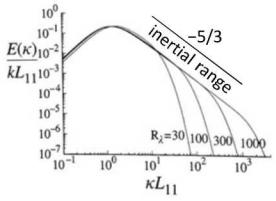

- Outer scale, δ = half width of the mean velocity profile
- Axial velocity fluctuations in the far field
- Longitudinal autocorrelation:
  Integral scale, L_{11} = area under curve
  Taylor scale, λ = intersection of parabola fitting the autocorrelation curve
- Model spectrum from Pope is consistent with experiments in a wide range of nonreacting turbulent flows,
  $Re_\lambda = u\lambda/\nu$ is a parameter

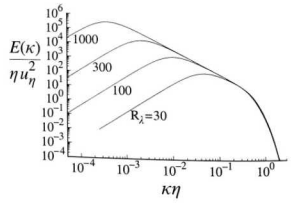

$k = \frac{1}{2}(u^2+v^2+w^2)$
$\eta = (\nu^3/\varepsilon)^{1/4}$
$u_\eta = (\nu\varepsilon)^{1/4}$

Turbulent Flows, Steve Pope, Cambridge Univ Press, 2000 (Ch 6, Ch 6.5)

Model Energy and Dissipation Spectra (3D)

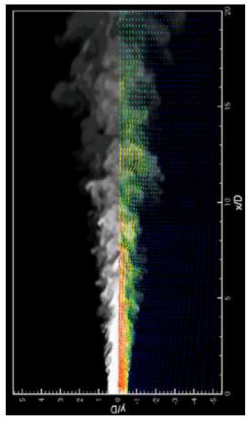

—— Re_λ = 1000
- - - Re_λ = 30

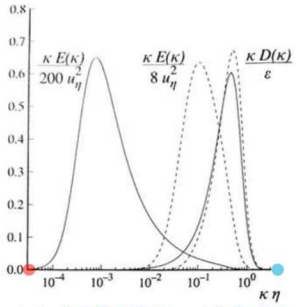

Cumulative kinetic energy and dissipation

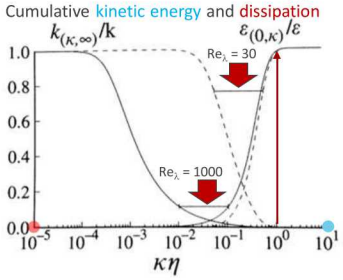

- At high Re_λ there is "separation of scales"
- At low Re_λ energy and dissipation spectra overlap
- Dissipation cutoff scale $\kappa\eta = 1$. Corresponding wavelength $\lambda_c = 2\pi\eta$

Turbulent Flows, Steve Pope, Cambridge Univ Press, 2000 (Ch 6, Ch 6.5)

Smallest Length Scales of Turbulence

Velocity: Kolmogorov scale, η

$$\eta = \left(\nu^3 / \langle\varepsilon\rangle\right)^{1/4}$$

- ν: kinematic viscosity
- $\langle\varepsilon\rangle$: mean rate of kinetic energy dissipation

Scalar: Batchelor scale, λ_B

$$\lambda_B = \left(\nu D^2 / \langle\varepsilon\rangle\right)^{1/4} = \eta\, Sc^{-1/2}$$

- D: mass diffusivity
- Sc: Schmidt number, $Sc = \nu/D$

- For gaseous flows and flames: $Sc \sim 1$ then $\eta \sim \lambda_B$
- Nonreacting jets (centerline, far field): $\lambda_B = 2.3\,\delta\,\mathrm{Re}_\delta^{-3/4}\,Sc^{-1/2}$
- Determined by local flow properties → ***How to estimate in flames?***

Sandia National Laboratories

65

Spatial Resolution Requirements: Nonreacting Flows

How much of the scalar (temperature) variance and dissipation are captured with a given probe resolution or sampling frequency?

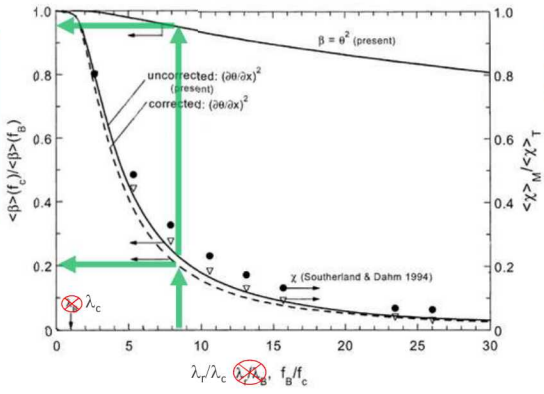

Passive Scalar Mixing (slightly heated air jet)

Mi & Nathan, Exp. Fluids, 2003
(see also Pitts et al., NISTIR 6393, 1999)

Fig. 2. Effect of probe spatial resolution on measurements of several scalar properties in the far field of a turbulent circular jet. Variances of the measured scalar fluctuation θ and its streamwise derivative $\partial\theta/\partial x$ for the present investigation (Re_j=180) were obtained from spectra (Φ_θ, $\Phi_{\partial\theta/\partial x}$) of θ low-pass-filtered at different cutoff frequencies f_c. The mean scalar dissipation rates (●, Re_j=32; ∇, Re_j=45) were measured at different spatial resolution scales λ_r by Southerland and Dahm (1994). The symbol λ_B denotes the Batchelor length scale

- Resolution capturing 95% of scalar variance only resolves 20% of dissipation
- Error in this and several other experimental papers has been to miss the factor 2π, so the label λ_B here should actually be λ_c, the dissipation cutoff scale, based on comparison with Pope's model spectrum

Sandia National Laboratories

66

Experimental Approach (UT Austin and Sandia)

- Use Rayleigh scattering to investigate scalar structure of turbulent flames
  - High SNR
  - Good spatial resolution

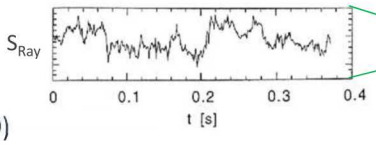

- $CH_4/H_2/N_2$ jet flames: DLR-A (Re_d = 15,200)
  DLR-B (Re_d = 22,400)
- Nearly constant Rayleigh cross section throughout flame, $\pm 3\%$
  (neglecting effects of differential diffusion, not OK near the nozzle)
- Measure energy and dissipation spectra of temperature fluctuations
- Compare to 1D form of model spectrum (Pope, Turbulent Flow, Ch 6.5)

Rayleigh scattering

- Not a laser spectroscopic method, but often applied in combination with spectroscopic methods
- Elastic scattering from all species in the laser probe volume
- Rayleigh signal:

$$S_{Ray} = C_{calib} I_{laser} NV \sum_i \boldsymbol{X_i \sigma_i}$$

(effective Rayleigh cross section)

$NV =$ (number density)(probe volume)
$X_i =$ mole fraction, $\sigma_i =$ Rayleigh cross section

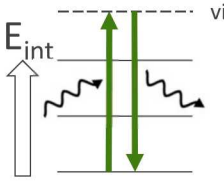

- Perfect gas law: $PV = nRT$ so $T \propto 1/S_{Ray}$
- For constant pressure and probe volume size; calibrate in room air

$$T_{Ray} = T_{air} \left(\frac{S_{air}/I_{air}}{S_{Ray}/I_{Ray}} \right) \left(\frac{\boldsymbol{\sigma_{eff}}}{\sigma_{air}} \right)$$

- Need to estimate or measure species mole fractions to measure T

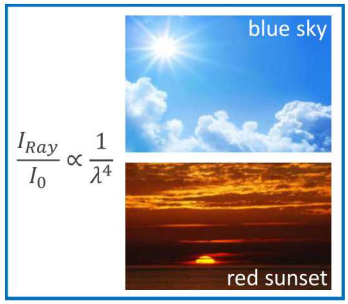

Rayleigh scattering

- For turbulent premixed flames, a laminar flame calculation can give an good estimate of $\sigma_{Ray}(T)$, then local temperature can be solved iteratively
- "Designer fuels" for non-premixed flames have small variation in σ_{Ray}, e.g., DLA-A,B flames ($CH_4/H_2/N_2$)
- These estimates are based on assumption about molecular diffusion (Le = 1 or Le = Le_i)
- Combine with Raman for accurate Rayleigh temperature measurements in flames
- Background measurement and subtraction is very important for 2D imaging;
- See Ruggles, Exp Fluids (2015) 56:202 and Frank & Kaiser, Exp Fluids (2008) 44:221 for examples of careful Rayleigh scattering experiments

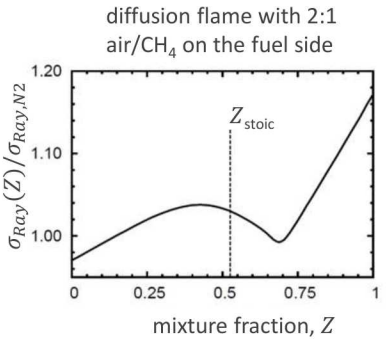

species	σ/σ_{N2}
N_2	1.0
O_2	0.846
CH_4	2.16
CO_2	2.32
H_2O	0.711
CO	1.25
H_2	0.216
He	0.013

Thermal dissipation by Rayleigh thermometry

- Wang et al. (UT Austin)
- High rep rate laser (72 W, 532 nm) → Time series of temperature

- 10 kHz sampling rate
- Optical resolution, 0.3 mm
- Redundant measurement, using two PMT's for the same focal volume
- $CH_4/H_2/N_2$ jet flame (DLR-A)
  Re = 15200
  d = 7.8 mm

Wang, Clemens, Varghese, *Proc. Combust. Inst.* 29 (2005)
Wang, Clemens, Varghese, Barlow, *Combust. Flame* 152 (2008)

Energy and dissipation spectra along centerline

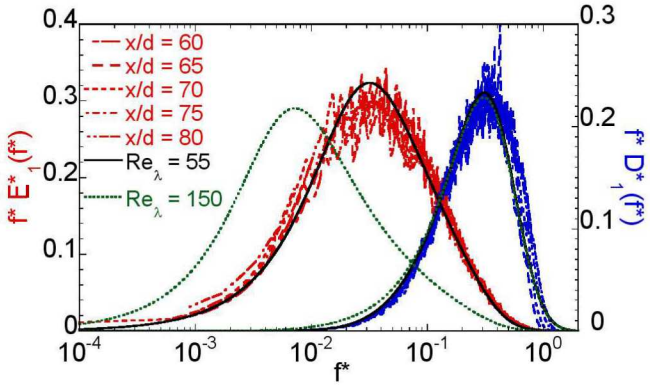

- Energy and dissipation spectra collapse at all downstream locations when scaled by Batchelor frequency ($f^*=f/f_B$)
- Good agreement with Pope model spectra using $50 < Re_\lambda < 60$
- Limited separation of scales for this Re_d = 15,200 flame

Sandia National Laboratories

Wang et al., *Combust. Flame* 152 (2008) 317-335

THE UNIVERSITY OF TEXAS AT AUSTIN

71

Effect of degrading resolution

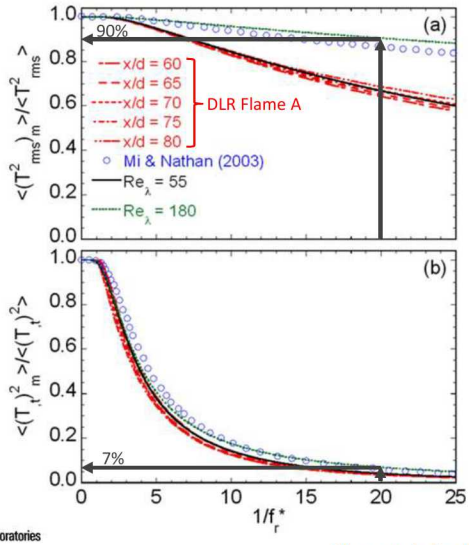

- Relative resolution = 1 to fully resolve temperature dissipation
- Variance curves:
  - Depend on Re_λ
  - Range of Re_λ consistent with local T

Scaling law for nonreacting jets

$$\lambda_B = 2.3\,\delta\,\mathrm{Re}_\delta^{-3/4}\;Sc^{-1/2}$$

- Dissipation curves:
  - Flame results agree well with model
  - Initial roll-off has little Re dependence

Sandia National Laboratories

Wang et al., *Combust. Flame* 152 (2008) 317-335

THE UNIVERSITY OF TEXAS AT AUSTIN

72

Aside: How to estimate fully-resolved scalar variance from under-resolved measurements, e.g., at high pressure

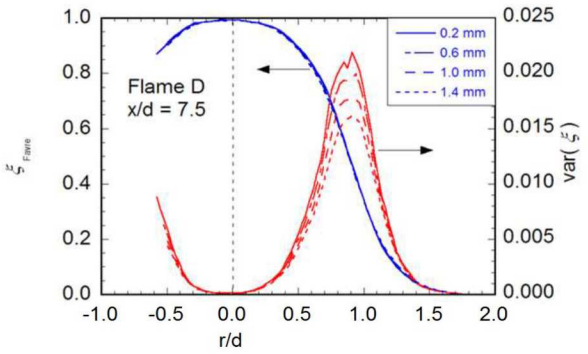

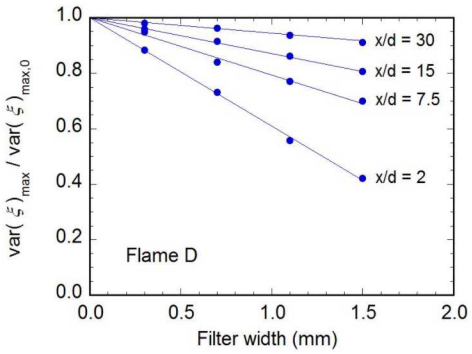

- Apply successive spatial filter to degrade resolution
- Near-linear behavior for filtered scalar variance
- Extrapolate to zero filter width
- Useful for high Re and high P flames where scales are very small

Sandia National Laboratories

Barlow & Karpetis, *FTC* 72 (2004) 427–448

73

Dissipation spectra from ensemble of 1D segments

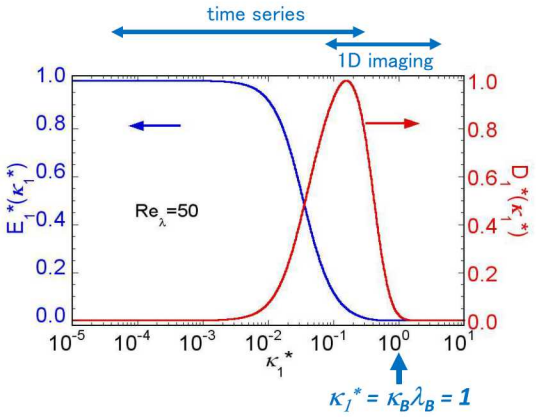

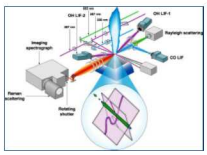

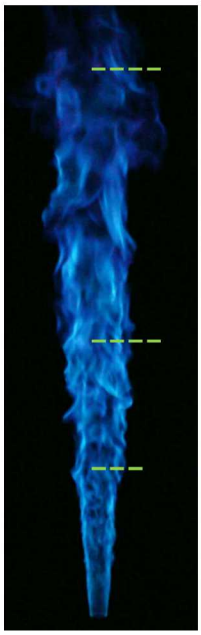

- Model 1-D dissipation spectrum (Pope, *Turbulent Flows*, 2000)
- $\kappa^*_1 = 1$ corresponds to ~2% of peak dissipation value, $\lambda_B = 1/\kappa_B$
- Physical wavelength is $2\pi\lambda_B$; Nyquist → ~$3\lambda_B$ for spectrally sharp filter; (commonly used central difference filter is not spectrally sharp)

Sandia National Laboratories

74

Dissipation cutoff scale in non-reacting C_2H_4 jets

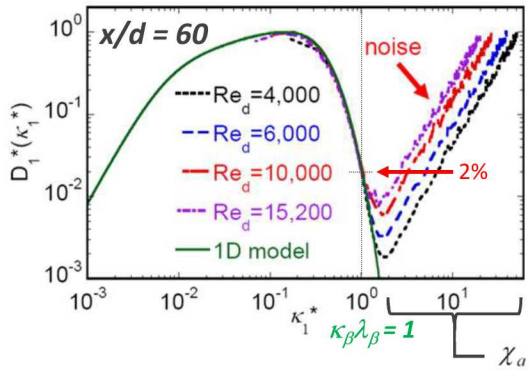

$$\chi_a = 4D_\xi \frac{\sigma_\xi^2}{2\Delta r^2}$$

"apparent dissipation"

- Demonstrate that the approach works in a non-reacting jet before trying it in a flame
- C_2H_4 density ~same as air
- Mixture fraction, ξ, from S_{Ray}
- "Apparent dissipation" due to noise

Scaling law for nonreacting jets

$$\lambda_B = 2.3\,\delta\,\mathrm{Re}_\delta^{-3/4}\,Sc^{-1/2}$$

Re_d	4,000	6,000	10,000	15,200	
λ_B (μm)	370	270	185	135	← Estimated using scaling law
λ_β (μm)	324	250	172	128	← Exp. determined (2% cutoff)

Sandia National Laboratories

75

Normalized 1-D "thermal dissipation" spectra

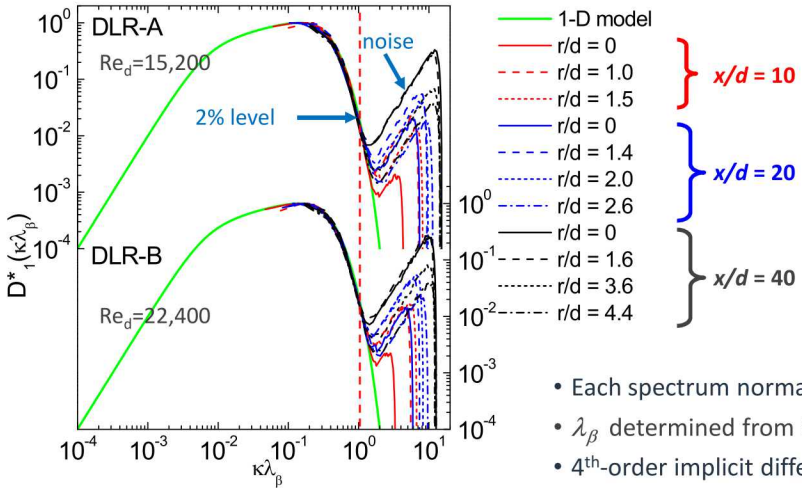

Gradient squared of fluctuations in $1/S_{ray}$

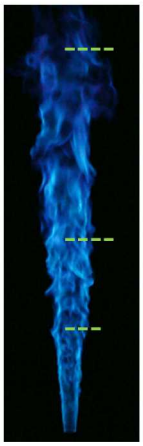

- Each spectrum normalized by its peak value
- λ_β determined from 2% of the peak
- 4th-order implicit differencing stencil (Lele, 1992)
- Cutoff scale for mixture fraction dissipation is equal or larger

Sandia National Laboratories

Wang et al., Combust. Flame 148 (2007) 62–75

76

Highly-resolved planar Rayleigh imaging

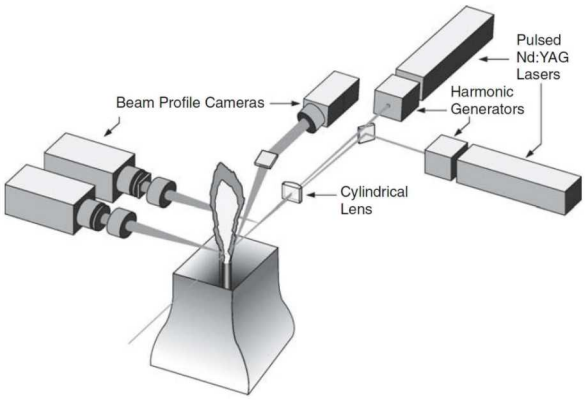

- Highly-resolved 2D Rayleigh imaging
- Structure of dissipation layers

Sandia National Laboratories

S.A. Kaiser, J.H. Frank, *Proc. Combust. Inst*. 31 (2007); J.H. Frank, S.A. Kaiser, *Exp. Fluids*. (2008)

77

Highly-resolved planar Rayleigh imaging

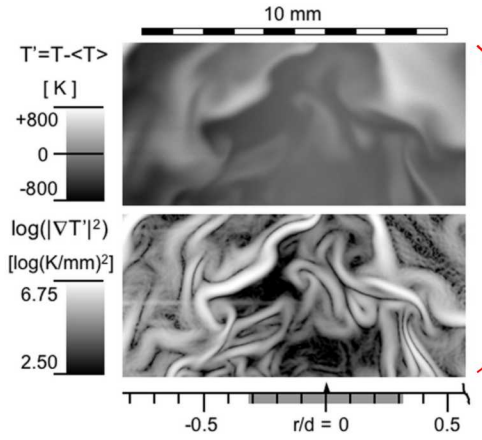

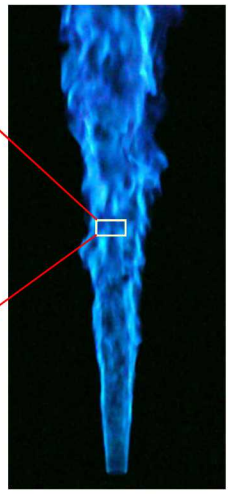

DLR-A, $CH_4/H_2/N_2$
Re = 15,200
x/d = 10

- Structure of temperature dissipation layers

Sandia National Laboratories

S.A. Kaiser, J.H. Frank, *Proc. Combust. Inst*. 31 (2007); J.H. Frank, S.A. Kaiser, *Exp. Fluids*. (2008)

78

Highly-resolved planar Rayleigh imaging

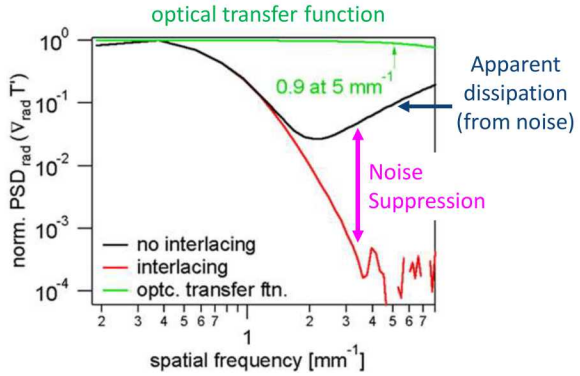

Interlacing for noise suppression

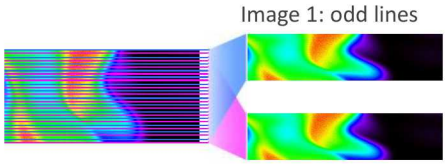

$$PSD_{rad} = \left| FFT\left(\partial T_1'/\partial r\right) FFT^*\left(\partial T_2'/\partial r\right) \right|$$

- Interlacing technique, or dual detectors (two PMT's), suppresses noise
- Power spectral density measured over three orders of magnitude (radial direction)

S.A. Kaiser, J.H. Frank, *Proc. Combust. Inst.* 31 (2007)

Comparison of 1D and 2D results from DLR flame A

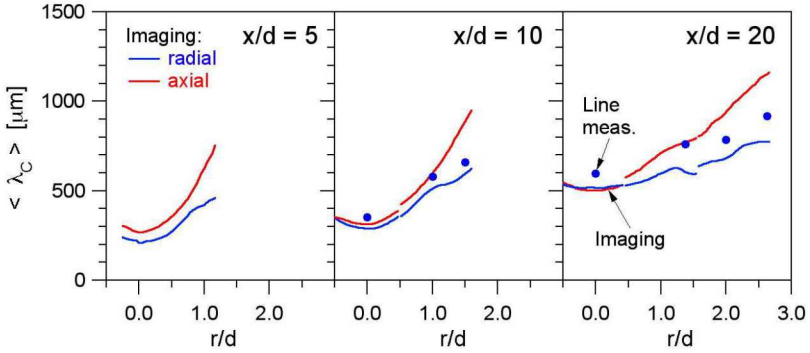

- Dissipation cutoff scale, $\lambda_c = 2\pi\lambda_B$ measured in radial and axial directions is ≥ 0.2 mm
- Nyquist sampling requires resolution of 0.1 mm
- Many lab-scale flames at modest Re can be fully resolved, at least in the high T regions
- For jet flames, use local mean T in estimating scales

$$\lambda_B = 2.3\,\delta\,\mathrm{Re}_\delta^{-3/4}\,Sc^{-1/2}$$

Outline

Coming up: Basics concepts of …

- Light-matter interaction
- Molecular spectroscopy
- Laser absorption
- Laser induced fluorescence
- Raman scattering

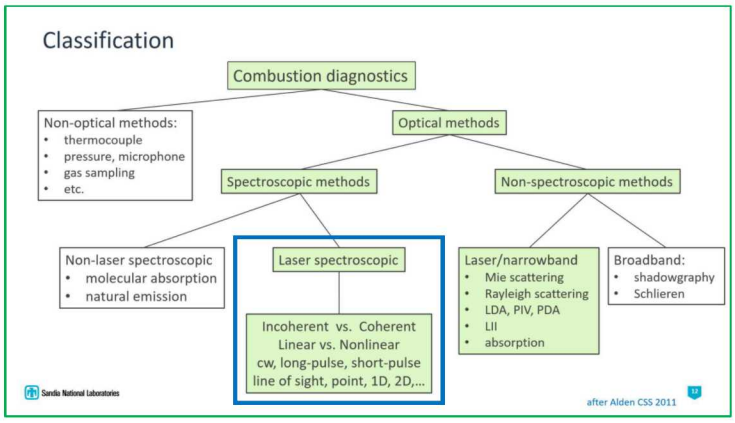

Light-matter interaction

- Absorption
- Emission

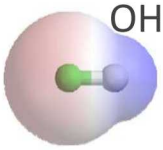

- Rayleigh scattering (elastic)

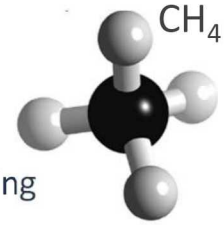

- Raman scattering (inelastic)
  - Stokes (red shift)
  - anti-Stokes (blue shift)

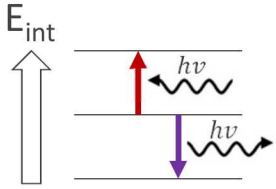

absorption

$\Delta E_{int} = h\nu = hc/\lambda_0$

$\Delta E_{int} = -h\nu = \quad /\lambda_0$

emission

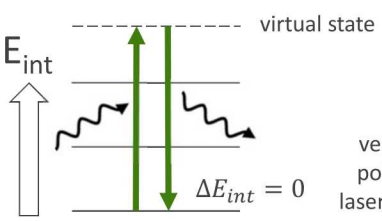

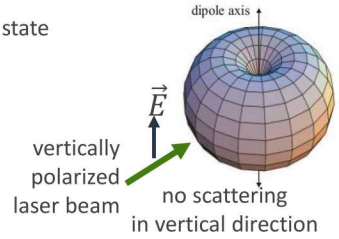

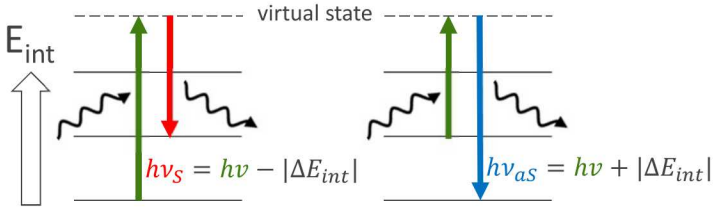

Sandia National Laboratories

Spectroscopy: Use emission or absorption of radiation to deduce properties of matter (in our case, gas-phase atoms and molecules)

Blue flame emission spectrum

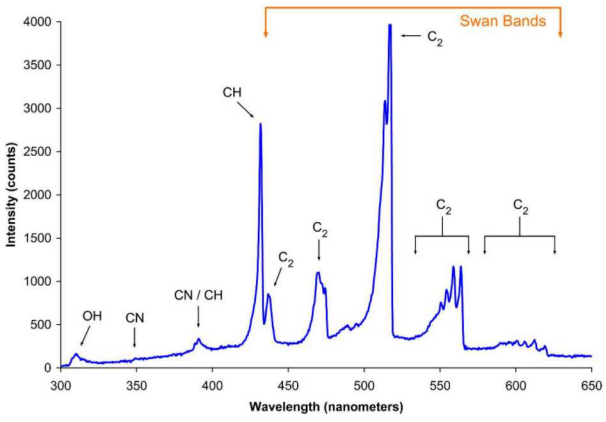

https://en.wikipedia.org/wiki/File:Spectrum_of_blue_flame.png

IR absorption spectra from HITRAN

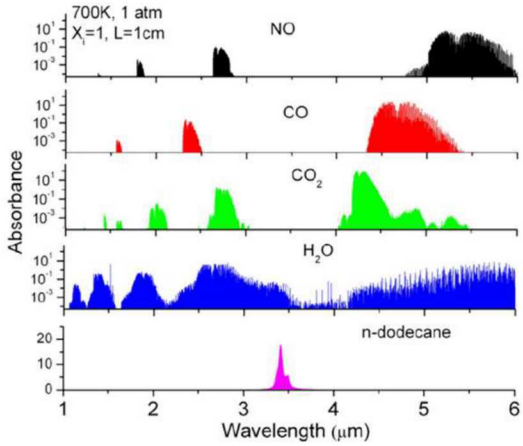

Hanson CISS 2018 Lecture 2

Sandia National Laboratories

84

Internal energy levels of a molecule are determined by quantum mechanics

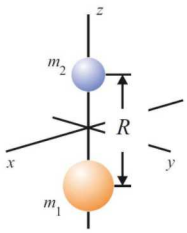

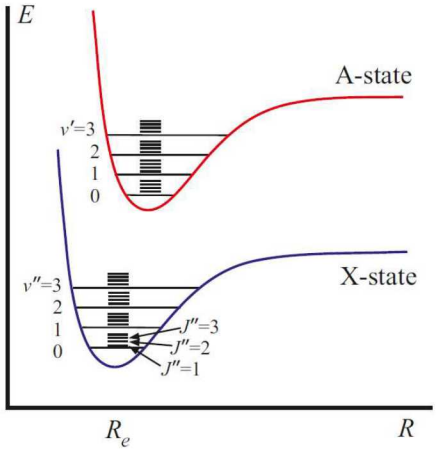

internuclear distance

- Internal energy
  $E_{int} = E_{elec} + E_{vib} + E_{rot}$
- Energy level differences
  $\Delta E_{elec} > \Delta E_{vib} > \Delta E_{rot}$
- Corresponding spectral regions
  UV-Vis IR μ-wave
- Quantum numbers
  - electronic *n*
  - vibrational *v*
  - rotational *J*

Energy levels for a rigid rotator

- Solutions to the Schrödinger equation for diatomic molecule with fixed bond length, r_0

rotational energy levels

$$E_J = \frac{h^2}{8\pi^2 I} J(J+1), \qquad J = 0,1,2,\ldots$$

moment of inertia

$$I = \mu r_0^2$$

reduced mass

$$\mu = \frac{m_1 m_2}{m_1 + m_2}$$

rotational energy levels in wavenumbers

$$F_J = \frac{E_J}{hc} = \frac{h}{8\pi^2 cI} J(J+1) = BJ(J+1) \quad [\text{cm}^{-1}]$$

rotational constant, B

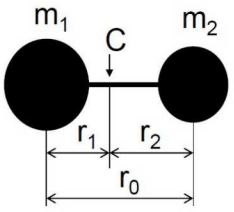

C – center of mass

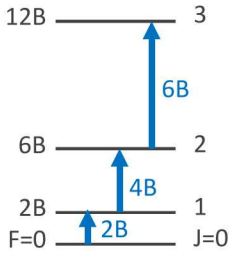

Energy levels for a rigid rotator

- Selection rule, $\Delta J = \pm 1$, so for absorption $\Delta J = +1$

$$F_J = BJ(J+1) \quad [\text{cm}^{-1}]$$

- Lines in rigid rotator absorption spectrum are evenly spaced (cm^{-1})

$$\bar{\nu}_{J'=1\leftarrow J''=0} = 2B(J''+1)$$

- $B_{CO} \sim 2\ \text{cm}^{-1} \Rightarrow \lambda_{J'=1\leftarrow J''=0} \sim 2.5\ mm$

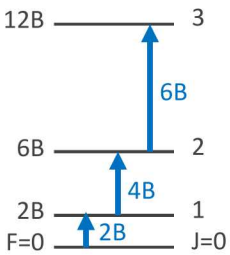

absorption spectrum for pure rotation

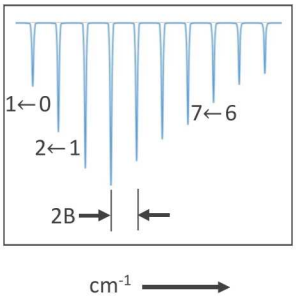

- Non-rigid rotator: add **centrifugal distortion term**, $F_J = BJ(J+1) - \boldsymbol{DJ^2(J+1)^2}$ …

- Interaction of light with a rotating dipole moment; only heteronuclear molecules

Vibrational-rotational (ro-vibrational) IR spectra

- Combine vibrational and rotational transitions (energies in the IR)

- Harmonic oscillator approximation (see Linne or Hanson for details, or Google)

- Total energy (vibration plus rotation)

$$T_{v,J} = G(v) + F(J)$$

$$T_{v,J} = \omega_e(v+1/2) - \underbrace{\omega_e x_e(v+1/2)^2}_{\text{first anharmonic correction}} + BJ(J+1) + \cdots$$

$$\omega_e = \nu/c\,, \qquad (cm^{-1})$$

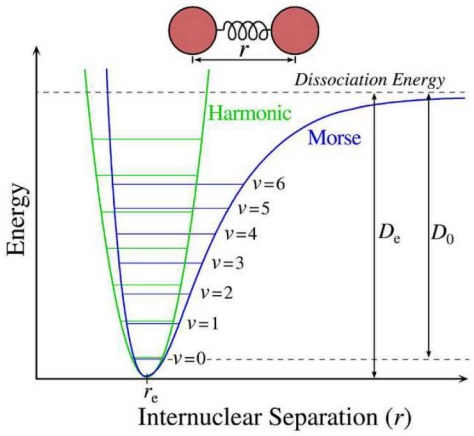

http://titan.physx.u-szeged.hu/~dpiroska/atmolfiz/molecular_structure_and_spectra.html

Ro-vibrational IR spectra

- Allow non-rigid rotation, anharmonic vibration, vib-rot interaction
- Total energy (vibration plus rotation)

$$T_{v,J} = \underbrace{\omega_e(v+1/2)}_{\text{simple harmonic oscillator}} - \underbrace{\omega_e x_e(v+1/2)^2}_{\text{first anharmonic correction}} + \underbrace{BJ(J+1)}_{\text{rigid rotator}} - \underbrace{D_V J^2(J+1)^2}_{\text{centrifugal distortion}}$$

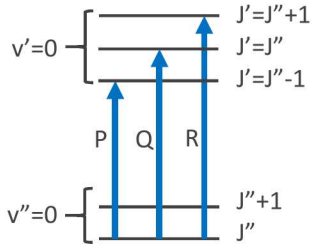

- Selection rule for electronic Σ state: $\Delta J = J' - J'' = \pm 1$; Otherwise: $\Delta J = 0, \pm 1$;
- Nomenclature for branches:

Branch	O	P	Q	R	S
ΔJ	-2	-1	0	+1	+2

NO spectrum centered near 5.35 μm, 1875 cm^{-1}

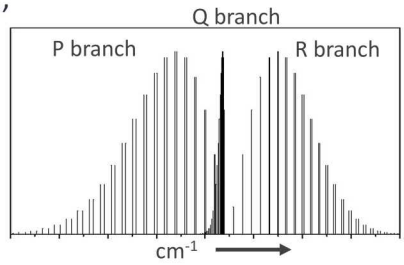

Sandia National Laboratories

Population distribution of internal energy states

- For a volume of gas in thermal equilibrium, the population distribution is given by Boltzmann statistics
- Boltzmann distribution function:
- $$f_{B,i} = \frac{N_i}{N} = \frac{g_i e^{(-E_i/kT)}}{\sum_j g_j e^{(-E_j/kT)}}$$

unique function of *T*

partition function, Q

where:

N = total number of molecules

g_i = degeneracy of level i

E_i = energy of level i

k = Boltzmann constant = 1.3806 × 10^{-23} m^2 kg s^{-2} K^{-1}

Sandia National Laboratories

90

Population distribution of rotational and vibrational energy states

- Internal energy: $E_{int} = E_{elec} + E_{vib} + E_{rot}$
- Partition function: $Q_{int} = Q_{elec}\, Q_{vib}\, Q_{rot}$

most relevant for combustion diagnostics

$$Q_{elec} = \sum_n e^{(-E_n/kT} \qquad Q_{vib} = \sum_v e^{(-E_v/kT} \qquad Q_{rot} = \sum_J g_I(2J+1)e^{(-E_J/kT)}$$

- "Boltzmann fraction" $f_{ro-vib} = f_v f_J = \frac{e^{(-E_v/kT)}}{Q_{vib}} \frac{g_I(2J+1)e^{(-E_J/kT)}}{Q_{rot}}$
- Equilibrium population fraction of molecules in a given ro-vibrational state before probing (ground state)

Population distribution of rotational and vibrational energy states

- As temperature increases, the population distribution shifts toward higher energy levels
- Basis for temperature measurements and quantitative species measurements

CO rotational line strength spectra (HITRAN) for absorption with vibrational transition 1←0

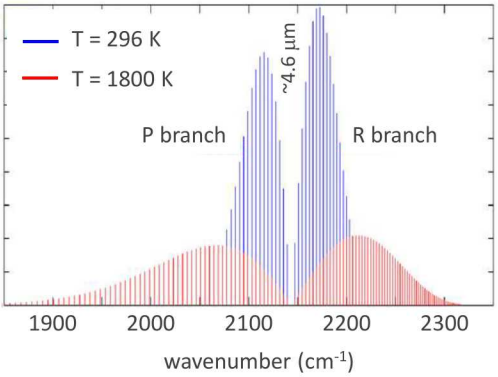

adapted from Bo Zhou MS thesis, Lund 2011

Calculated spontaneous Raman spectra of N2 at 300K up to 2400K

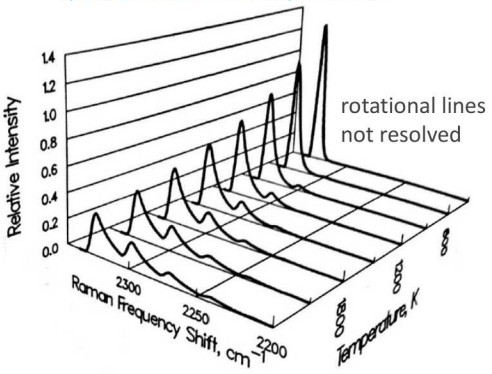

Eckbreth, Laser Diagnostics for Combustion Temperature and Species, 1996

HITRAN/HITEMP database

- Resource for IR spectroscopy data on gases relevant to atmospheric science and combustion
- https://hitran.org/

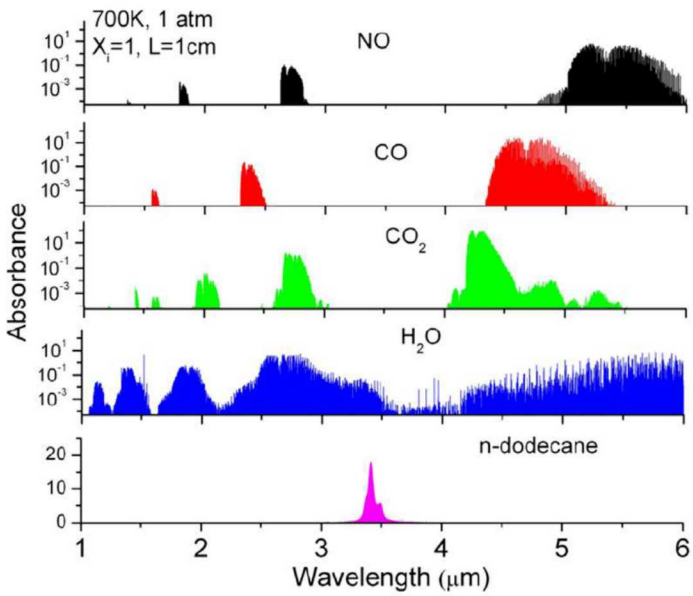

Sandia National Laboratories

Hanson CISS 2018 Lecture 2

93

Line broadening and line shapes

Absorption/emission lines are broadened mainly by two processes

- **Doppler broadening** (thermal broadening)
  - Gas molecules have a translational energy distribution that gets wider with increasing temperature
  - Movement toward (*away from*) the laser or detector shifts the light to higher (*lower*) frequency
  - Velocity distribution is Gaussian, so Doppler broadening produces a **Gaussian line function**

$$\phi_D(\nu) = \frac{2\sqrt{\ln 2}}{\sqrt{\pi}\Delta\nu_D}\exp\left[-\left(\frac{2\sqrt{\ln 2}}{\Delta\nu_D}(\nu-\nu_0)\right)^2\right]$$

$$\Delta\nu_D\ (\text{FWHM}) = 2\sqrt{\frac{2kT\ln 2}{mc^2}}\nu_0 = 7.17\times10^{-7}\nu_0\sqrt{T/M}$$

m particle mass
M g/mole of emitter/absorber
k Boltzmann constant
ν_0 center frequency

- **Collisional broadening** (pressure broadening)
  - Collisions between molecules perturb the radiative decay process, shortening the lifetime of the emitter
  - Uncertainty principle → shorter time, broader line
  - Time limiting process, **Lorentzian line function**:

$$\phi_C(\nu) = \frac{1}{\pi}\frac{\Delta\nu_C/2}{(\nu-\nu_0)^2+(\Delta\nu_C/2)^2}$$

$$\Delta\nu_C\ (\text{FWHM}) = 2P\sum_i X_i\gamma_{i,0}\left(\frac{T_0}{T}\right)^{n_i}$$

ν_0 center frequency
P pressure (atm)
X_i species mole fractions
$\gamma_{i,0}$ broadening coeff. at T_0 (cm^{-1} atm^{-1})
n_i temperature exponent

See Hanson CISS 2018 Lecture 6 for more details

Sandia National Laboratories

94

Line broadening and line shapes

Combine effects of collisional and Doppler broadening

- **Voigt profile**
  - Convolution of collisional (Lorentzian) and Doppler(Gaussian) line shape functions

$$\phi_V(\nu) = \phi_C(\nu) * \phi_D(\nu) = \int_{-\infty}^{\infty} \phi_C(u)\,\phi_D(\nu - u)\,du$$

$$\phi_V(\nu) = \underbrace{\left\{\frac{2\sqrt{\ln 2}}{\sqrt{\pi}\Delta\nu_D}\right\}}_{\phi_D(\nu_0)} \underbrace{\left\{\frac{a}{\pi}\int_{-\infty}^{\infty}\frac{\exp(-y^2)dy}{a^2+(w-y)^2}\right\}}_{\equiv V(a,w)}$$

Voigt function

$$a \cong \sqrt{\ln 2}\,(\Delta\nu_C/\Delta\nu_D)$$

$$w = 2\sqrt{\ln 2}\,(\nu - \nu_0)/\Delta\nu_D$$

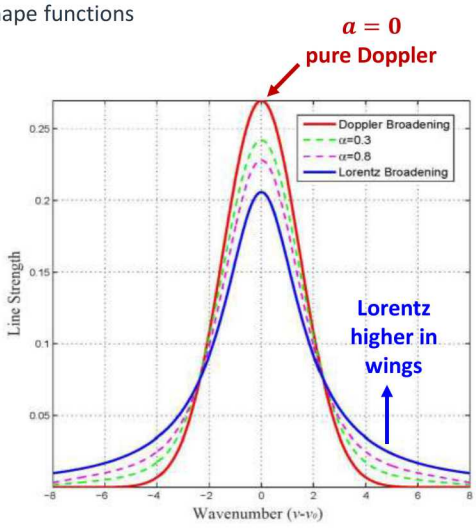

Sandia National Laboratories

Laser absorption spectroscopy (LAS)

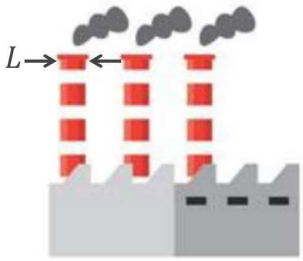

- Governed by Beer's law :

Transmission, $\tau_\nu = \left(\frac{I}{I_0}\right)_\nu = \exp(-\sum_{i,j} P X_i S_{i,j}\,\phi_{\nu,i,j} L)$

where $P =$ pressure (atm)
$X_i =$ mole fraction of ith species
$S_{i,j}(T) =$ line strength of jth transition of ith species (cm^{-2}/atm)
$\phi_{\nu,i,j} =$ line shape function
$L =$ absorption path length (cm)
(uniform medium)

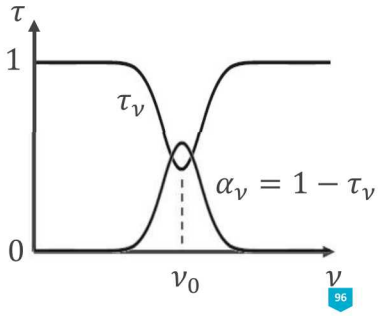

- Scan tunable laser across absorption line
- Measure laser intensity before and after the sample
- Direct absorption can have noise issues; limited sensitivity

Sandia National Laboratories

96

Scanned wavelength modulation spectroscopy

- Developed by Ron Hanson's group (Stanford)
- Cancels out several noise sources affecting direct absorption
- Superpose two voltage wave forms to modulate the tunable diode laser wavelength
  - Low frequency triangle wave (e.g., f_{scan} ~1 kHz)
  - Higher frequency sinusoid (e.g., f_{mod} ~100 kHz)
  - Sample the detector much faster (e.g., f_{sample} ~10 MHz)
- Apply digital signal processing to extract harmonics
- Recover absorption from $2f_{mod}/1f_{mod}$

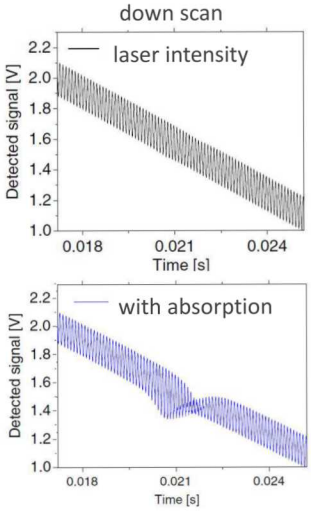

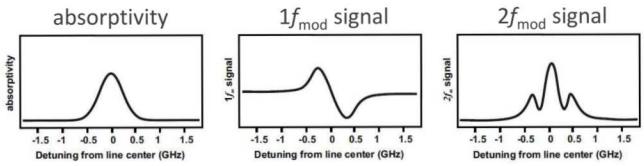

Sandia National Laboratories

Linne CISS 2016, Hanson CISS 2018

97

Application example: TDLAS of H_2O, CO_2, CO, and temperature

- Peng et al., "Single-ended mid-infrared laser-absorption sensor for simultaneous in situ measurements of H_2O, CO_2, CO, and temperature in combustion flows," Applied Optics 55 (2014)

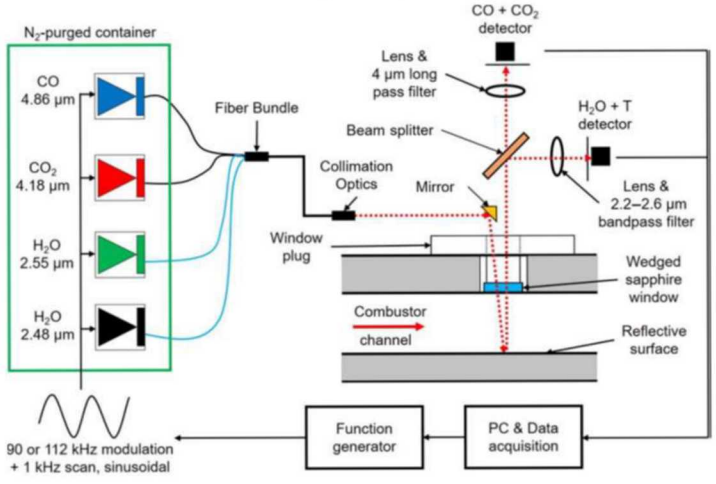

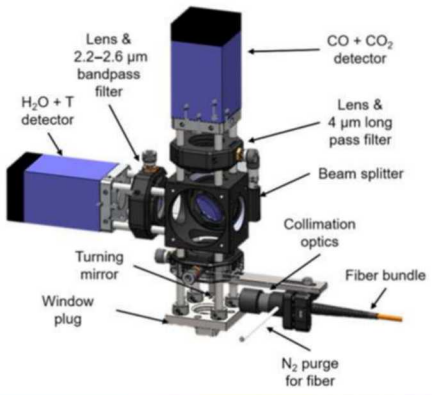

Species	ν_0 (cm^{-1})	E'' (cm^{-1})	S (296 K) (cm^{-2}/atm)
H_2O	3920.08	704.2	6.35×10^{-1}
H_2O	4029.52	2660.95	1.10×10^{-4}
CO_2	2394.41	3329.0	7.39×10^{-5}
CO	2055.40	886.9	6.20×10^{-1}

Sandia National Laboratories

Application example: TDLAS H_2O, CO_2, CO, and temperature

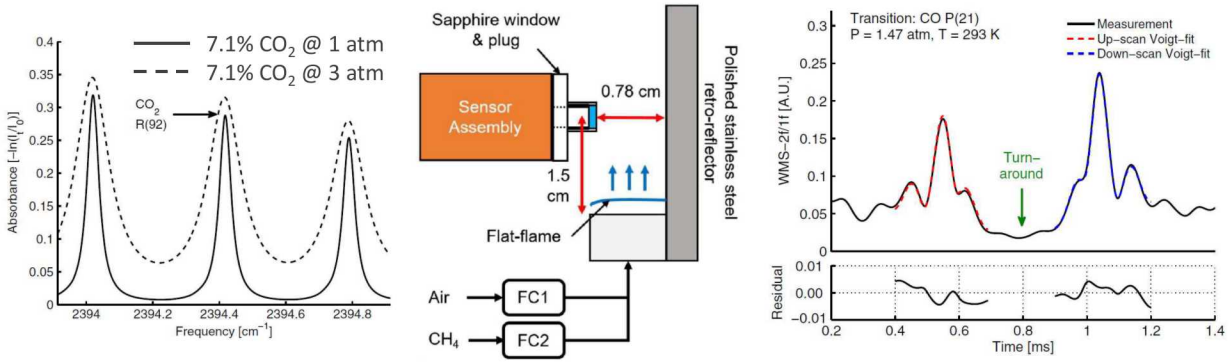

- Simulated absorption spectra of CO_2 in products of ϕ=1.2 CH_4/air flame (T=1500K, L=15 mm)
- 0.78 cm path length across flat flame products
- Scanned-wavelength-modulation spectroscopy with 2nd harmonic detection and 1st harmonic normalization (scanned-WMS-2*f*/1*f*) suppresses several noise sources
- WMS spectral fitting routing

Sandia National Laboratories

Peng et al., *Applied Optics* 55 (2014)

99

Summary: Tunable diode laser absorption spectroscopy (TDLAS)

- Absorption of IR laser light by ro-vibrational transitions
- Many species of interest in combustion are accessible
- Significant recent (~10 yrs) developments in IR lasers and detectors
- Can be very sensitive (multi-pass cell, cavity ring-down, modulation spectroscopy)
- Temperature derived by measuring two or more lines of a molecule
- Line of sight technique; temperature and composition should be uniform along the path length
- Systems can be very compact; fiber optics to "throw and catch"
- Multiplexing: simultaneous measurement of multiple lines and species to get concentrations and temperature
- Applications: shock tube kinetics, exhaust stream monitoring, propulsion test rigs, …
  NOT turbulent flames

- Detailed treatment in Ron Hanson's CISS 2018 lecture notes
- Approachable explanation of the physics in Mark Linne's CISS 2016 lecture notes

Sandia National Laboratories

100

Electronic transitions: Example OH

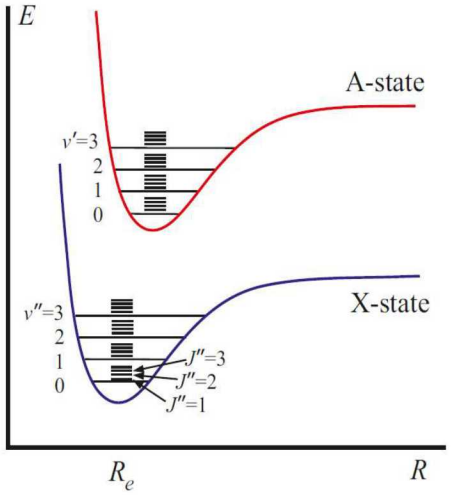

- Internal energy: $E_{int} = E_{elec} + E_{vib} + E_{rot}$
- Energy differences (and thereby wavelengths for absorption or emission) can be calculated from molecular parameters

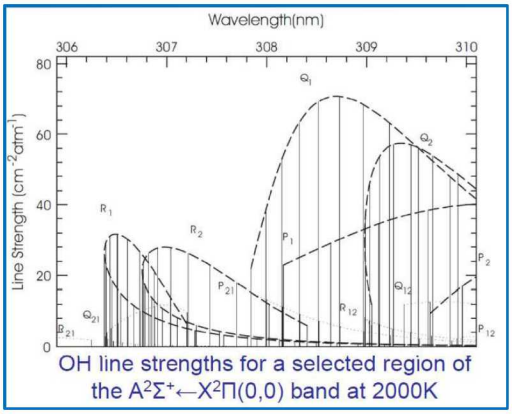

Hanson CISS 2018 Lecture 3

Sandia National Laboratories

Electronic transitions: OH laser induced fluorescence (LIF)

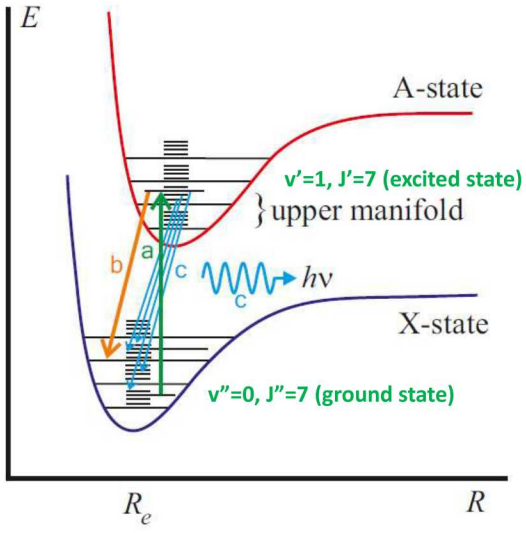

- Typical strategy for OH LIF or PLIF imaging
- Excitation (molecule absorbs, **a**, usually single line)

$$Q_1(7)\ A^2\Sigma^+ \leftarrow X^2\Pi(1,0) \quad (283.2\ \text{nm})$$

- Most molecules relax via collisions (process **b**)
- Detection (molecule emits after rotational and vibrational energy transfer; many different transitions, process **c**)

$$A^2\Sigma^+ \rightarrow X^2\Pi(1,1),(0,0) \quad (305\text{-}320\ \text{nm})$$

- To make a quantitative measurements, we need to know (among other things):
  - population of the ground state (v"=0, J"=7)
  - efficiency of excitation and fluorescence
  - collisional quenching rate

Sandia National Laboratories

Linne CISS 2016

Basics of laser induced fluorescence (LIF)

- Two level model (simplified theory)
- Einstein A and B coefficients
- Rates per unit volume:

$N_1 b_{12}$	absorption	$N_2 A_{21}$	spontaneous emission
$N_2 b_{21}$	stimulated emission	$N_2 Q_{21}$	collisional quenching

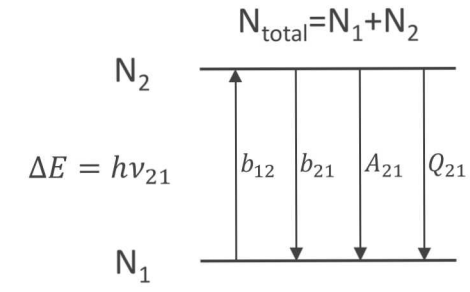

- Assume steady state, linear regime (low laser power) and skip a few steps… fluorescence signal in photons

$$S_F = N_1 V b_{12} \left(\frac{A_{21}}{A_{21}+Q_{21}}\right)\left(\frac{\Omega}{4\pi}\right)\eta_{opt}$$

photons absorbed | fluorescence efficiency | fraction collected

$A_{21} \ll Q_{21}$

"overlap integral"

$$b = \frac{B}{c}\int_\nu I_\nu(\nu) g(\nu) d\nu$$

laser intensity | absorption lineshape

Need to know collisional quenching rate to make LIF quantitative in concentration!!

Sandia National Laboratories

also detector efficiency to convert photons to electronic signal

103

A few important combustion species detected by LIF

Molecule	Excitation	Detection
OH	~283 nm, ~314 nm	306-320 nm
NO	~226 nm	236-280 nm
CH	~314, ~387, ~431 nm	various 314-460 nm
CO	~230 nm (2 photon)	~484 nm
CH_2O	~355	360-550 nm
HCO	~258 nm	276-284 nm

- References:
  - Applied Combustion Diagnostics, Kohse-Höinghaus and Jeffries, Eds., Chapter 2, 2002
  - LIFBASE software for LIF of diatomic molecules (Luque and Crosley)
    Download version 2.1 (free); https://www.sri.com/engage/products-solutions/lifbase

Sandia National Laboratories

104

Application example: Multi-species PLIF and Rayleigh scattering

- Combine PLIF imaging of OH + CH with PLIF of CH_2O (formaldehyde) and Rayleigh scattering

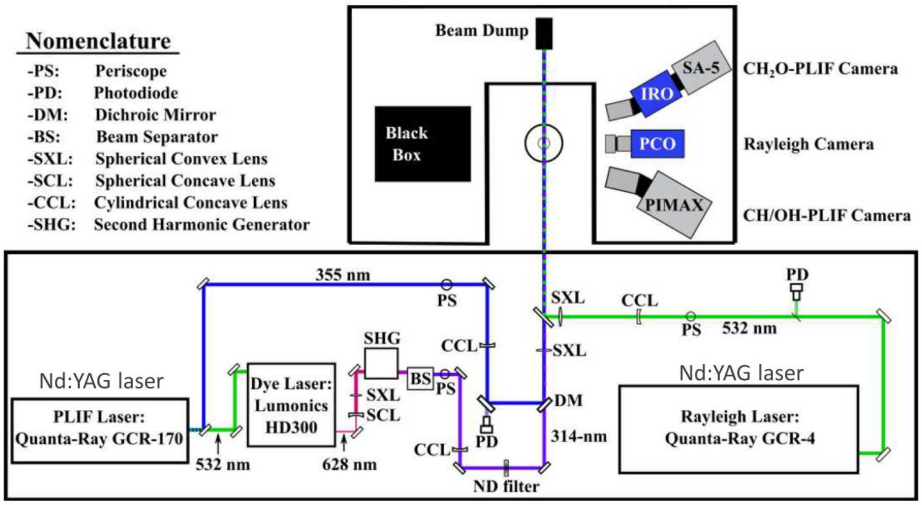

Skiba et al., *Combust. Flame 189* (2018) supplemental material

Application example: Multi-species PLIF and Rayleigh scattering

- Novel scheme implemented by Cam Carter and coworkers to allow PLIF of OH or CH or both, using a single Nd:YAG-pumped dye laser system (*smart diagnostics*)

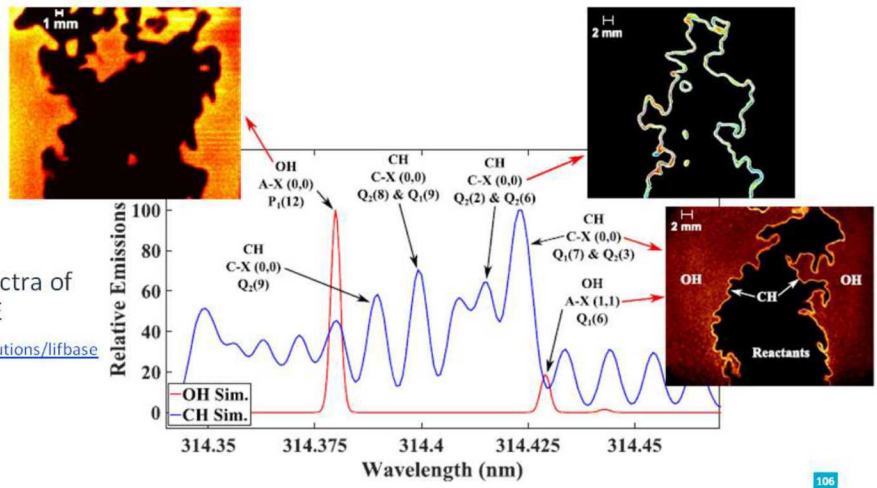

- Computed excitation spectra of CH and OH using LIFBASE

https://www.sri.com/engage/products-solutions/lifbase

Skiba et al., *Combust. Flame 189* (2018)

Application example: Multi-species PLIF and Rayleigh scattering

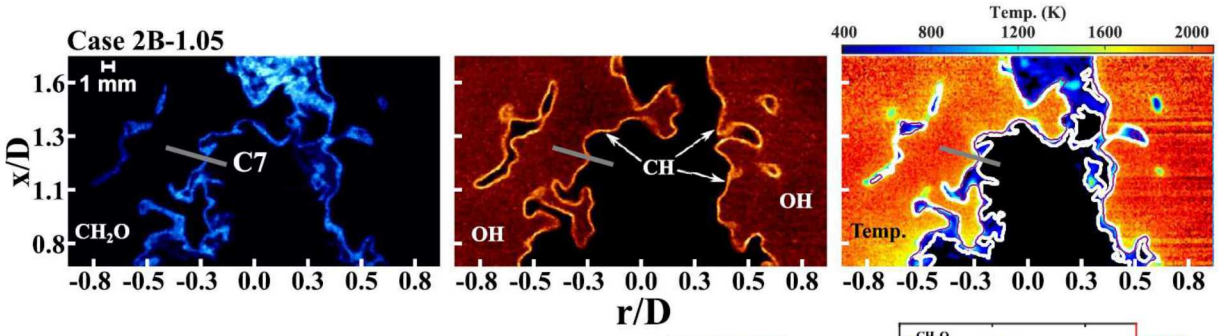

- Applied to highly turbulent premixed flames (Michigan HiPilot burner)
- Investigate reaction zone structure
  - broadened preheat zone (CH_2O)
  - thin reaction zone
- Question: Which way are the lasers pointing?

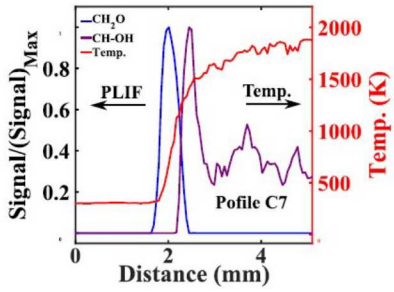

Sandia National Laboratories

Skiba et al., *Combust. Flame 189* (2018)

Next: Raman scattering (my favorite diagnostic)

- ~~Light-matter interaction~~
- ~~Molecular spectroscopy~~
- ~~Laser absorption~~
- ~~Laser induced fluorescence~~
- Raman scattering

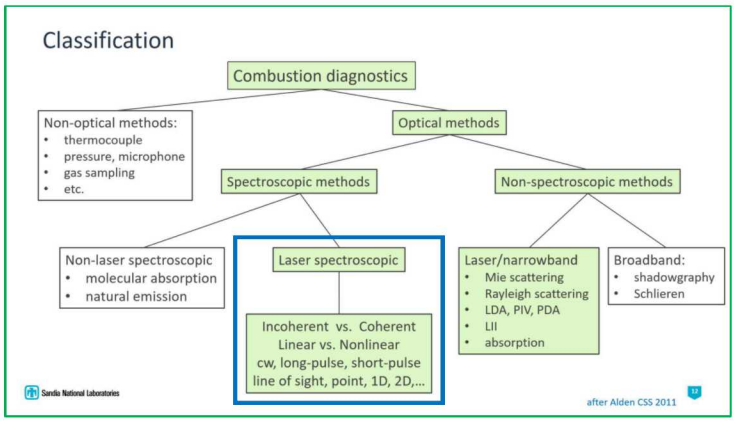

Sandia National Laboratories

108

Spontaneous Raman scattering

- Raman scattering (inelastic)
  - Stokes (red shift)
  - anti-Stokes (blue shift)
- Raman shift (cm^{-1}) is the difference between rotational and ro-vibrational levels in each molecule; rovibrational spectra of all Raman-active species are "imprinted" on the scattered light
- Raman scattering cross sections ~$\sigma_{Ray}/1000$

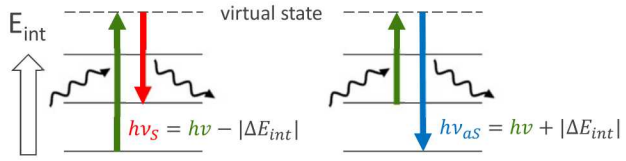

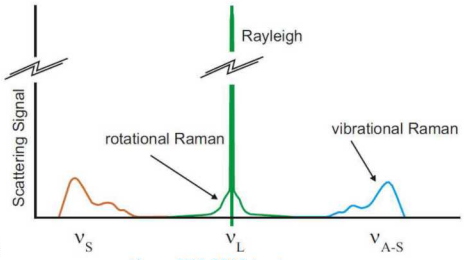

Linne CISS 2016 Lectures

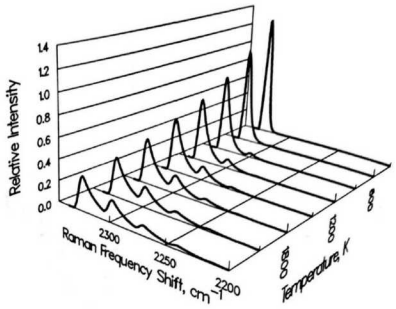

Calculated spontaneous Raman spectra of N_2 at 300K up to 2400K (rotational lines not resolved) Eckbreth, Laser Diagnostics for Combustion Temperature and Species, 1996

Sandia National Laboratories

109

Line imaging of Raman scattering in laminar CH_4/air jet flame

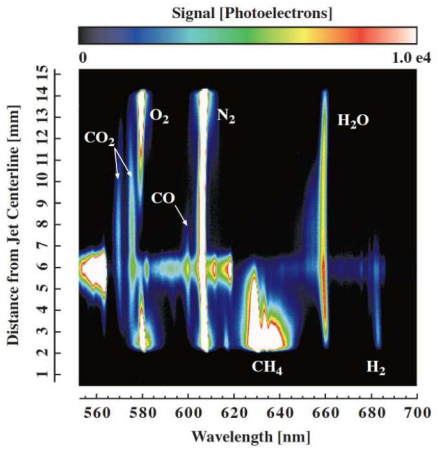

vibrational Raman shift

species	~shift (cm^{-1})
CO_2	1285, 1388
O_2	1556
CO	2145
N_2	2331
CH_4	2915, 3017
H_2O	3657
H_2	4160

Eckbreth, 1996

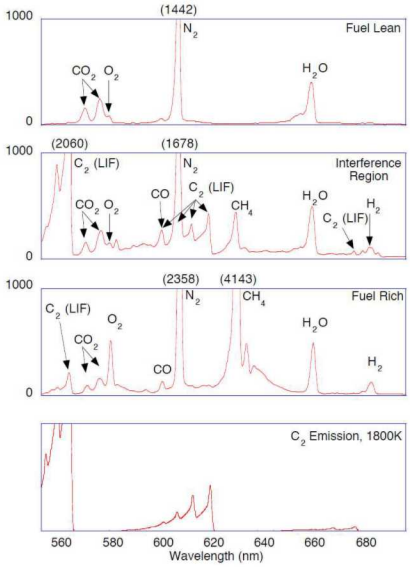

- Partially premixed (3:1 air/CH_4); average of 500 shots
- Fluorescence interference centered near r = 6 mm (fuel rich)

Barlow, Miles PCI 28, 2000

Sandia National Laboratories

110

Spontaneous Raman scattering

- **PROS**
- All major species concentrations using one laser wavelength
- Non-resonant; no laser tuning
- Linear with laser intensity & concentration
- Detection in the visible allows high efficiency optics, detectors
- Combine with Rayleigh and LIF (with all major species you can calculate $\sigma_{Ray} = \sum_i X_i \sigma_i$, T, Boltzmann fraction, and collisional quenching rate)

- **CONS**
- Requires high laser pulse energy to get good signal with a single shot
- Fluorescence interference from large hydrocarbons (soot precursors) can swamp the Raman signals
- Even flame luminosity can be a problem (intense combustion, CO or syngas flames)
- Limited to non-sooting flames of simple fuels
- Limited to 1D if measuring all major species

Sandia National Laboratories

111

Application example: Simultaneous Raman/Rayleigh/LIF

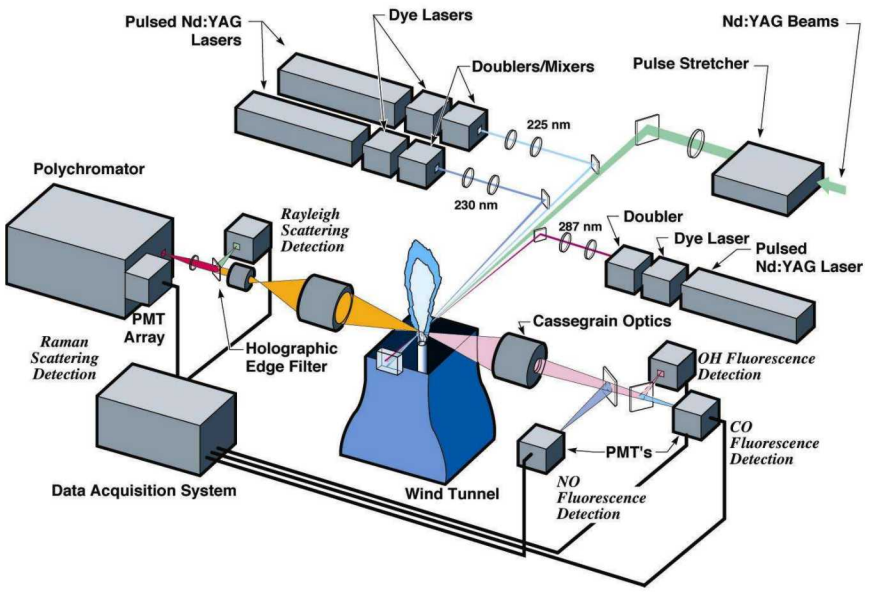

- Sandia point measurement system (1995-2001)
- Raman/Rayleigh plus LIF of OH, NO, CO
  - Linear LIF of OH, NO
  - 2-photon CO LIF (more complicated)
- Several TNF Workshop data sets on the web came from this system (tnfworkshop.org)
- Exploratory science AND validation experiments

112

Calibrations, Precision, and Accuracy

Hencken Burner – CO/H_2/air near adiabatic

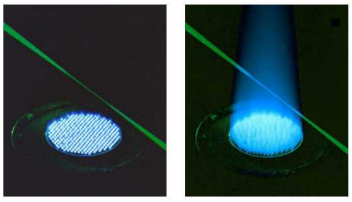

Lean Rich

- Calibration in well-known reference flames and detailed documentation of experimental uncertainties are required for useful comparisons with models.
- Calibration of flow controllers is essential!

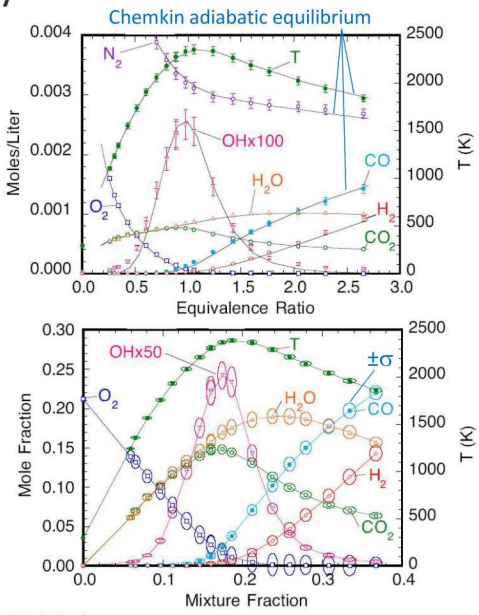

Barlow et al. C&F 120:549-569 (2000)

Laminar Opposed Flow Flame (Reality Check)

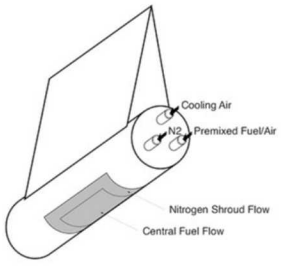

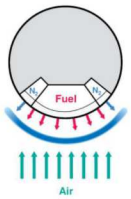

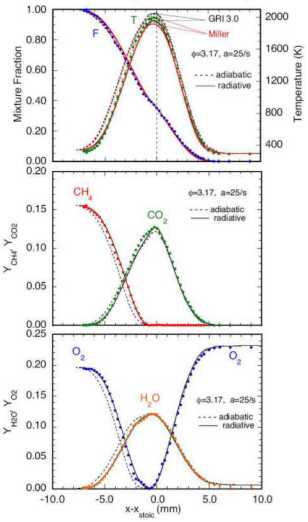

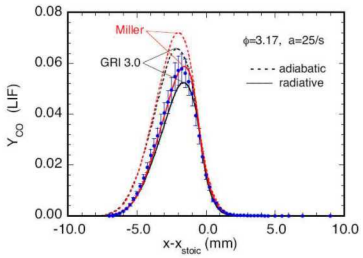

Radiation makes a big difference for NO

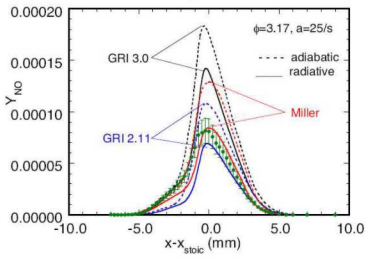

- Tsuji burner; strain parameter, $a = 2U_\infty / r$; partially premixed CH_4/air (1:3 by volume)
- Buoyancy induced flow increases strain rate; match mixture fraction profile

Barlow et al. C&F 127 (2001) 2102-2118

Point measurements from Sandia flame D (piloted 1:3 CH_4/air jet flame)

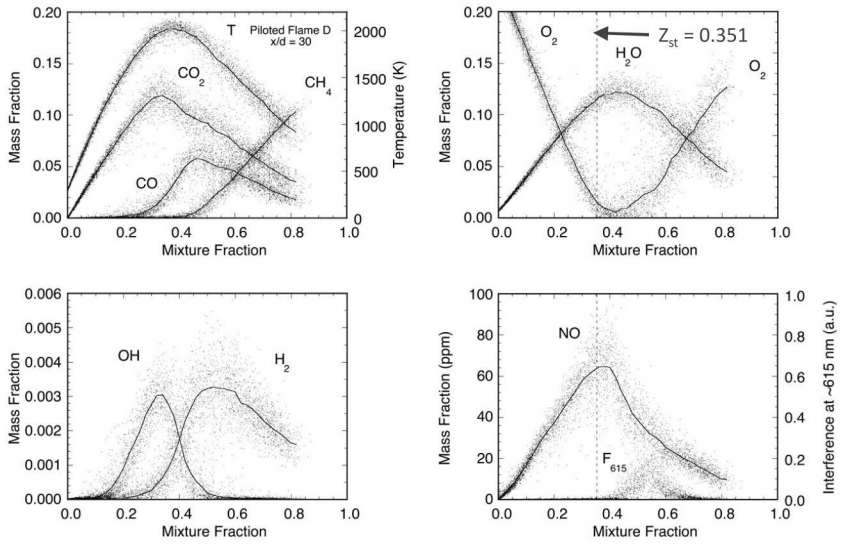

- Lines show conditional means
- Mixture fraction: fraction of mass in the sample that originated from the jet
- Temperature calculated from Rayleigh signal, using species mole fractions from Raman (iterative)
- Higher scatter in these measurements than in later measurements
- OH and NO corrected for shot to shot variations in Boltzmann fraction and collisional quenching rate
- NO detection limit 1-2 ppm

Sandia National Laboratories

Barlow and Frank, PCI 28, 1998

115

Importance of LIF corrections for OH and NO

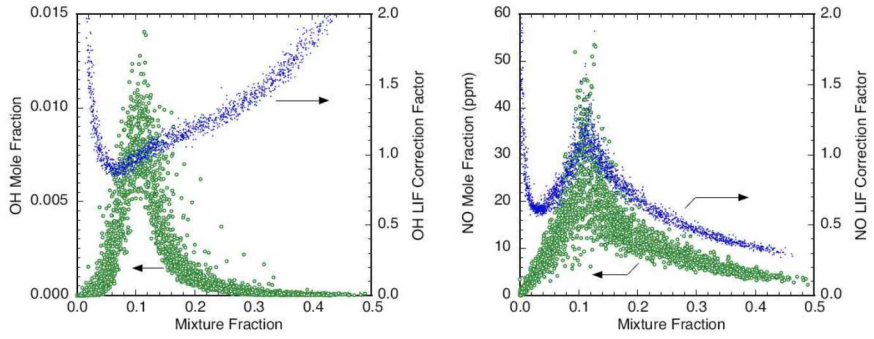

- Scatter plots of OH and NO mole fraction and their corresponding single-shot correction factors from experiments in a turbulent H_2/N_2 jet flame
  - Corrections for Boltzmann fraction $f(T)$ and collisional quenching rate $Q(T,X_i)$
  - Within roughly ±15% in region of high OH (can be reduced by picking optimal OH transition)
  - Corrections are more important for NO
  - Calibrate at flame conditions; Purdue/Sandia method for NO calibration

Sandia National Laboratories

Barlow, Carter, Pitz, "Multiscalar Diagnostics in Turbulent Flames," in Applied Combustion Diagnostics, Kohse-Höinghaus, Jeffries, Eds. Taylor and Francis 2002

116

Application of CO-LIF in the Delft III Jet Flame (piloted natural gas)

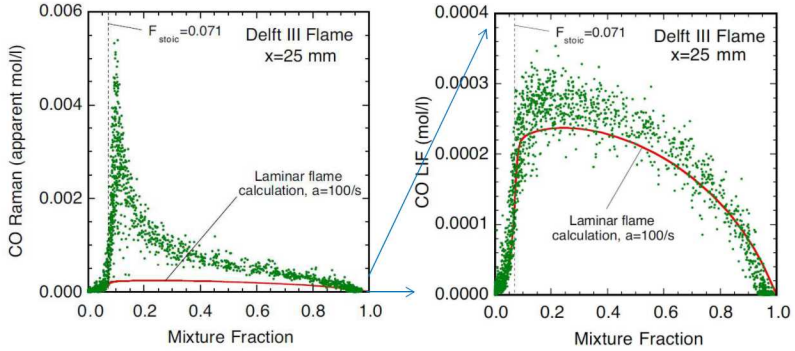

- High levels of interference from soot precursors render CO Raman measurements useless
- CO LIF is relatively unaffected by interference
- Excitation: 2 photons at 230.1 nm; third photon can ionize the excited state CO; adjust laser for power dependence of 1.1-1.2 to suppress effect of quenching; calibrate response (works well in methane flames; does not work in oxy-fuel flames)

Sandia National Laboratories

Nooren et al. Appl. Phys. B 71, 2000; Sevault et al, Combust. Flame 159, 2012

117

Where do diagnostic advances come from?

- Innovations and improvements in combustion diagnostics are often made possible when new laser or detector technologies become commercially available
- Sometimes major improvements can be gained from innovative methods of data analysis without any new hardware:
  - Wavelet-Based Optical Flow Velocimetry (Jeff Sutton group)
  - Scanned-wavelength-modulation spectroscopy (Ron Hanson group)
- Sometimes a combination of custom engineered hardware and innovative methods of data acquisition and analysis can give a big payoff in diagnostic performance:
  - Example: Multiscalar measurement capabilities at Sandia (1995 – 2018)
  - Developments driven by the goal of measuring mixture fraction gradients and scalar dissipation in Raman-friendly turbulent flames
  - Long-term DOE investment into research on fundamentals of turbulence-chemistry interactions

Sandia National Laboratories

118

Multiscalar Experiments at Sandia

- Gen 3: Turbulent Diffusion Flame Lab (1995-2001)
  - Point measurements of T, major species, OH, NO, CO
  - Probe volume: 0.75-mm L x 0. 5-mm D = **0.14 mm³**
- Gen 4: Turbulent Combustion Lab (2001-2007)
  - Line imaged Raman/Rayleigh/CO-LIF and crossed planar OH-LIF
  - Mixture fraction gradient, scalar dissipation, length scales
  - Probe volume: 0.2-mm L x 0.22-mm D = **0.0073 mm³**
- Gen 5: Turbulent Combustion Lab (2007-2013)
  - Better spatial resolution, precision, and accuracy
  - Premixed and stratified flames
  - Probe volume: ≤ 0.1-mm L x 0.22-mm D ≤ **0.0036 mm³**
- Gen 6: Turbulent Combustion Lab (2014-2018)
  - Second Raman/Rayleigh detection system
  - Polarized-depolarized detection (subtract interference)
  - Dual-resolution Raman detection of multiple hydrocarbons
  - Demonstration experiments only

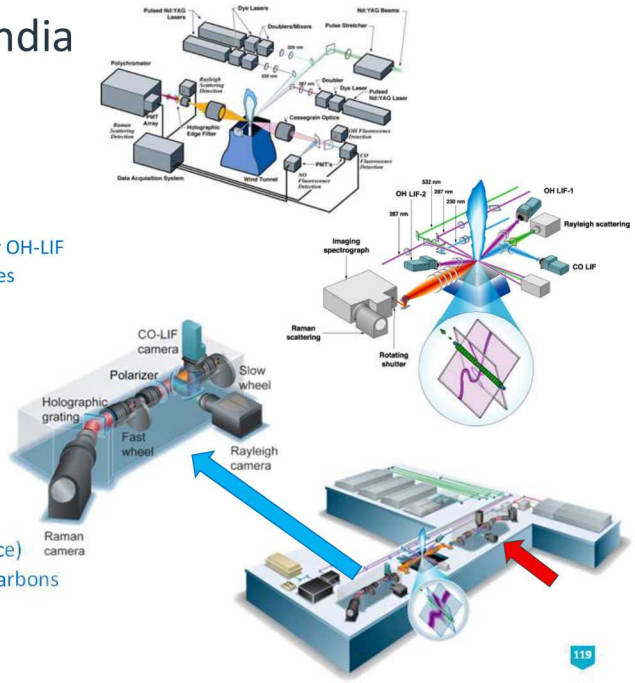

Sandia National Laboratories

119

Progress on precision and spatial resolution

- Table compares signal-to-noise ratios (SNR = mean/rms)
- Gen 3 versus Gen 5
  - Line imaging vs. point
  - Factor ~40 smaller volume of gas
  - 2.5-4 times higher Raman SNR
- Even better SNR with wavelet denoizing

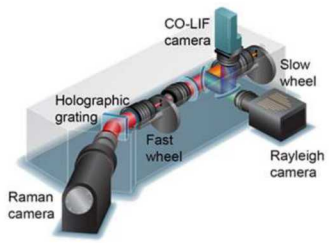

Air (294 K)	Gen 3 750 μm*	Gen 5 100 μm†	denoised†
Y_{N2}	90	400	700
Y_{O2}	30	125	210
T_{Ray}	400‡	410‡	430‡

CH_4/air flat flame (2050 K, ϕ = 1.28)

Y_{N2}	50	130	190
Y_{H2O}	20	50	88
Y_{CO2}	15	29	45
Y_{CO_LIF}	17	16	23
Y_{H2}	6	17	24
T_{Ray}	100	150	200
phi	20	65	86

* 750 μm values from Barlow & Frank (1998) using 1.2 J/pulse

† Representative SNR from 100-shot files using 1.8 J/pulse

‡ SNR for T_{Ray} limited by accuracy of laser energy measurements

Sandia National Laboratories

120

Simultaneous Raman/Rayleigh/CO-LIF and crossed OH PLIF

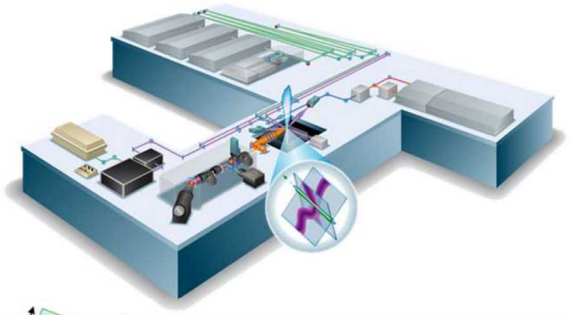

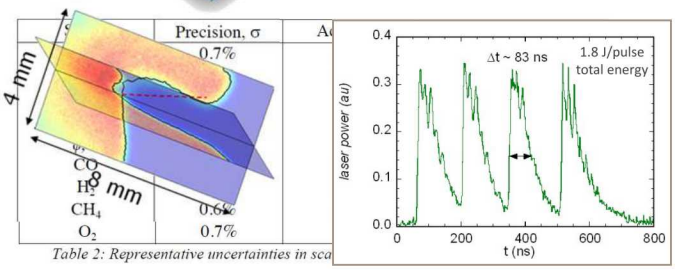

Table 2: Representative uncertainties in sca

- **Raman/Rayleigh**
  - Four Nd:YAG lasers (1.8 J/pulse, ~400 ns)
  - Rotating shutter (21000 rpm, 3.9 μs gate)
  - High-efficiency holographic transmission grating
  - Low-noise CCD (-110 C) for Raman
  - **T, N_2, O_2, CH_4, CO_2, H_2O, H_2, CO**
  - **6-mm probe length**
- **CO-LIF**
  - 230.1 nm 2-photon excitation; ~484 nm detection
  - Lower noise, less interference
- **State of mixing, progress of reaction, 1D gradients**
- **Crossed OH PLIF → "3D" gradients, curvature**
- **Hybrid matrix inversion**
  - Temperature dependent response table based on theoretical Raman spectra
- **Wavelet adaptive thresholding & reconstruction (WATR)** developed by Matt Dunn
  - **Reduced noise** in all signals
  - 20 μm data spacing, **50 μm resolution**

Sandia National Laboratories

121

Fuest, et al. (Proc. Combust. Inst. 33, 2011); Sweeney, et al. (Combust. Flame 160, 2013)

Line-imaging detection system

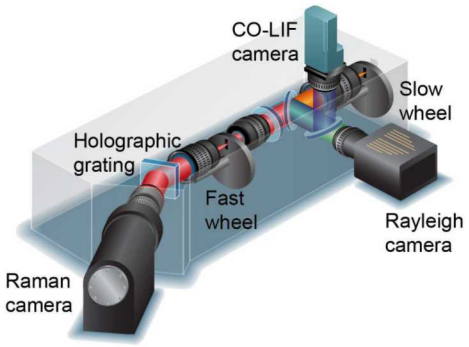

- Three cameras
  - Rayleigh: unintensified CCD
  - Raman: cryo-cooled CCD
  - CO LIF: intensified CCD
- Custom grating (Kaiser Optical)

  90% efficiency at 625-nm
- Fast wheel:

  21000 rpm (3.9 μs gate FWHM)
- Slow wheel: 3000 rpm (300μs)
- PLL motor control

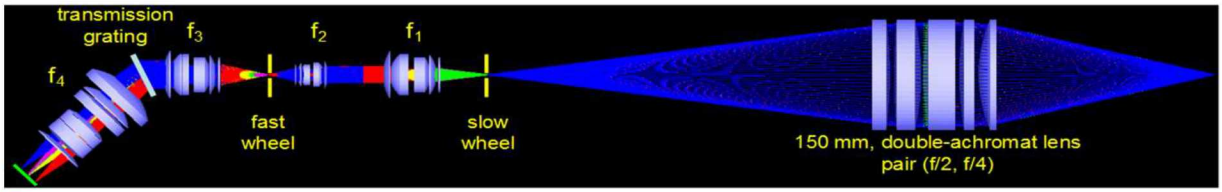

Sandia National Laboratories

122

Line-imaging detection system

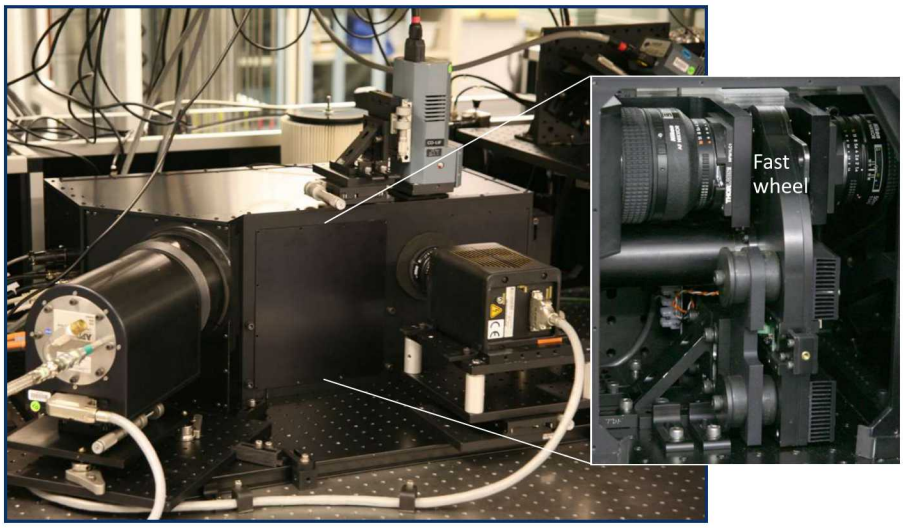

Sandia National Laboratories

123

Data acquisition and reduction

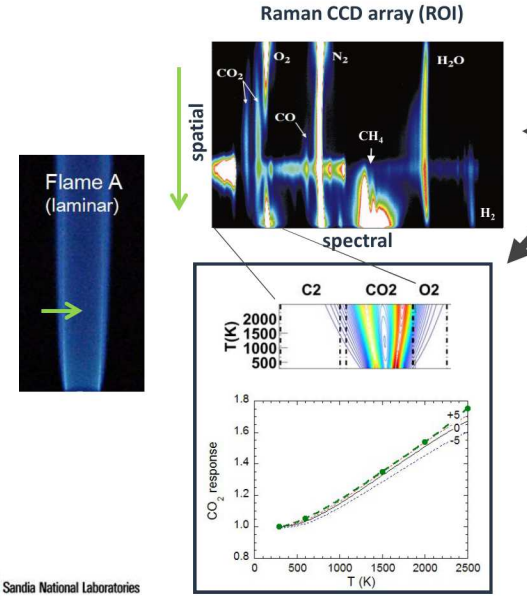

1. Averaged laminar flame image
2. On-chip binning to reduce readout noise
3. Temperature dependence based on theoretical spectra (Ramses code from TU Darmstadt)
4. Iterative "hybrid matrix inversion"

$$\begin{bmatrix} S_{CO2} \\ S_{O2} \\ S_{CO} \\ S_{N2} \\ S_{CH4} \\ S_{H2O} \\ S_{H2} \\ S_{CO\text{-}LIF} \\ F560 \\ b3 \end{bmatrix} = \begin{bmatrix} N_{CO2} \\ N_{O2} \\ N_{CO} \\ N_{N2} \\ N_{CH4} \\ N_{H2O} \\ N_{H2} \\ N_{CO\text{-}LIF} \\ \text{"C2"} \\ Bck \end{bmatrix}$$

Sandia National Laboratories

Fuest et al. PCI 33 (2011)

124

Laminar unstrained premixed flame (ϕ = 0.73) compared with Chemkin calculation (daily reality check for premixed flames)

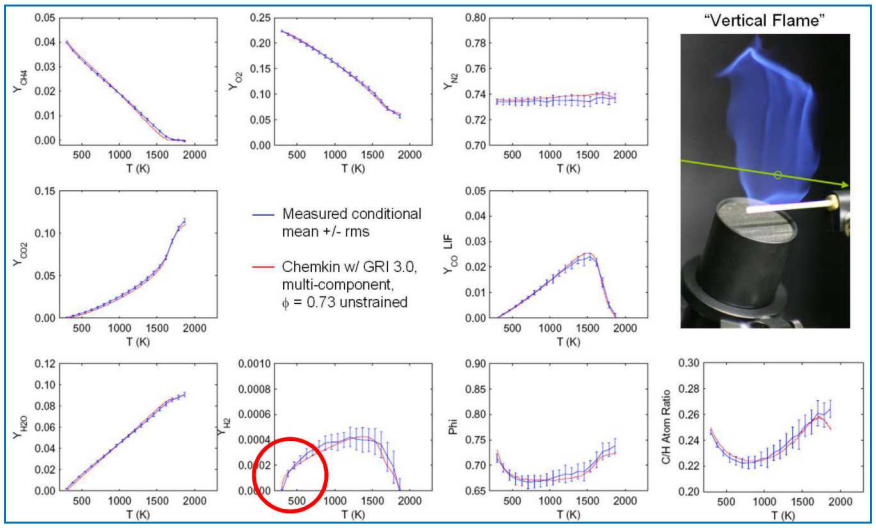

differential diffusion of H_2 ϕ and atom ratios not constant

Wavelet adaptive thresholding & reconstruction (WATR)

- Sample 1D Raman, Rayleigh, and CO-LIF at ~20 μm spacing
  - Pixel-to-pixel noise at scale smaller than physical scales in the flow and smaller than optical resolution
- Apply wavelet denoising algorithm to individual raw signals
  - 9 Raman channels, Rayleigh, CO-LIF
  - Decomposition parameters based on expected noise at the local signal level on each camera
  - Locally adaptive filter, preserves high gradients
- Process denoised signals using hybrid matrix inversion method

Black box overview (single-shot N_2 Raman signal)

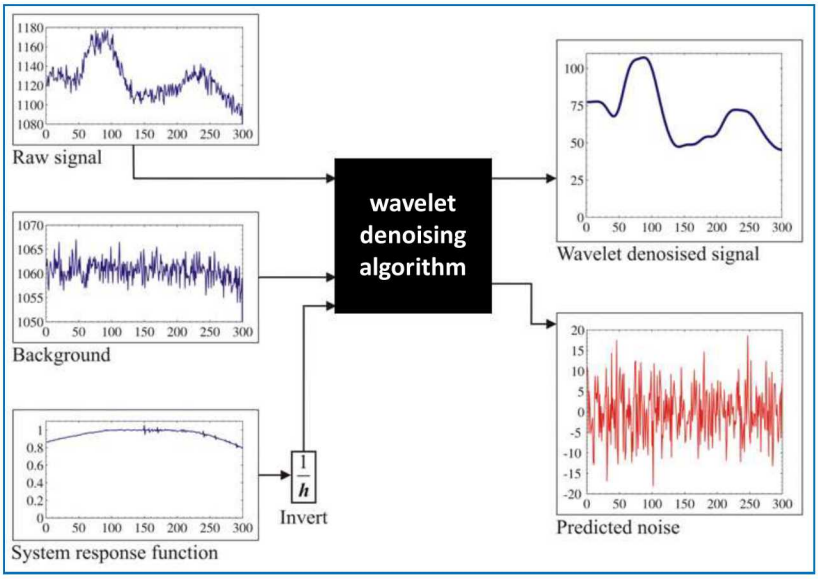

Sandia National Laboratories

127

Denoising of single shot T and mixture fraction profiles

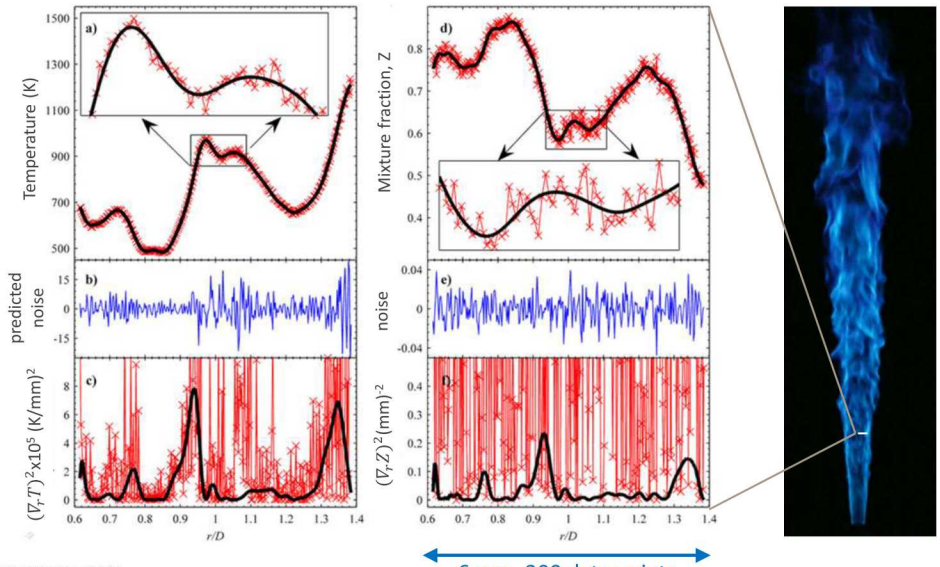

DLR-B flame
$CH_4/H_2/N_2$
d = 8 mm
x/d = 10
r/d = 1.0
λ_B ~ 70 μm

Fuel-rich region where T dependence on mixture fraction is near linear.

Sandia National Laboratories

128

Thermal Dissipation Spectrum (Inverse Rayleigh Signal)

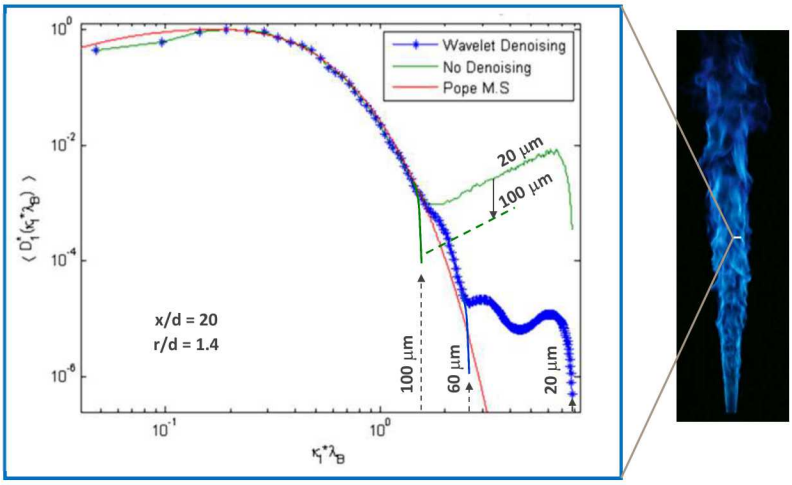

- Preserves spectrum up to the noise tail. ~Noise free at 60 μm.
- Locally adaptive filter. Single-shot dissipation is directly available.

Outline

Turbulent combustion phenomena

- Different modes and regimes of turbulent combustion
- Some things we have learned about turbulent flames and the interactions of turbulence, chemistry, and molecular transport
  - Differential diffusion of species in jet flames and premixed bluff-body flames
  - Dynamics and statistics of local extinction and relight
  - When is a premixed flame not a premixed flame?
  - How to identify premixed and non-premixed reaction zones in partially-premixed flames
  - Multi-regime combustion

Different modes of turbulent combustion

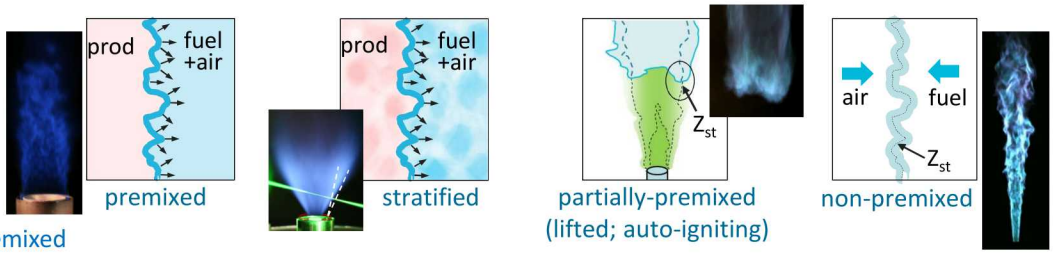

- Premixed
  - Propagation of a reacting front through a homogeneous, flammable mixture of fuel and oxidizer
  - Turbulence increases flames surface area and the rate of consumption of reactants
- Stratified (or "stratified-premixed")
  - Propagation through an inhomogeneous mixture (lean or rich, but not both)
  - Back-supported flames are more robust than premixed flames at the same equivalence ratio
- Partially premixed
  - Broad category coves everything between premixed and non-premixed; most applications are partially premixed
  - Local reaction zones can have characteristics of both premixed and non-premixed flames
- Non-premixed
  - Fuel and oxidizer come from opposing sides of stoichiometric the reaction zone
  - Reaction zone location is dictated by the fluid mechanics of mixing

Combustion modes and regimes

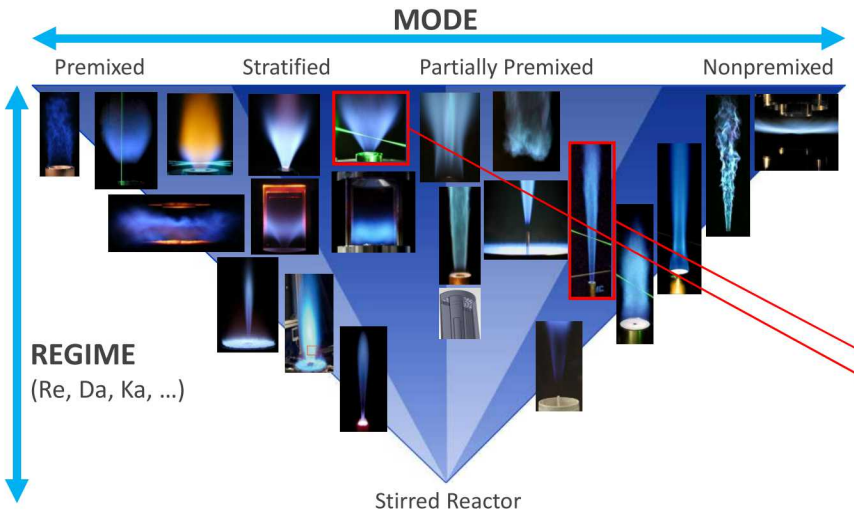

- Interactions of turbulence, molecular transport, and chemistry are expressed differently in the different combustion modes and regimes
- How important is differential diffusion in turbulent flames?
  - Jet flames
  - Stratified and premixed flames

Differential diffusion is normally ignored in turbulent combustion models

Multi-component Transport

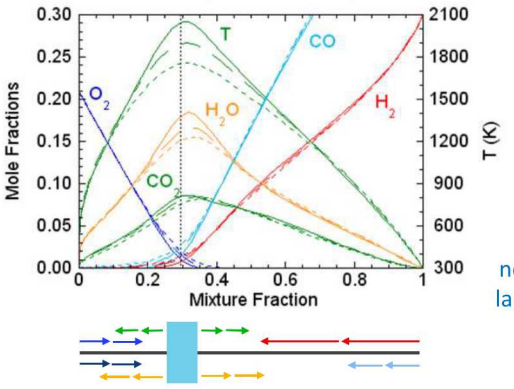

non-premixed laminar flames
30% H_2
40% CO
30% N_2

Equal Diffusivities ($Le_i = \alpha/D_i = 1$)

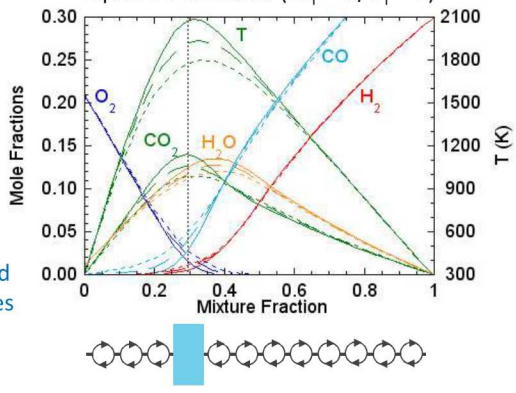

- Transport assumption has factor of two effect on C/H ratio at stoichiometric in laminar calculations
- Driven by high mobility of H_2 compared to CO and products

Molecular and turbulent transport can both be important

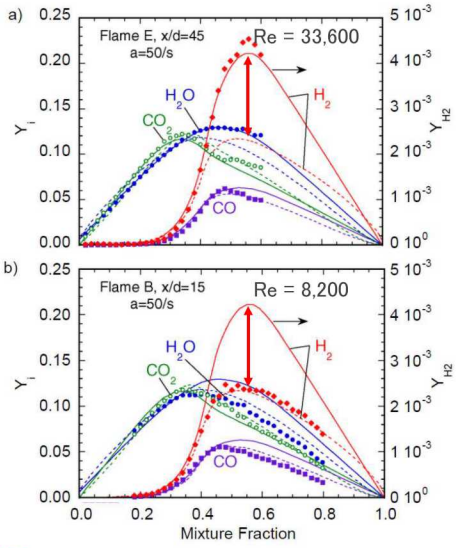

Symbols: conditional means mass fractions
Solid lines – equal diffusivities ($Le_i = \alpha/D_i = 1$)
Dashed lines – multi-component transport

Re = Ud/ν, U-jet exit velocity, d-nozzle diameter, ν-kinematic viscosity

- Methane flame: diff-diff of H_2 only after reaction
- Differential molecular diffusion is important in the near field and at low Reynolds number.
  - Sandia flame B is not turbulent, only transitional (wiggly laminar flame)
- Turbulent transport becomes dominant in jet flames with increasing downstream distance and increasing Reynolds number, Re.
  - Re > 20000 preferable for model comparisons (the higher the better)

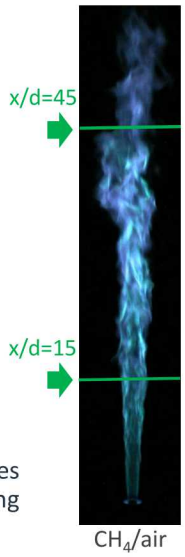

Sandia National Laboratories

Barlow, PCI 31 (2007) 49–75

135

Cambridge/Sandia Stratified Swirl Burner

UNIVERSITY OF CAMBRIDGE

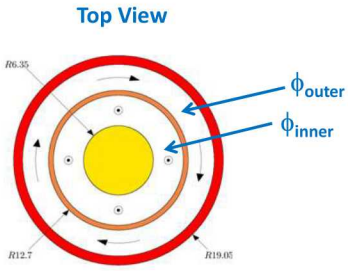

- Double annular construction
- Ceramic center body, 12.7-mm diameter
- Variable swirl in outer annular flow
- Isolate effects of mixture stratification on flame structure; include recirculation, shear, swirl

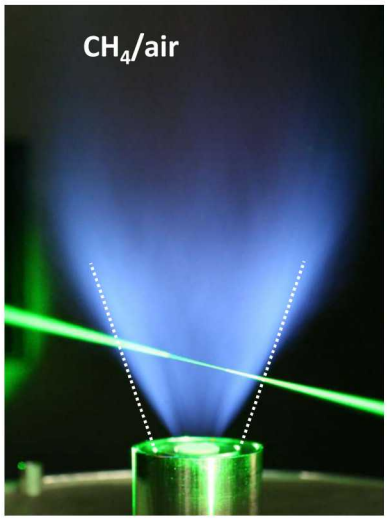

Sandia National Laboratories

Sweeney et al., *Combust Flame* 159 (2012) a,b; 160 (2013)

136

Cambridge/Sandia Stratified Swirl Burner

UNIVERSITY OF CAMBRIDGE

U_i = 8.3 m/s U_o = 18.7 m/s U_{cf} = 0.4 m/s

Re_i = 5,960 Re_o = 11,540

Vary stratification ratio and swirl

- Radial profiles
  - z = 10, 20, 30, … mm
  - 300 shots at each location, 1500 in flame brush
  - 103 μm data spacing
- Long records
  - crossing of flame & mixing layer
  - 30,000 shots
  - 20 μm data spacing
  - Wavelet denoising
- Velocity (PIV, LDA at Cambridge)

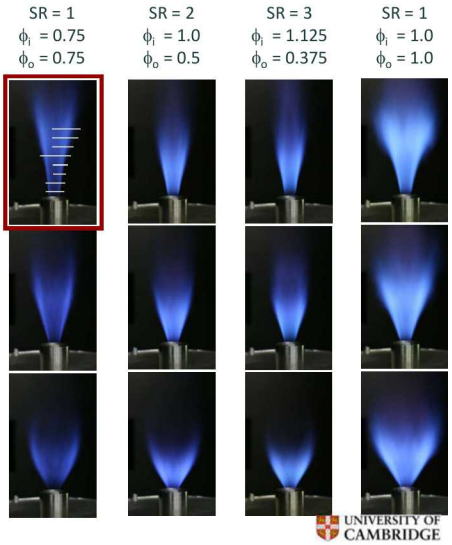

Sandia National Laboratories

UNIVERSITY OF CAMBRIDGE

137

Sweeney et al., *Combust Flame* 159 (2012) a,b; 160 (2013)

Cambridge/Sandia Stratified Swirl Burner

UNIVERSITY OF CAMBRIDGE

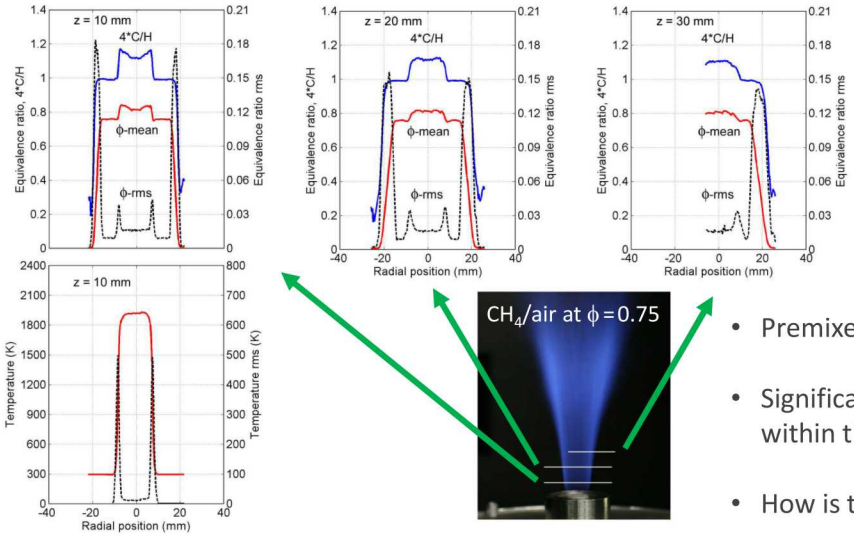

- Premixed flame w/o swirl (SwB1)
- Significant increases in ϕ and C/H within the recirculation zone
- How is that possible!?

Sandia National Laboratories

138

Barlow et al., *Combust. Flame* 159 (2012)

Cambridge/Sandia Stratified Swirl Burner

UNIVERSITY OF CAMBRIDGE

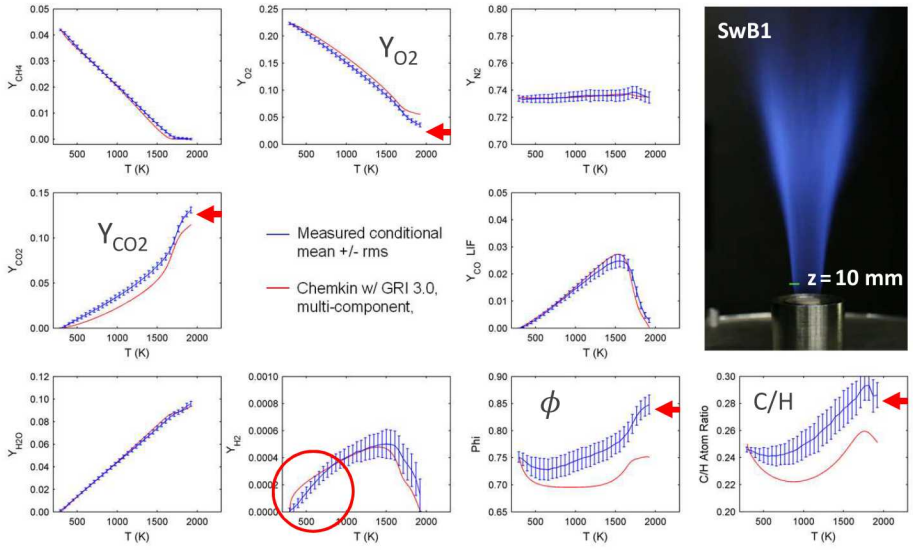

- SwB1 is fully premixed with $\phi_i = \phi_o = 0.75$
- 1500 shots with probe volume centered on the reaction zone
- Conditional means

Sandia National Laboratories

Barlow et al., *Combust. Flame* 159 (2012)

139

Hypothesis based on laminar flame structure

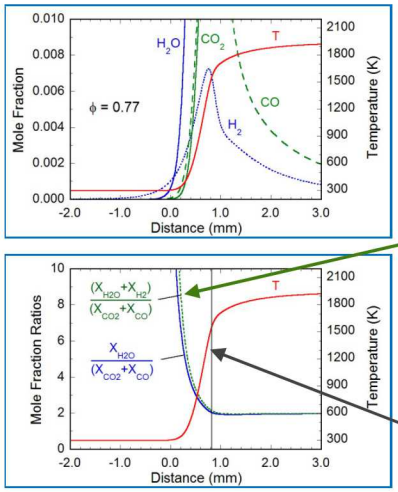

$$\frac{X_{H2O} + X_{H2}}{X_{CO2} + X_{CO}}$$

max heat release

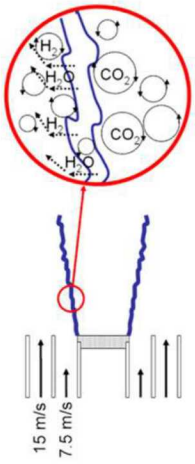

- Chemkin with GRI Mech 3.0, multi-component transport, Soret effect
- Combined effect of H_2 diff-diff and kinetics → H_2O production at lower T than CO_2
- Hypothesis: H_2 and H_2O move ahead of CO, CO_2 and are transported downstream by shear flow

Sandia National Laboratories

Barlow et al., *Combust. Flame* 159 (2012)

140

Experiments and simulations confirm physical mechanisms

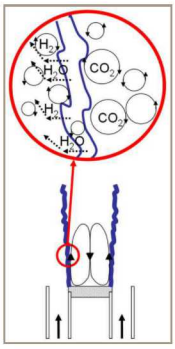

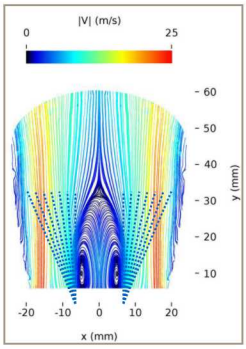

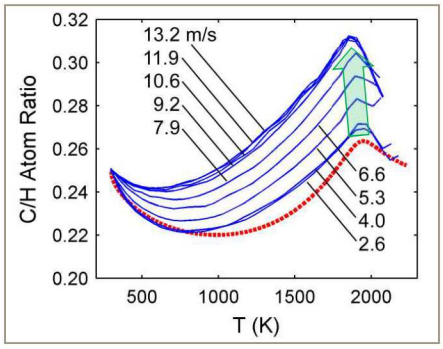

- Combination of preferential transport, high shear, and a strong, compact recirculation zone that amplifies the transport effects
- Saturates at highest velocities; can this affect high Re flames?

Combustion modes and regimes

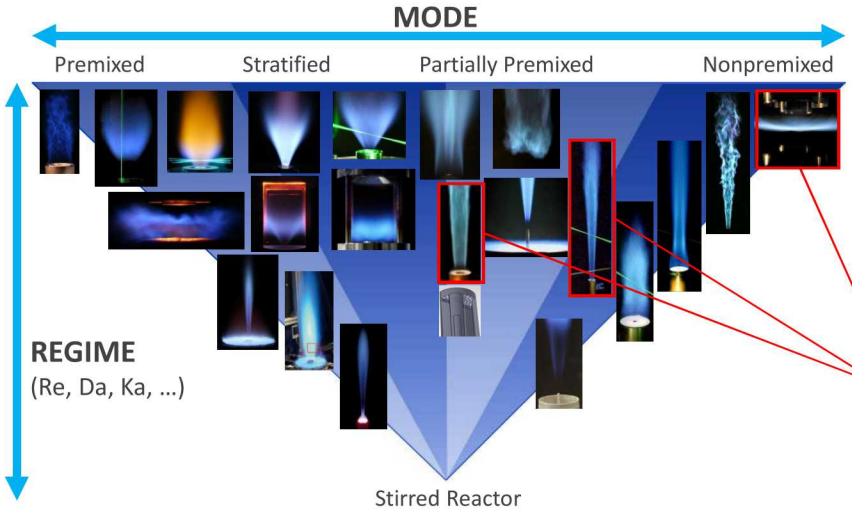

- Interactions of turbulence, molecular transport, and chemistry are expressed differently in the different combustion modes and regimes
- Dynamics and statistics of local extinction and relight
  - Opposed flow flames
  - Jet flames

Time evolution of strain rate induced extinction: Laminar

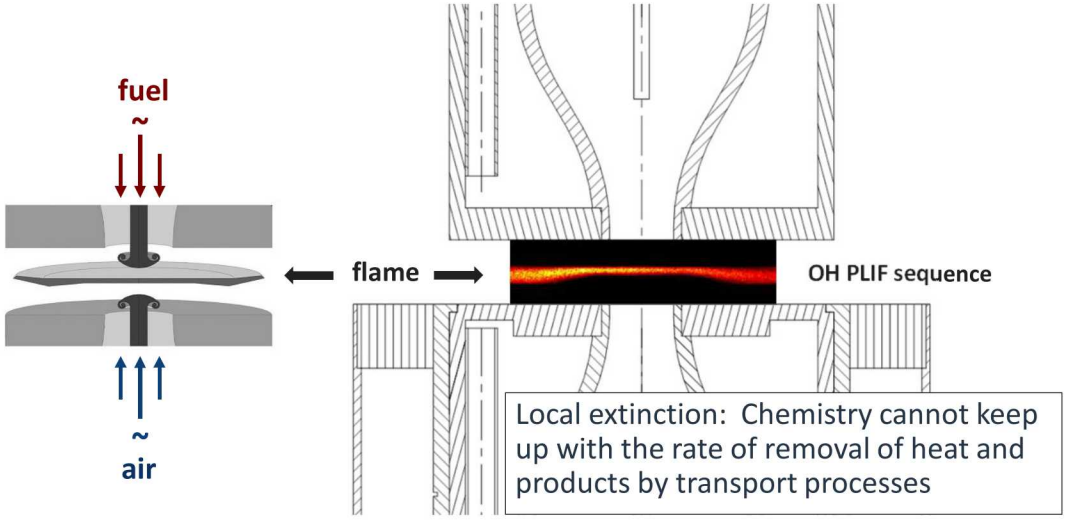

Sandia National Laboratories

Courtesy of Jonathan Frank

143

Time series on local extinction and relight in DLR flame

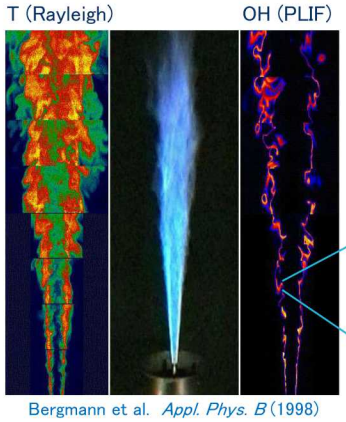

Bergmann et al. *Appl. Phys. B* (1998)

$CH_4/H_2/N_2$ jet flame, "DLR flame"

Time series of planar OH LIF images, Δt = 125 μm

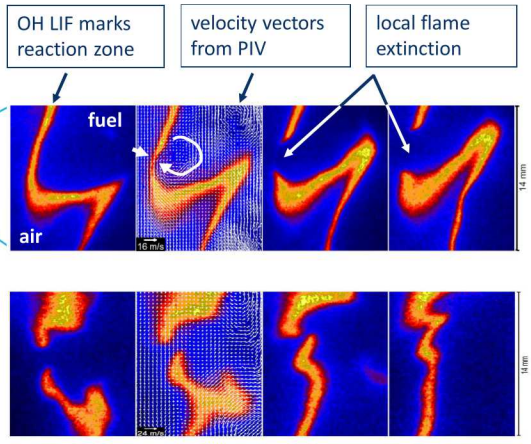

Sandia National Laboratories

Hult et al. (2000) http://ltces.dem.ist.utl.pt/lxlaser/lxlaser2000/papers/pdf/26_2.pdf

144

Effects of local extinction on T and species

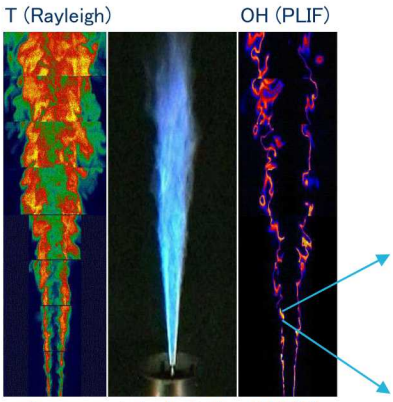

Bergmann et al. *Appl. Phys. B* (1998)

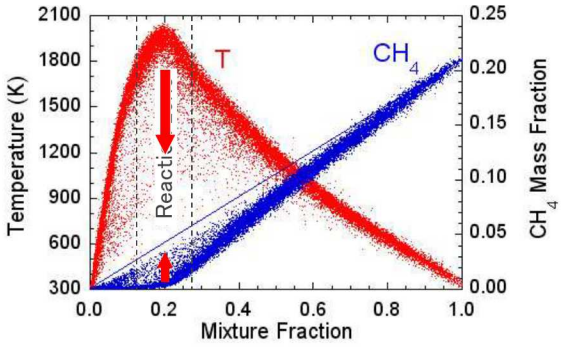

$CH_4/H_2/N_2$ jet flame, "DLR flame"

Experimental collaborations:
DLR-Stuttgart, Sandia, TU Darmstadt, Purdue, Lund University, UT Austin

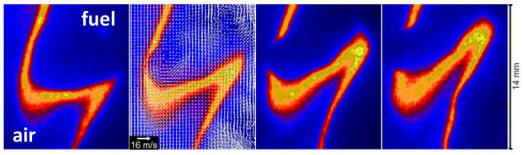

Sandia National Laboratories

145

High-Speed Multi-Frame OH PLIF Imaging + Stereo PIV

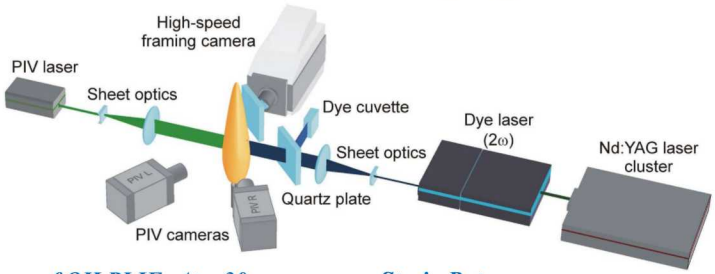

Six Frames of OH PLIF, $\Delta t = 30\ \mu s$

Strain Rate

$CH_4/H_2/N_2$

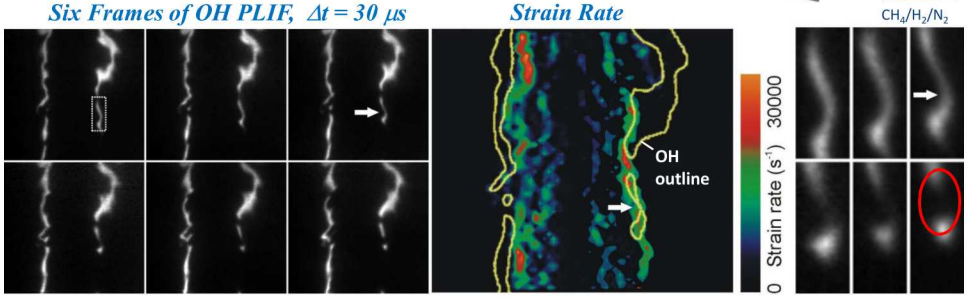

Sandia National Laboratories

J. Hult, U. Meier, W. Meier, A. Harvey, C.F. Kaminski, *Proc. Combust. Inst.* 30 (2005) 701–709.

146

Oxy-Fuel Combustion: Collaboration with SINTEF, Norway

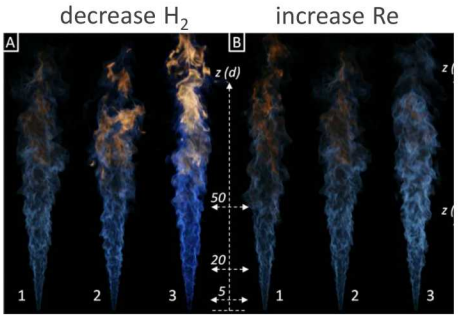

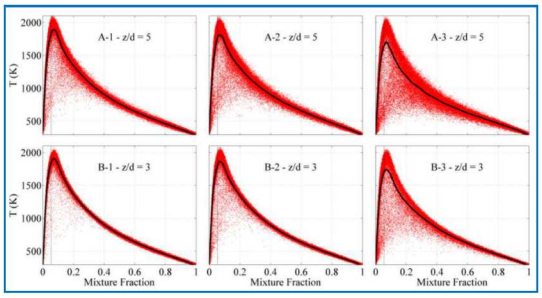

- CH_4/H_2 fuel jet in O_2/CO_2 coflow
- Vary Re, hydrogen content
- Measure scalar structure, differential diffusion effects, and local extinction
- Burning index is easily compared to simulations; average of T/T_{eq} for mixture fraction interval near stoichiometric

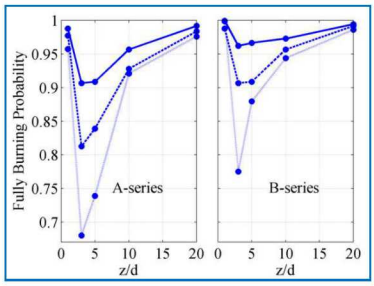

Sandia National Laboratories

Sevault et al., CNF (2012)

147

Sandia piloted CH_4/air jet flames

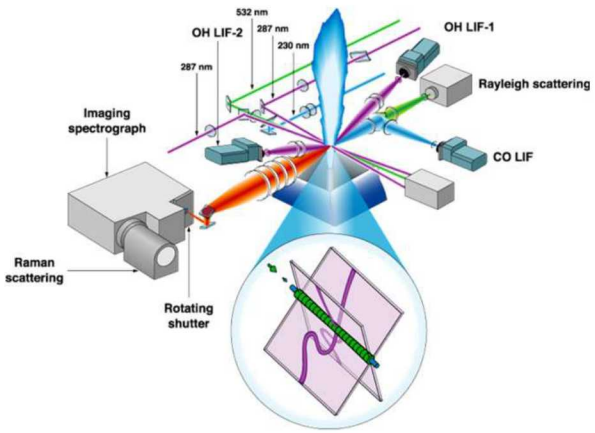

increasing probability of local extinction

Flame	Re_j	u_{exit} (m/s)
C	13,400	38
D	22,400	64
E	33,600	96
F	44,800	128

Premixed Pilot Flame

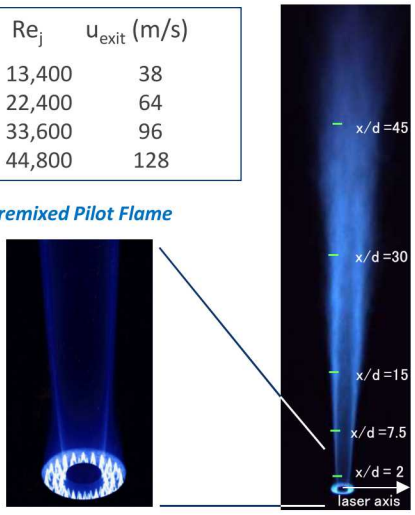

Sandia National Laboratories

148

Doubly conditioned statistics in flame with extinction $(Y_i|\xi,\chi)$

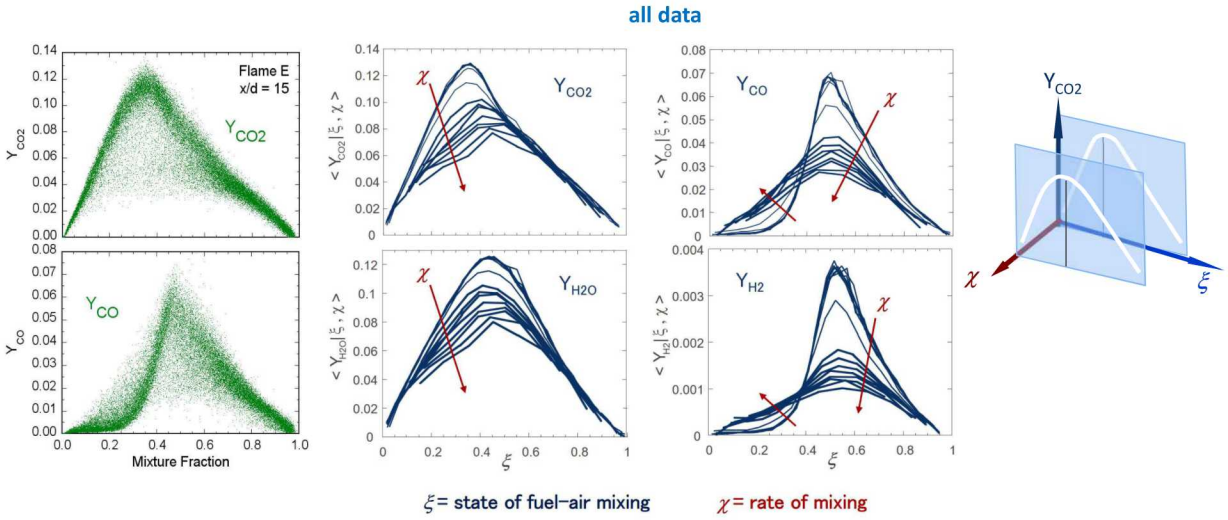

Sandia National Laboratories

149

Barlow & Karpetis, *Proc. Combust. Inst.* 30 (2005)

Inclined structures with high scalar dissipation

Scalar dissipation in 2D images

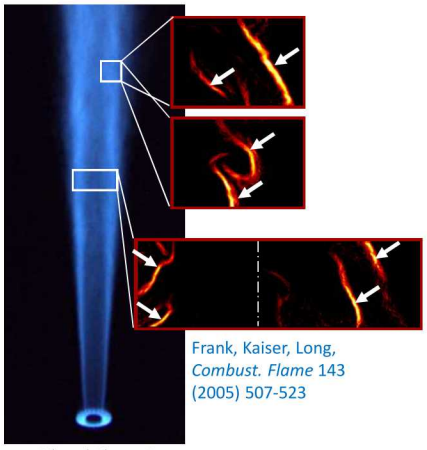

Frank, Kaiser, Long, *Combust. Flame* 143 (2005) 507-523

Piloted Flame D

Scalar dissipation in Large Eddy Simulations

from Andreas Kempf

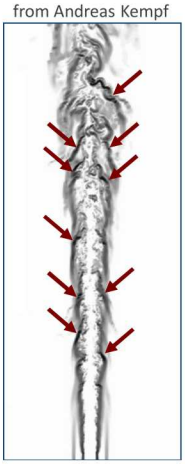

from Heinz Pitsch

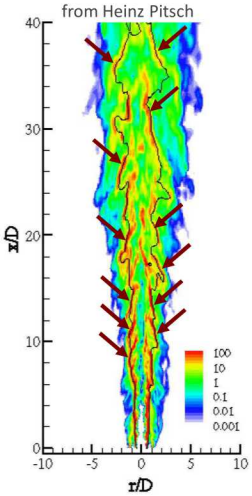

- Suggests direct coupling of large and small scales
- May be important for local extinction and differential diffusion

Sandia National Laboratories

150

Compressive Strain Rate in Turbulent Partially-Premixed Jet Flame

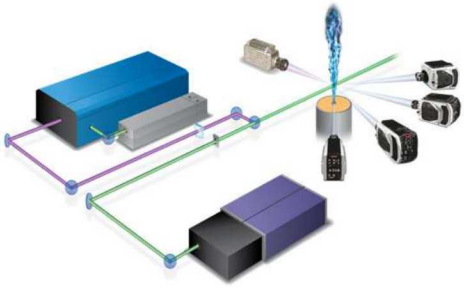

Tomographic PIV and
OH PLIF at 10 kHz

Coriton, Steinberg, Frank, Exp. Fluids (2014)

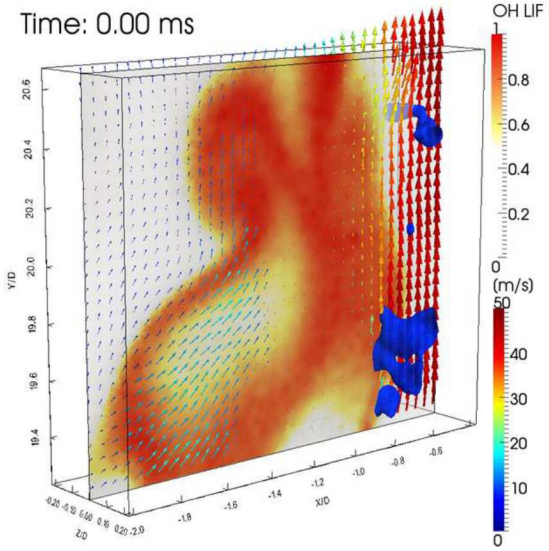

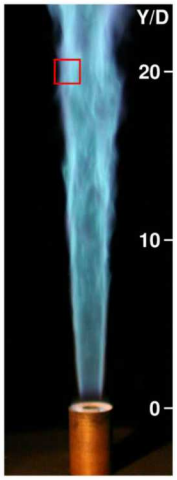

Blue isosurfaces: $\Gamma^{3D} = -15{,}000\ s^{-1}$

Sandia National Laboratories

151

Time evolution of strain rate induced extinction

Tomographic PIV and OH PLIF at 10 kHz

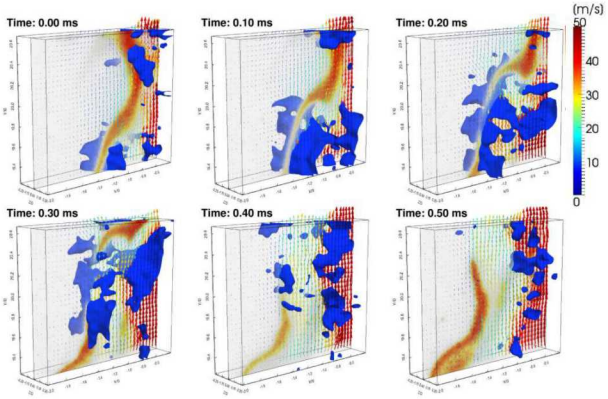

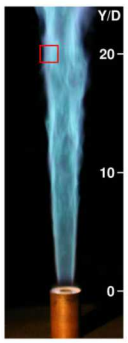

DME/air
Re=29,300

Preferred alignment

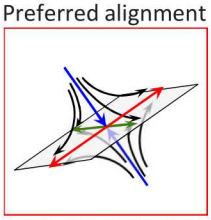

$s_1 > s_2 > s_3$
extensive int. compressive

- Time history of interaction is critical (high intensity, short duration)

Blue isosurfaces: $s_3 = -15{,}000\ s^{-1}$

Steady laminar extinction limit: 817 s^{-1} (Zhou); 933 s^{-1} (Kaiser)

Sandia National Laboratories

Coriton, Steinberg, Frank, Exp. Fluids (2014)

152

Heat release increases agglomeration of strain rate structures

Increasing Heat Release

Air Jet | Flame C_{LP} | Flame *C*

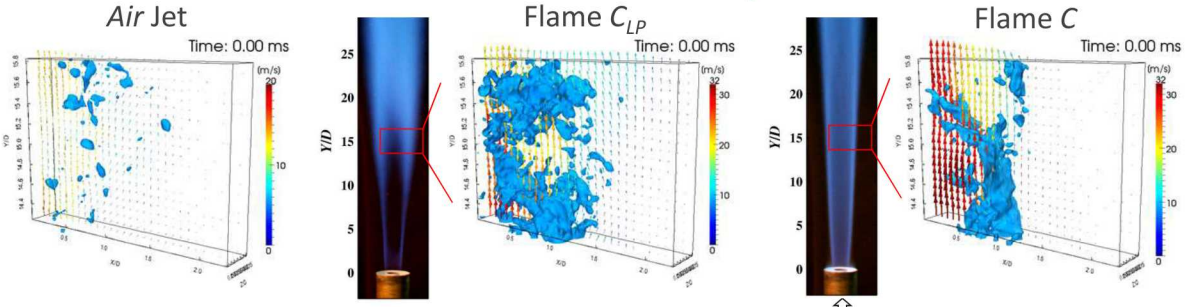

- Bursts of large strain rate structures
- Air Jet: small fragmented structures throughout jet
- Flame C: large elongated structures concentrated near reaction zone
- Flame C_{LP}: localized extinction → intermittent features of both non-reacting and reacting flows

Isosurfaces: $|s_{thrs}| = 7{,}000\ s^{-1}$

$|s| = (s_1^2+s_2^2+s_3^2)^{1/2}$

Sandia National Laboratories

Coriton, Frank, Proc. Combust. Inst. (2015)

P 153

Enhanced coupling of strain rate and vorticity

Strain Rate Isosurfaces
Vorticity Isosurfaces

Increasing Heat Release

Air Jet | Flame C_{LP} | Flame *C*

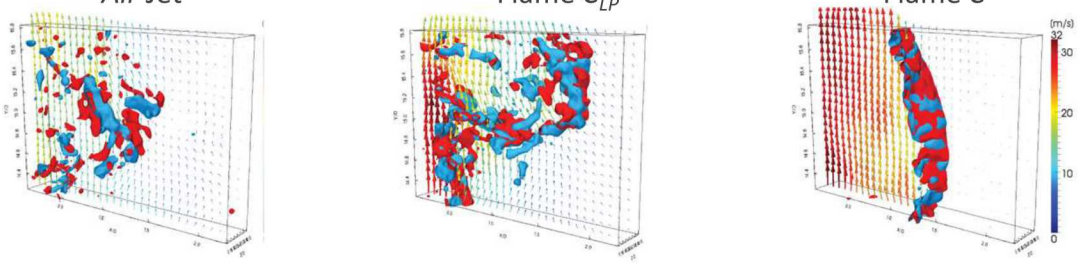

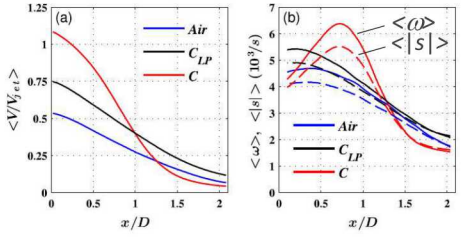

- **Heat release in Flame C reduces air entrainment, preserving high velocities in the fuel-rich core**
- **Larger peak vorticity (solid) and strain rate (dashed) in Flame C**

Sandia I

Coriton & Frank, Physics of Fluids (2016)

P 154

Preferential vorticity alignment with extensive strain increases vorticity production

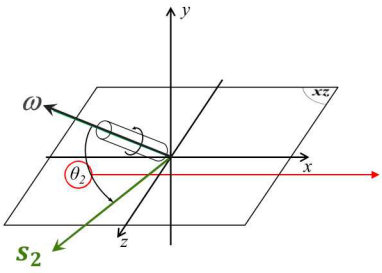

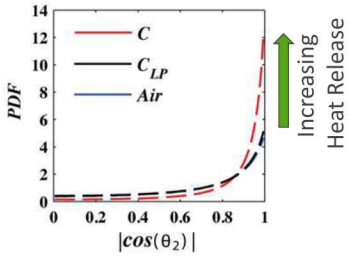

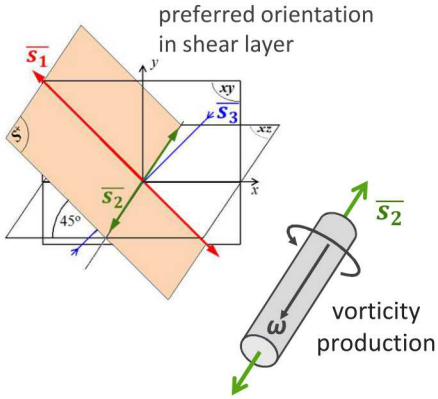

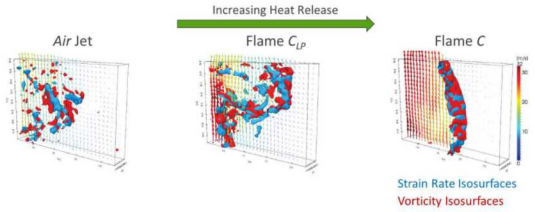

- **Heat release induces alignment of vorticity and s_2 strain**
- **Large vorticity preferentially aligned with *mean* extensive s_2 strain**

Sandia National Laboratories

Coriton & Frank, Physics of Fluids (2016)

P 155

Combustion modes and regimes

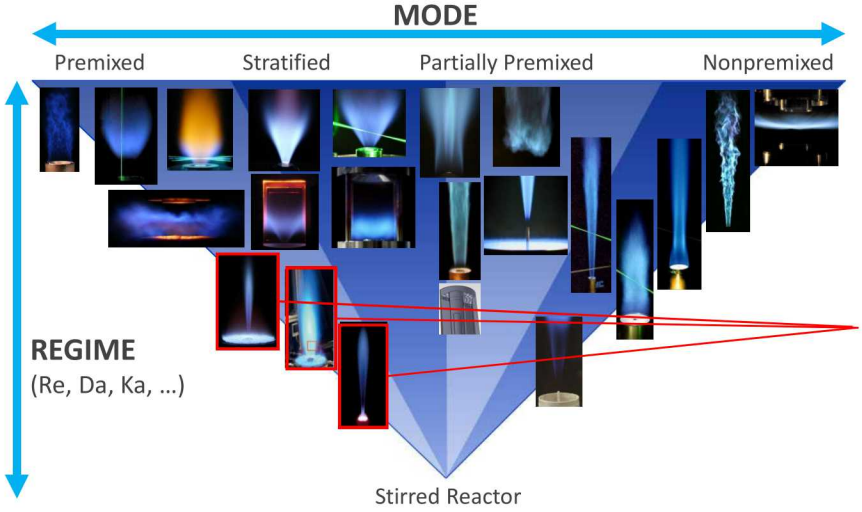

- Interactions of turbulence, molecular transport, and chemistry are expressed differently in the different combustion modes and regimes
- Reaction zone structure in highly turbulent premixed flames

Sandia National Laboratories

156

Background on highly turbulent (high Ka) Premixed Flames

Sydney PPJB
(Dunn et al.)

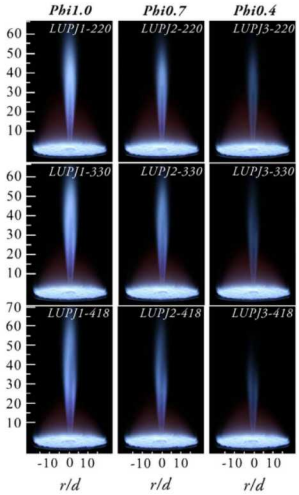

Lund JHCF
(Zhou et al.)

Michigan HiPilot
(Wabel, Skiba et al.)

Sandia National Laboratories

157

Background on highly turbulent (high Ka) Premixed Flames

- Proposed new boundaries on regime diagram (Skiba et al., CNF 2018)
- $Ka_{T,P} = (u'/S_L^{3/2})\,(L/\delta_{F,L,P})^{-1/2}$
- $\delta_{F,L,P} = (\lambda/c_p)_R/(\rho S_L)_0 = D^*/S_L$ (Peters)

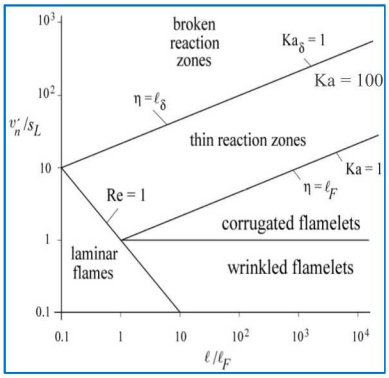

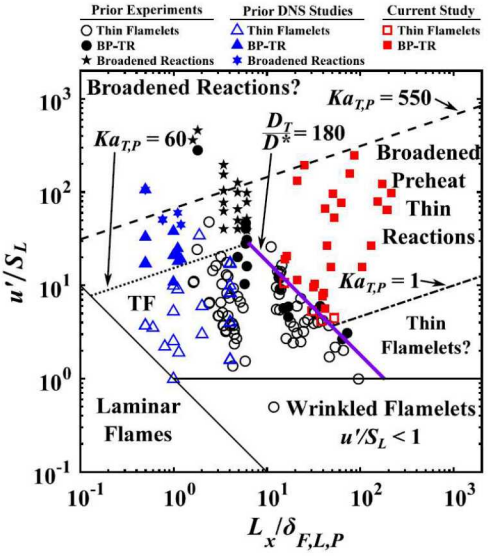

Sandia National Laboratories

158

Background on highly turbulent (high Ka) Premixed Flames

- PROBLEM: Highest Ka experimental cases are actually stratified flames
  - HiPilot
  - Lund JHCF
  - Sydney PPJB (H_2/air pilot)
- Evidence come from
  - Sandia measurements of HiPilot
  - DNS of the Lund jet flames
- Stratified flames should not be used to define boundaries on a premixed regime diagram

from Skiba et al. CNF 2018

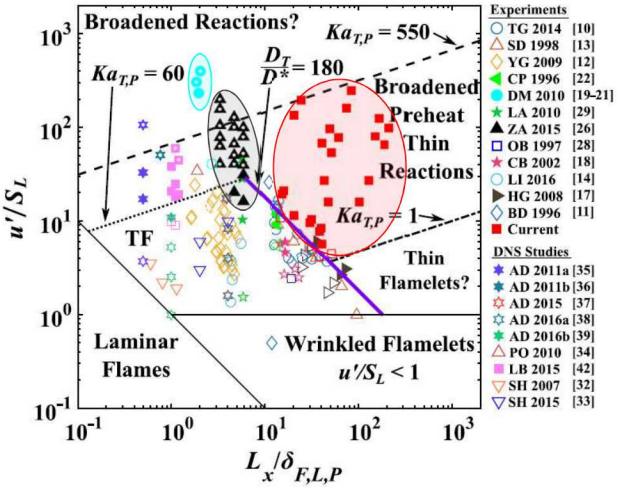

Sandia National Laboratories

159

Summary of experiments

- Four flames: HP3_65, **HP4_65**, HP3_85, HP4_85
- Vary jet velocity and equivalence ratio
- Radial profiles of T and major species

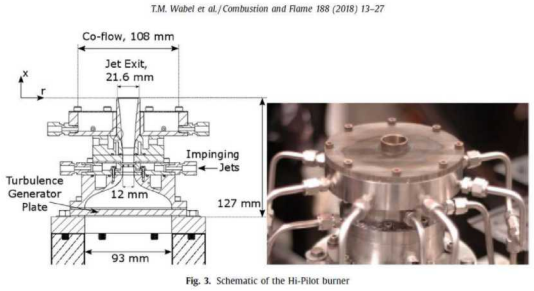

Fig. 3. Schematic of the Hi-Pilot burner

- Equivalence ratio calculated from major species (oxygen needed/oxygen available):

$$\phi = \frac{X_{CO_2} + 2X_{CH_4} + X_{CO} + 0.5(X_{H_2O} + X_{H_2})}{X_{CO_2} + X_{O_2} + 0.5(X_{CO} + X_{H_2O})}$$

- Normalized progress variable (Barlow et al. CNF 2017):

$$c_O = \frac{Y_{CO2}\left(\frac{w_{O2}}{w_{CO2}}\right) + Y_{CO}\left(\frac{w_O}{w_{CO}}\right) + Y_{H2O}\left(\frac{w_O}{w_{H2O}}\right)}{\left(Y_{CO2}\left(\frac{w_{O2}}{w_{CO2}}\right) + Y_{CO}\left(\frac{w_{O2}}{w_{CO}}\right) + Y_{H2O}\left(\frac{w_O}{w_{H2O}}\right) + Y_{H2}\left(\frac{w_O}{w_{H2}}\right) + Y_{CH4}\left(\frac{2w_{O2}}{w_{CH4}}\right)\right)}; \quad \phi < 1$$

Sandia National Laboratories

Tim Wabel, Adam Steinberg, Robert Barlow (submitted to CNF)

160

Case HP4: ϕ_{jet} = 0.65, ϕ_{pilot} = 0.9

- Peak CO occurs near the location of max heat release rate
- Color coded by measured local ϕ
- Peak CO occurs at intermediate ϕ values
- Local extinction (straight-line mixing between the reactant and pilot conditions) is rare

Y_{CO} vs. T

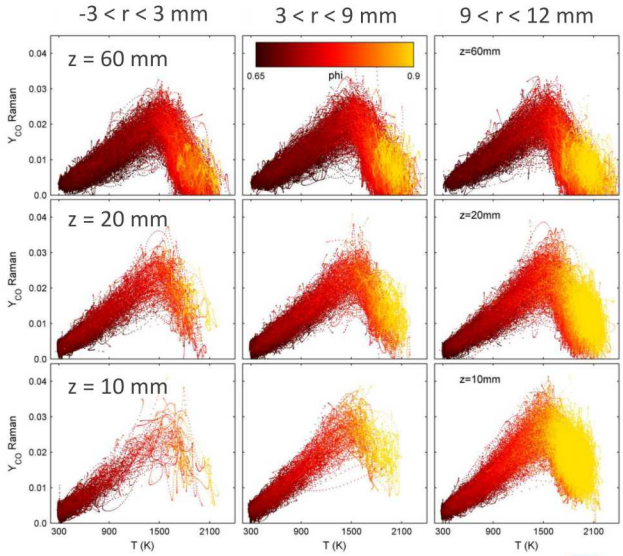

Sandia National Laboratories

Tim Wabel, Adam Steinberg, Robert Barlow (submitted to CNF)

161

PDFs of ϕ conditioned on progress variable

- Equivalence ratio condition on progress variable, $P(\phi|0.7 \le c_o \le 0.8)$
- Low flame speed at phi=0.65 leads to mixing before reaction
- Peak moves from ~0.78 @ 10 mm to ~0.69 @ 60 mm

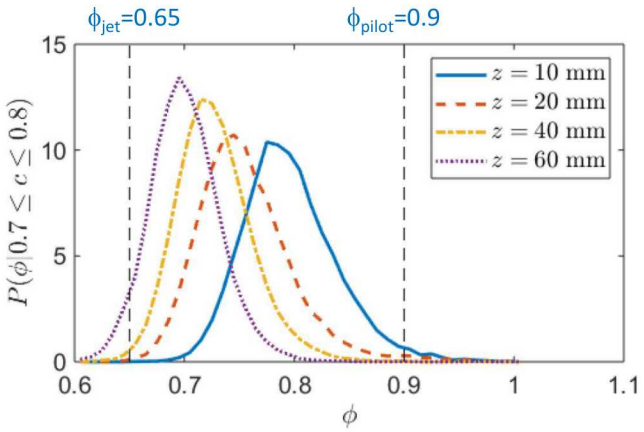

Sandia National Laboratories

Tim Wabel, Adam Steinberg, Robert Barlow (submitted to CNF)

162

Combustion modes and regimes

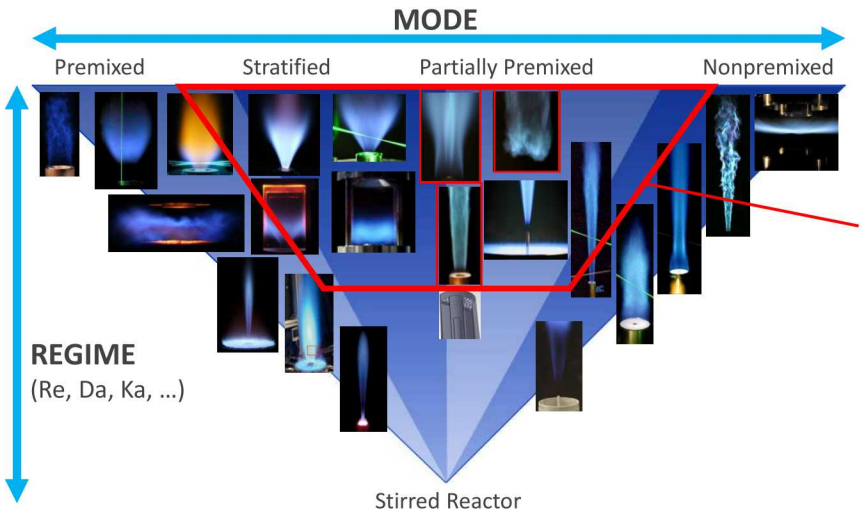

- Interactions of turbulence, molecular transport, and chemistry are expressed differently in the different combustion modes and regimes
- Partially premixed flames can combine multiple types of reaction zones within the same overall flame structure
- "Multi-regime" combustion is not well understood at a fundamental level
- Challenging for models
- Topic for TNF workshop

Multi-regime combustion is common in practical systems

Gas turbine combustion

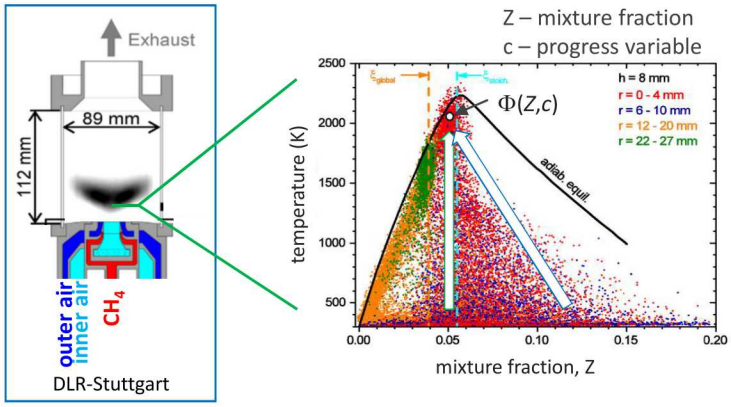

Diesel engine combustion

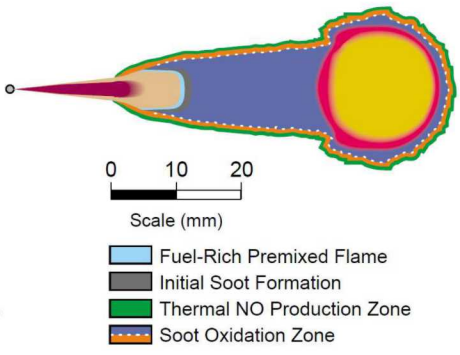

- Meier et al., Experimental Thermal and Fluid Science 73 (2016) 71–78
- Dec 1997 SAE paper 970873 DOI: https://doi.org/10.4271/970873

Partially Premixed Combustion

Laminar Opposed Flow

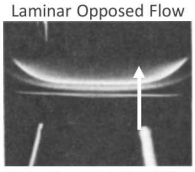

Sohrab et al. PCI 1984

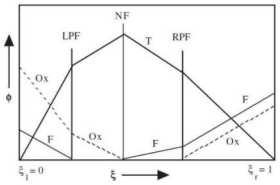

S.K. Aggarwal, PECS 35 (2009) 528–570

Laminar Edge (Triple) Flame

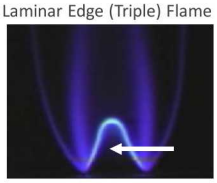

S.K. Aggarwal, PECS 35 (2009) 528–570

- Takeno Flame Index (Yamashita, PCI 1996): $\nabla Y_F \cdot \nabla Y_O$
  - Identify premixed/nonpremixed flame structures in lifted H_2 jet flame DNS (Mizobuchi et al. PCI 2002)
  - Normalized flame index: $(\nabla Y_F \cdot \nabla Y_O)/|\nabla Y_F \cdot \nabla Y_O|$
    +1 for premixed, -1 for nonpremixed.
    Still used, but overly simplistic and potentially misleading
- Good discussion in: Domingo et al. (CNF 2005), Fiorina et al. (CNF 2005), Masri (topical review on partially premixed & stratified flames; PCI 2015)
- Knudsen & Pitsch (more advanced regime indicators; CNF 2009, 2012)
- Numerical flame index and regime indicators require 3D gradients & more

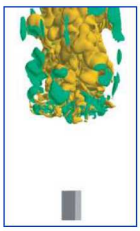

Lifted H_2 flame DNS

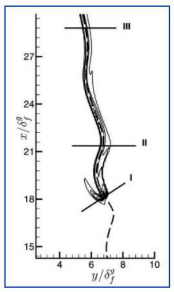

Lifted HC flame DNS
Domingo, et al. (2005)

Sandia National Laboratories

165

Gradient-free regime identification (GFRI)

Regime identification from Raman/Rayleigh line measurements in partially premixed flames

Hypotheses:

1. Major species and temperature from experiments are a footprint of full thermochemical state of each sample — **Experiment**
2. That full thermochemical state can be approximated by a constrained homogeneous reactor calculation — **Approximation**
3. Relevant flame markers can be calculated from the approximate state — **Flame markers**
4. Combinations of flame markers can reliably detect and characterize reaction zones — **Identification**

Sandia National Laboratories

Hartl et al., Combust. Flame 189, 2018; Hartl et al., Proc. Combust. Inst. 37, 2019

166

GFRI – Flame markers

Bilger mixture fraction (element based) [1]:

(characterizing non-homogeneous systems)

$$Z = \frac{\frac{2(Y_C - Y_{C,ox})}{W_C} + \frac{Y_H - Y_{H,ox}}{2W_H} - \frac{Y_O - Y_{O,ox}}{W_O}}{\frac{2(Y_{C,fuel} - Y_{C,ox})}{W_C} + \frac{Y_{H,fuel} - Y_{H,ox}}{2W_H} - \frac{Y_{O,fuel} - Y_{O,ox}}{W_O}}$$

Chemical explosion mode analysis [2,3]:

(zero-crossing identifies premixed reaction zones or auto-ignition events)

- Evaluate the eigenvalues of the chemical Jacobian
- Eigenvalue with max. real part is defined as λ_e

$$\mathrm{CM} = \mathrm{sign}(\mathrm{Re}(\lambda_e)) \times \log_{10}(1 + |\mathrm{Re}(\lambda_e)|)$$

Heat release rate [4]:

(use local value to detect reaction zones)

$$\mathrm{HRR} = -1/\rho \sum_{i \in N} \dot{\omega}_i h_{f,i}$$

Sandia National Laboratories

167

[1] R.W. Bilger et al., Combust. Flame 80 (1990) [2] T.F. Lu et al., J. Fluid Mech. 652 (2010) [3] R. Shan et al., Combust. Flame 159 (2012) [4] P. Domingo et al., Combust. Flame 140 (2005)

Procedure to approximate the full thermochemical state

$$\Phi^{exp,RR} = [T, Y_{CH_4}, Y_{CO_2}, Y_{H_2O}, Y_{CO}, Y_{H_2}, Y_{O_2}, Y_{N_2}]$$

Raman/Rayleigh experimental data $\Phi^{exp,RR}$ → constrained homogeneous reactor → approximate full state $\Phi^{exp,RR}_{app}$ → calculate flame markers Z, HRR, CM, ΔCM

- For methane flames, major species > 0.99 mass fraction
- Constrained homogeneous reactor: constant temperature, constant pressure, long residence time
- Allow minor species, radicals to build up from zero to steady state → approximate full state
- Calculate flame markers
- Original approach: Constrain major species to stay within experimental uncertainty
- Current approach: Constrain major species (except CH_4) to initial values (best available information); Separately evaluate sensitivity to experimental uncertainty using UQ methods

Sandia National Laboratories

168

Identification criteria developed using laminar flame simulations

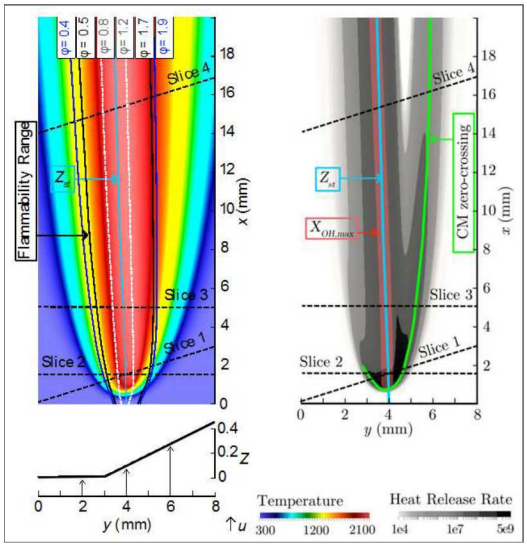

- 1D CH_4/air counterflow flames:
  - Non-premixed
  - Partially premixed
  - Premixed
- 2D CH_4/air triple flames:
  - Lean and rich premixed branches
  - Trailing non-premixed flame
- Identification criteria

Premixed	**Non-Premixed**
• CM zero-crossing • HRR local max near crossing	• negative CM values • significant HRR near Z_{st}

Sandia National Laboratories

169

Hartl, Geyer, Dreizler, Magnotti, Barlow, Hasse (Combust. Flame, 189, 2018)

GFRI method was validated using counterflow flame experiments

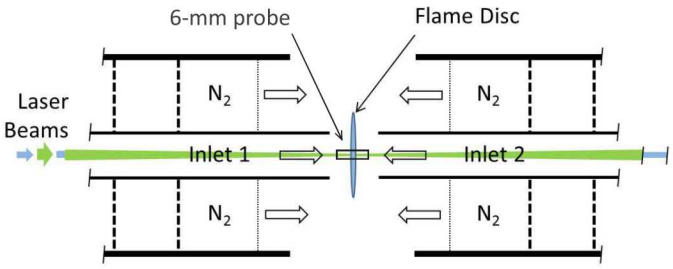

Three partially premixed flames

	Inlet 1		Inlet 2		
	φ_1	u (m/s)	φ_2	u (m/s)	a (1/s)
PP1	0.7	0.29	1.4	0.39	114
PP2	0.4	0.22	1.8	0.16	60
PP3	0	0.31	4.8	0.3	101

PP1 – both inlets flammable
PP2 – both inlets outside flammability limits
PP3 – fuel side matches Sydney piloted inhomogeneous jet flames (air/CH_4 = 2)

Sandia National Laboratories

170

Hartl, Geyer, Dreizler, Magnotti, Barlow, Hasse (Combust. Flame, 189, 2018)

Laminar counterflow flame results

- Flame PP1: ϕ_1=0.7, ϕ_2=1.4
- CM
  - Approximation yields accurate zero crossings
  - Good agreement across most of the profile
- HRR
  - More sensitive to uncertainty
  - local peaks can still be identified

- **Flame markers and reaction zones are correctly identified from the Raman/Rayleigh data**
- **Relative strength of different reaction zones can be assessed**

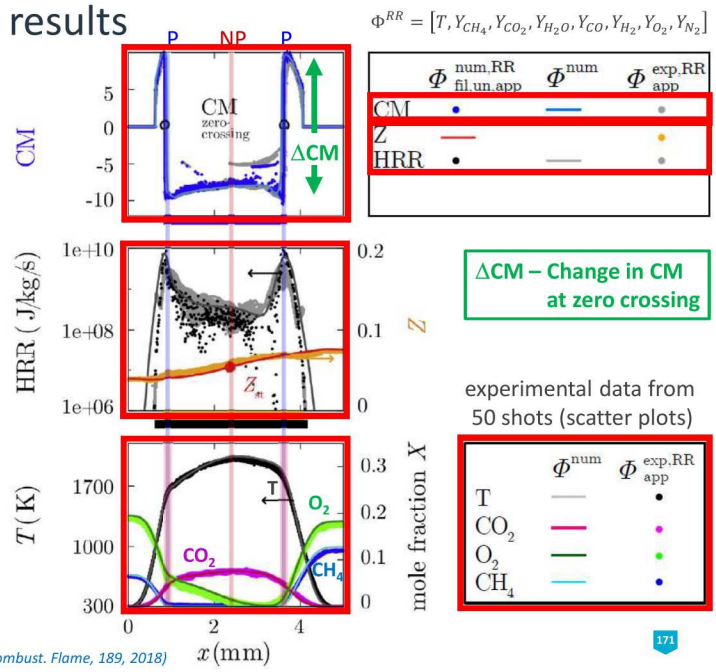

ΔCM – Change in CM at zero crossing

experimental data from 50 shots (scatter plots)

Sandia National Laboratories

Hartl, Geyer, Dreizler, Magnotti, Barlow, Hasse (Combust. Flame, 189, 2018)

171

Lifted flames and the correlation of Z_{CM}, ΔCM, HRR

- Mildly turbulent lifted flames
  - D = 8.0 mm
  - 0.3 m/s coflow
  - Re_{jet} = 2000, 7330
  - liftoff heights: h/D = 4.5, 16
- 2D laminar triple flame simulation

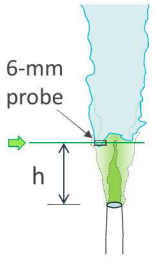

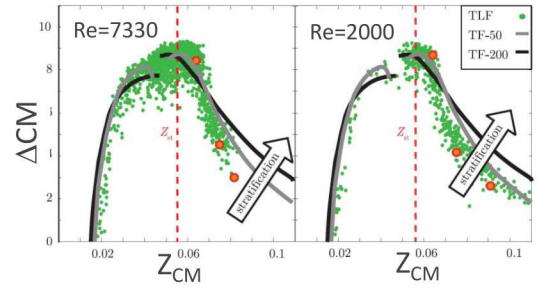

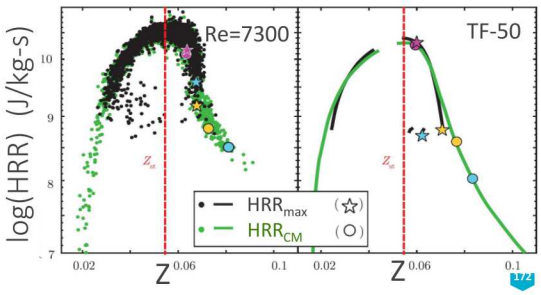

- **ΔCM and HRR_{CM} decrease as Z_{CM} moves away from most reactive range**
- **HRR_{max} switches to non-premixed reaction zone as premixed zone weakens**
- **Similar in experiment and simulation**

Sandia National Laboratories

Hartl et al., Proc. Combust. Inst. 37, 2019

172

Darmstadt Multi-Regime Burner (MRB)

TECHNISCHE UNIVERSITÄT DARMSTADT

h_da HOCHSCHULE DARMSTADT UNIVERSITY OF APPLIED SCIENCES

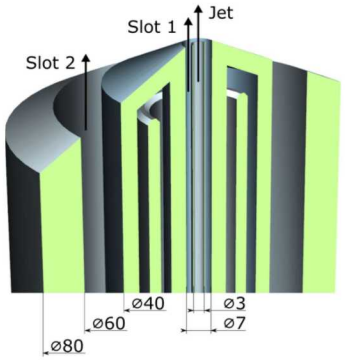

	jet		slot 1			slot 2	
	φ	u [m/s]	φ	u [m/s] a	u [m/s] b	φ	u [m/s]
MRB14	1.4	105	0	7.5	15	0.8	20
MRB18	1.8						
MRB22	2.2						
MRB26	2.6						

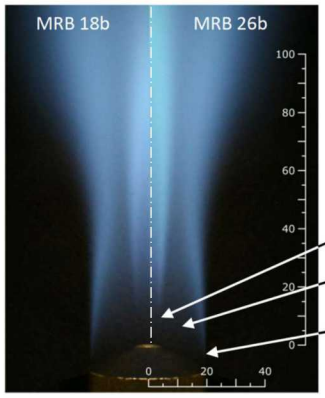

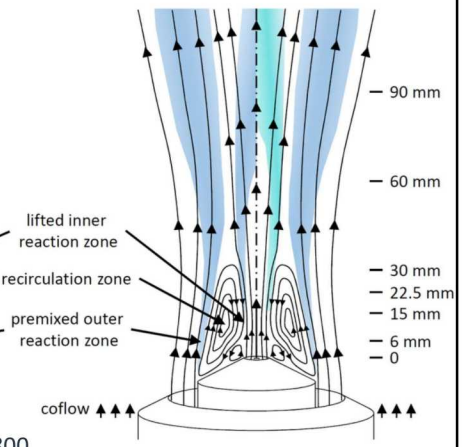

- $Re_{jet} \cong 18500$; $Re_{slot2} \cong 20800$
- Eight cases studied: Raman/Rayleigh/LIF; PIV and SO_2 PLIF
- Focus on two cases: MRB18b, MRB26b

Sandia National Laboratories

Butz, Hartl, Popp, Walther, Barlow, Hasse, Dreizler, Geyer (submitted to CNF last week)

173

Temperature vs. mixture fraction

- The profile at 6 mm is below the inner flame stabilization zone

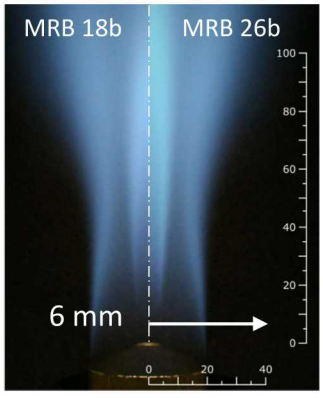

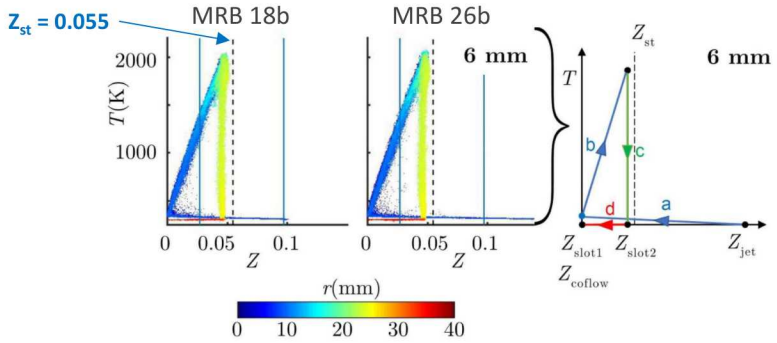

- Line **a**: mixing of jet fluid with slot 1 air (warm)
- Line **b**: mixing of slot 1 air with slot 2 products
- Line **c**: traverses the outer premixed flame from products to reactants
- Line **d**: mixing of slot 2 reactants and coflowing air

Sandia National Laboratories

174

Temperature vs. mixture fraction

- Evolution in reactant composition

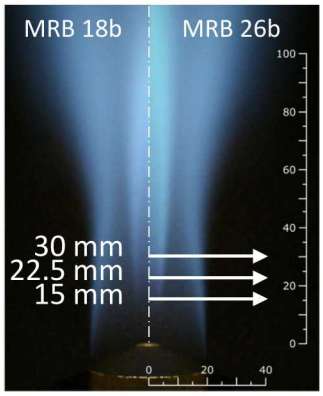

flammability limits

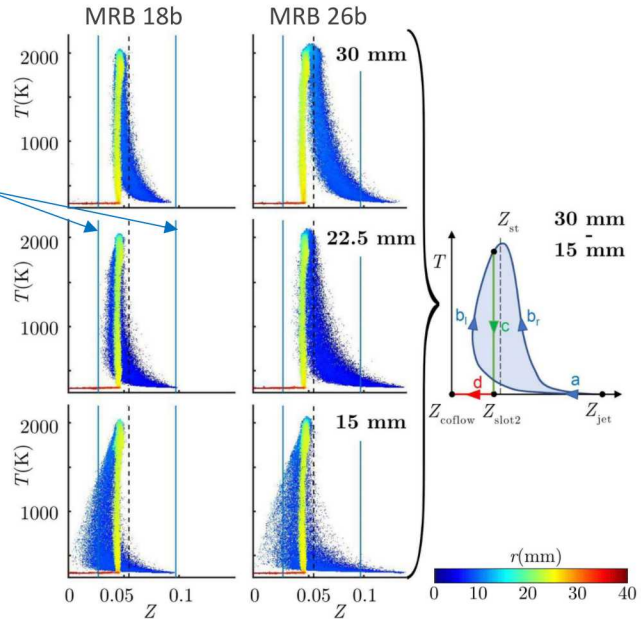

- Many samples moving to elevated T within flammability limits; lean and rich trajectories (illustrated by b_l … b_r)

Sandia National Laboratories

Criteria for characterizing reaction zones

- Instantaneous 1D scalar profiles
- Region of interest (ROI) 0.5 mm wide from crossing into negative CM region
- HRR_{CM} = max within ±100 μm of crossing
- HRR_{NP} = max within ROI (outside 100 μm)
- Reaction zone index based on relative heat release of premixed and non-premixed reaction zones in close proximity:

$$\eta = (HRR_{CM} - HRR_{NP})/ HRR_{max}$$

$$HRR_{max} = \max(HRR_{CM}, HRR_{NP})$$

(+1 – premixed, -1 – non-premixed)

- Multi-regime: $0.8 > \eta > -0.8$

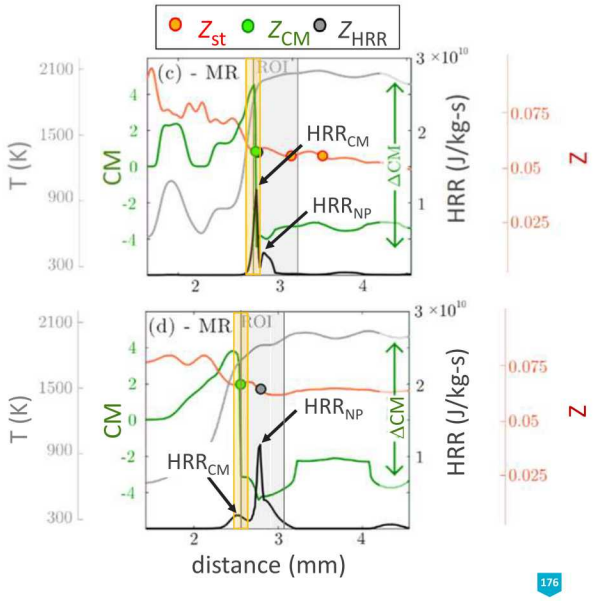

Sandia National Laboratories

176

Criteria for automated characterization of reaction zones

premixed	P	$\eta > 0.99$, no detectable NP character
dominantly premixed	DP	$0.99 > \eta > 0.80$
multi-regime	MR	$0.80 > \eta > -0.80$
dominantly non-premixed	DNP	$-0.80 > \eta > -0.99$
non-premixed	NP	$\eta \leq -0.99$; HRR_{max} within $0.055<Z<0.07$, no CM zero crossing
lean back-supported	LBS	$Z_{CM} < Z_{HRR} < Z_{slot\ 2}$ (special case)

Sandia National Laboratories

177

Population fractions of different reaction zone structures

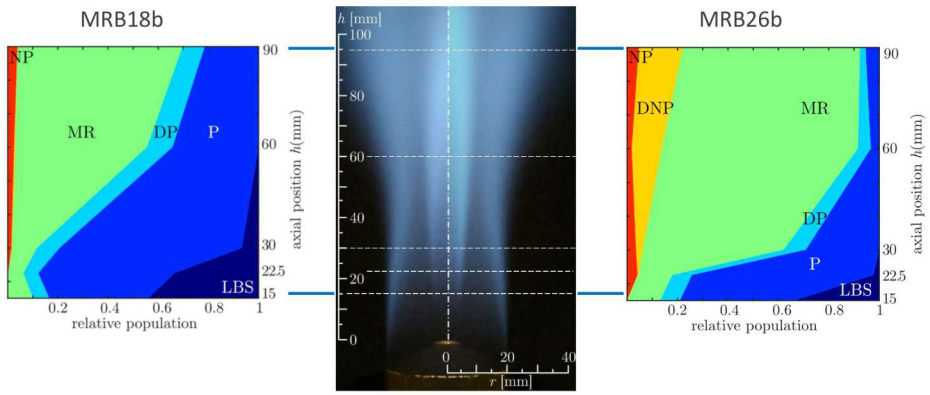

- Near field primarily premixed and stratified-premixed structures (P, DP, LBS) in both flames
- Increasing probability of multi-regime (MR) structures with downstream distance, especially in MRB26b
- Increasing DNP in the richer flame, but fully non-premixed structures are rare in both flames
- Results are <u>not</u> highly sensitivity to characterization parameters

Sandia National Laboratories

178

Butz, Hartl, Popp, Walther, Barlow, Hasse, Dreizler, Geyer (submitted to CNF)

Useful Reviews

- Springer Handbook of Experimental Fluid Mechanics, Tropea, C., Yarin, A. L. and Foss, J. (Eds), Springer, 2007, http://www.springer.com/materials/mechanics/book/978-3-540-25141-5
- Westerweel, J., G.E. Elsinga, R.J. Adrian, Particle Image Velocimetry for Complex and Turbulent Flows, Annual Reviews of Fluid Mechanics (2013). http://www.annualreviews.org/doi/full/10.1146/annurev-fluid-120710-101204
- Miles, R.B., W.R. Lempert, J.N. Forkey, Laser Rayleigh scattering, Meas. Sci. Technol. 12 (2001) R33-R51.
- Daily, J.W., Laser Induced Fluorescence Spectroscopy in Flames, Prog. Energy Combust. Sci. 23 (1997) 133-199.
- Schulz, C., V. Sick, Tracer-LIF diagnostics: quantitative measurement of fuel concentration, temperature and fuel/air ratio in practical combustion systems, Prog. Energy Combust. Sci. 31 (2005) 75–121 doi:10.1016/j.pecs.2004.08.002. http://linkinghub.elsevier.com/retrieve/pii/S0360128504000619
- Roy, S., J.R. Gord, A.K. Patnaik, Recent advances in coherent anti-Stokes Raman scattering spectroscopy: Fundamental developments and applications in reacting flows, Prog. Energy Combust. Sci. 36 (2010) 280–306 doi:10.1016/j.pecs.2009.11.001. http://www.sciencedirect.com/science/article/pii/S0360128509000586
- Schulz, C., B.F. Kock, M. Hofmann, H. Michelsen, S. Will, B. Bougie, et al., Laser-induced incandescence: recent trends and current questions, Appl. Phys. B. 83 (2006) 333–354 doi:10.1007/s00340-006-2260-8. http://link.springer.com/10.1007/s00340-006-2260-8.
- Linne, M., Imaging in the optically dense regions of a spray: A review of developing techniques, Prog. Energy Combust. Sci. 39 (2013) 403-440. http://dx.doi.org/10.1016/j.pecs.2013.06.001
- Drake, M.C., D.C. Haworth, Advanced gasoline engine development using optical diagnostics and numerical modeling, Proc. Combust. Inst. 31 (2007) 99-124. doi:10.1016/j.proci.2006.08.120

Books

- R. K. Hanson, R. M. Spearrin, and C. S. Goldenstein, Spectroscopy and Optical Diagnostics for Gases, 1st ed. (Springer, 2015)
- M. A. Linne, Spectroscopic Measurement: An Introduction to the Fundamentals (Academic Press, 2002)
- K. Kohse-Höinghaus and J. Jeffries, eds., Applied Combustion Diagnostics (Elsevier 2002)
- A. C. Eckbreth, Laser Diagnostics for Combustion Temperature and Species (Gordon and Breach, 1996)
- S. B. Pope, Turbulent Flows (Cambridge University Press, 2000)


Thank you for
your attention
Del Valle Reservoir, Livermore, California Sep 30, 2018